COMMUNICATIONS

Dear reader,

as you probably know the Department of Mechatronics and Electronics is one of the departments existing at the Faculty of Electrical Engineering of the University of Zilina. Since established in 2005, it provides education of specialists in the study branches Power- and Applied Electronics, and Electrical Systems in Mechatronics and carries out research in the same fields. This issue of the Communications – Scientific Letters is devoted to the latter branch. Mechatronics is the conjunction of smart mechanics, electronics, and control techniques, i.e. control of mechanical motion by means of electronic devices and software tools. From this point of view we can talk about a highly promising field of engineering as the majority of 'high-tech' applications are based on branches covered by mechatronics. I strongly believe that we shall come across these systems on the pages of the Communications again in the near future.

Branislav Dobrucký

Ladislav Jurišica *

MECHATRONICS SYSTEMS

The term mechatronics refers to systems with special characteristics that can be achieved only as a whole, and cannot be realized through other means. Integrating mechanical and electronic components with control systems and informatics during design was introduced due to new performance requirements on system quality, its overall reliability, dynamics, low energy consumption, low weight, etc. The paper is focused on the basic information about mechatronics.

Keywords: mechatronics, robotics, integration, electortechnics, control

Introduction

Many systems in industry and other areas are designed for controlling mechanical movement. Although earlier systems were using only mechanical energy, most of the current mechatronics systems contain components for mechanical movement and parts that control it. The main drawback of earlier systems stems from the use of only simple laws of control, which in turn required system redesign for any control adjustments. Introducing electrical components into systems increased their flexibility. Additional significant improvement was enabled by microprocessors, which enabled to execute tasks by programs instead of purely by hardware. Combined, these improvements substantially increased the complexity of tasks that could be executed.

Integrating electrical, electronic and control systems with computers and mechanical systems established a new approach to design and use of manufacturing systems and other systems with mechanical movements.

Universal control systems comprise multiple components for: specification of control signals, implementation of control laws for static and dynamic events in the system, amplification of control commands, measurement of actual system state, and communication infrastructure. Control systems are usually implemented using computers, sensors for system state assessment, electric actuators for moving mechanical parts, and electric or optoelectric communication systems. The term *mechatronics* refers to such integrated systems with computer control of electric and mechanic subsystems.

Mechatronics

Growing demands for extended properties and capabilities of machines increase their complexity, which in turn requires improving the quality of these systems to the point when further improvements were not possible without integrating mechanical and electric systems during their design and use. Main directions of this approach, called mechatronics, were described in the 60-ties, and further developed by defining its principles in the 70-ties. Mechatronics relates to the start of modern robotics, and robots represent typical mechatronics systems. The main goal of this field is to design new generation of powerful and intelligent machines.

Although the term mechatronics was introduced in 1970, there is still discussion about its meaning. One line of thought defines mechatronics as nothing more than a good engineering design with systematic approach [2]. However, there are several definitions that clearly define goals of mechatronics as a scientific field, and there is plenty of research interest in the field [3, 4, 5, 6, 7, 8, 9, 10, 11, 12].

Currently, many fields and technologies synergistically integrate with computer science, resulting in increased use of autonomous, intelligent computerized control systems. This integration marks the beginning of "mechatronics age", which is characterized by fusion of diverse technologies and significant shortening of system design cycle.

In the past, system design was characterized by a sequential integration of individual design stages:

- Specifying mechanical components.
- Integrating sensors, actuators, and regulators.
- Adding control subsystems and programs.

In contrast, mechatronics follows an integrated and comprehensive approach to system design, where all design stages and components are integrated simultaneously. The result of such design approach should be a high-quality integrated system, which could not be achieved by sequential integration of individual design stages.

Mechatronics is the result of increased demands on automation, electronic and informatics approaches in engineering, and systems, in which mechanical movement needs to be precisely and flexibly controlled.

* **Ladislav Jurišica**
chairman of SOK committee for mechatronics, Faculty of Electrical Engineering and Information Technology, Slovak Technical University, Bratislava, E-mail: ladislav.jurisica@stuba.sk

Mechatronics integrates diverse techniques, approaches and principles including mechanics, electronics, control and information theory, and computer science to synthesize available subsystems to achieve required goals. Mechatronics system comprises non-separable combination of mechanical and electronic components, which facilitate exchange of energy and information. Mechatronics is unique since it enables building systems that are qualitatively different from any previous designs [1]. The usual graphical representation of mechatornics is presented in Figures 1–3.

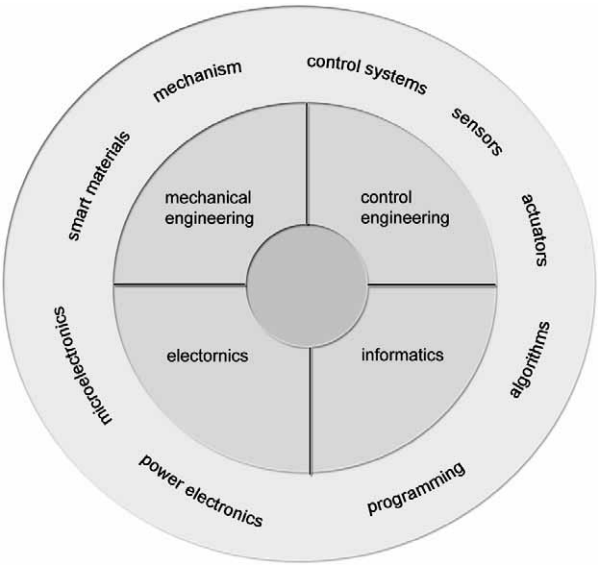

Fig.1. Mechatronics and its components

Technical systems with the software-oriented control may contain features, which were not attainable in the past, but may create challenges as well. Software is implemented in the computer system, but at the same time, it is a self-determining component, independent from the system implementation. Taking this into account, it is necessary to consider software quality and safety. Thus, new technologies require new methodology for software design, which has to be considered in the current definition of mechatronics.

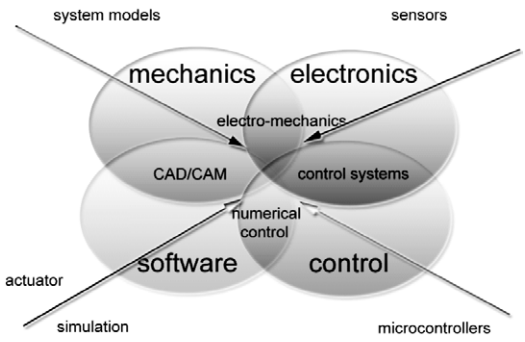

Fig. 2 Mechatronics as a combination of diverse technological and scientific disciplines

The classic definition characterizes mechatronics as a synergistic integration of precision machinery, electronics, computers, control systems, and system approach to design of processes and systems. *More recent definitions* include an important component – application of comprehensive decision-making process during the control of technological systems. The key element in mechatronics is the integration of all components in both the design and manufacturing processes. The important principle in mechatronics is the flexibility and ease of system and process control. The main goal is to create modules with "plug and play" features, and those having local autonomy.

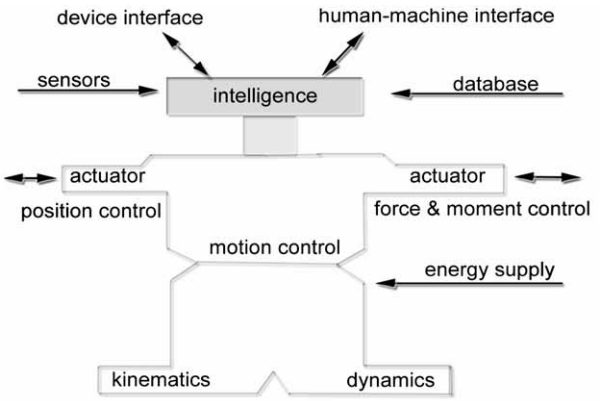

Fig. 3 Mechatronics systems and its integration with the environment

Mechatronics is a modern, interdisciplinary, technological and scientific field, which combines mechanics, electronics, informatics and cybernetics. Its goal is a synergistic integration of individual subsystems, in a comprehensive approach to design, manufacturing and use of machines, systems, components and products, in which main activity comprises mechanical principles.

Mechatronics focuses on computer-controlled electro-mechanical systems – mechatronics systems, their analysis and synthesis with the goal to achieve synergistic effect among individual subsystems, which are contained in the full system. Additional research focus also includes individual analysis and synthesis methods, design and manufacturing approaches, and experimental validation methods, since it is precisely those methods that are essential in achieving synergistic effect.

Mechatronics Systems

Mechatronics systems characterize a separate class of objects, which are qualitatively defined by the artificial systems with specific, intelligent behavior. This behavior is achieved by controlling generalized movements of individual parts of the system, and controlling energy interaction among individual diverse subsystems (including mechanical stiff and flexible matter, electromagnetic current, liquid, gas). For example, CNC machines, robots, technological automatic systems, mobile machines, transportation and manipulation systems, special machinery, consumer products, etc.

A special class comprises micro-mechatronics systems – micro-electro-mechanical systems (MEMSs).

One of the main requirements in mechatronics systems is to achieve intelligent properties for these systems. *Intelligent systems* could achieve the following:

- Sensing the environment and recognizing important and relevant information required for achieving the task.
- Anticipating changes in the environment considering the used model.
- Using information about the environment and expert knowledge for intelligent decision making.
- Planning the task execution required for achieving the given task and their adaptation to the actual state of the system environment.
- Communication and collaboration with other intelligent systems during problem solving.
- Learning from the past experience during solving the same or similar tasks.
- Adapting to a new environment.

The main goal of intelligent control is to achieve high system performance, high reliability, effective use, and automated fault response and recovery. Systems with sensors for monitoring the process are using decision support systems during considering imprecise information about parameters and changed signal, fuzzy control, artificial neural networks, learning, and other intelligent planning systems using artificial intelligence.

Mechatronics systems comprise three essential components: 1) energy components, 2) information-control component, and 3) mechanical subsystems.

Energy component comprises *mechanisms, actuators* and *their connecting subsystems*. The chief characteristic is the energy interaction among individual components.

Information-control component comprises *sensors, communication and control subsystems* (usually distributed), which process information and coordinated communication in mechatronics systems. Information system extension in mechatronics systems contains monitoring and diagnostics subsystems, visualization and automation systems for assessing quality of performed tasks, or the overall production quality. Information-control component is characterized by information processes and interactions.

Micro-mechatronics comprises integration of mechanical and electrical systems, where both subsystems are measured in microns. Micro-mechatronics requires combination of components such as microprocessors, microsensors and microactuators, with all functionality supported by intelligent computational systems. Additional essential features of such systems are their high functional reliability, low manufacturing cost, high reproducibility of functional characteristics, and low power requirements.

Design and manufacturing of microsystems require deep knowledge of physics principles of micro-components, and the ability to use powerful computer-aided design systems and simulators. The central assumption is the knowledge of microelectronics and micro-manufacturing technologies. Micro-mechatronics is the future focus of mechatronics, in which existing composite materials will increasingly be complemented by novel materials, including biological.

Conclusions

Mechatronics is linked to increased demands on system performance. Gradually, electro-mechanical systems achieved intelligent properties. We can expect to achieve qualitatively new results only when comprehensive approach is used in design and synthesis of such systems.

Mechatronics systems comprise mainly electronic and opto-electronic components, for obvious reasons. It is precisely the advancement in micro-electronics and electronic materials that enabled realization of compact systems with sufficient mechanical power. Sophisticated structures, extensive sensor systems, powerful control-computer systems and actuators further enable new types of applications, including complex manufacturing processes.

Mechatronics approach to design is based on optimal system construction. This approach also leads to the use of smart materials in these systems.

References

[1] AUSLANDER, D. M.: *What is Mechatronics?*, IEEE/ASME Trans. on Mechatronics, 4/1996, pp. 5–9

[2] HEWIT, J. R., KING, T. G.: *Mechatronic Design for Product Enhancement*, IEEE/ASME Trans. on Mechatronics, 2/1996, pp. 111–119

[3] ACAR, M., PARKIN, R. M.: *Engineering Education for Mechatronics*, IEE Trans. on Ind. Electronics, 1/1996, pp. 106–112

[4]. FUKUDA, T., UEYAMA, T.: *Self-Evolutionary Robotic System*, J. of Robotics and Mechatronics, 2/1992, pp. 96–103

[5]. THIELEMANS, H.: *HERDA - Heterogenous Distributed Real-time Architecture*, Proc. Tampere Int. Conf. Machine Automation, 1994, pp. 627-639

[6] BOLTON, W.: *Mechatronics. Electronic controlsystems in mechanical and electrical engineering,* Pearson, Prentice Hall, 2003.

[7] DOVICA, M.: *Components and modules in mini- and micro-mechanisms (in Slovak)*, Typo press, Košice 2002, ISBN 80-7099-878-4

[8] GMITERKO, A.: *Mechatronics. Driving forces, characteristics and conceptual design of mechatronics systems (in Slovak)*, Košice, 2004, ISBN 80-8073-157-8

[9] http://sk.wikipedia.org/wiki/Mechatronika

[10] Mechatronics, AT&P Journal Plus, 6/2005, ISSN 1336-5010

[11] Application of Artificial Intelligence, AT&P Journal Plus, 7/2005, ISSN 1336-5010

[12] Mechatronics Systems, AT&P Journal Plus, 1/2006, ISSN 1336-5010

P. Bauer – J. Sitár *

ANALYSIS OF ELECTROMECHANICAL ACTUATOR BASED ON FEM – CIRCUIT SIMULATOR COUPLING

Abstract: Design and simulation of an electromechanical system is multidisciplinary. In this paper three different types of co-simulation of a mechatronic system are compared. The co-simulation is realized between two different programs (power electronic circuit simulator – control part and finite element analysis – magnetic and mechanic model part). The simulations were realized for an electromechanical actuator fuel injection system. The output waveforms for coil current, forces, inductances and position are compared. Finally the measured waveforms are presented too.

I. Introduction

Design and construction of modern types of electromechanical actuators is often verified by simulation. Analysis of a typical electromechanical system with power electronic converter consists of many aspects and is often multidisciplinary. Such a design can be realized only by different software packages. A classical electromechanical system consists of three different parts: electrical circuit (simulation of electrical circuit and control part), magnetic circuit (forces, co-energy, inductances) and mechanical part (torque, revolution). There is not a single simulation program which can handle such a system in a single way and consider all aspects at the same detailed level. Therefore, the design of an electromechanical system drive is mostly created step by step in different programs. The first step is usually building the magnetic circuit of a machine. Simulation results are often used in the next step, which is the simulation of electric circuit and control part of the machine. Simulation of mechanical loads and forces can be computed together with the first step in magnetic circuit simulation. However, the simulation of electric and magnetic circuit can not be decoupled because they interact with each other.

In this paper the simulation of a fuel injection system is investigated. There are two different parts in this system. Magnetic circuit and magnetic model specifications consist of forces, material properties and mechanical quantities such as movement, speed, shift and deformation. The electric circuit consists of a control circuit simulator together with the signal generator. To achieve an analysis of a complete system, two different programs are used. For this model type it is very suitable to use co-simulation, where two different programs are co-operating.

II. Basic co-simulation principles

In the first two cases of co-simulation it is possible to describe the program cooperation in the same way (Fig. 1). The difference is only in the obtained results. The dynamic power electronic model calculation is based on static finite element model calculation. From this the static values for inductance, magnetic force and coil current are obtained and used in the power electronic calculation. In the second case the difference is only for finite element model calculation where the power electronic output results were verified by the static loop calculation.

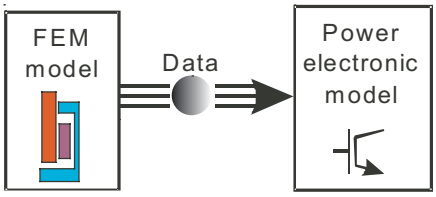

Fig. 1: Simple principle for data exchange at the first and second co-simulation

The computing like this one is accurate for a solenoid actuator description but from these first two co-simulation types there is no possibility to determine the transient behaviour. For this reason the third co-simulation possibility between the programs (Fig. 2) was realized. In this case it is necessary to realize the primary static computing in the finite element program too. After that the full dynamic co-simulation can start. This calculation is transient and during simulation the results are saved as data table.

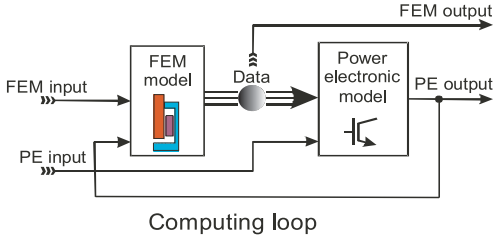

Fig. 2: Principle for full variable data exchange during co-simulation

* P. Bauer[1], J. Sitár[2]
[1]Delft University of Technology/Power Electronic and Power Processing, Delft, The Netherlands, P.Bauer@tudelft.nl
[2]Alexander Dubcek University of Trencin, Faculty of Mechatronics, Trenčín, Slovakia

The main question remains: on what level these programs must co-operate. Three different levels of data exchange will be defined as shown in Figs. 3, 4, and 5. These levels bring different kind of abstraction and simplification of the subsystems. Different kind of levels of the co-simulation will result in different output values. This paper will give an answer to the question, how the different level of co-simulation influences the results of the investigated system. The conclusions about the usefulness of these different levels of co-simulation are given. The best know simulation package for magnetic circuit analysis are Ansys, Femag, Femlab, Maxwell, Femm and there are many others. For simulation of electrical circuit the best know are Spice, Caspoc, Matlab/Simulink, Dynast and others. Some of these mentioned programs have a connection option with open interface, which can make the co-simulation. For example: Maxwell can be connected together with the Simplorer and Caspoc has a connection with Ansys and Matlab/Simulink. Here co-simulation between Caspoc and Ansys will be created and the results are presented. Basic structures, analyses and mathematical models of solenoid are described in [8]. In literature the magnetic circuit model is presented together with control circuit.

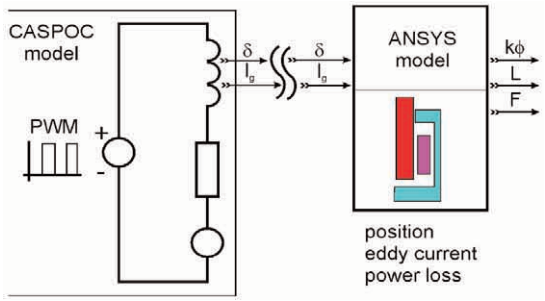

Fig. 3: Block circuit for one value co-simulation and data exchange

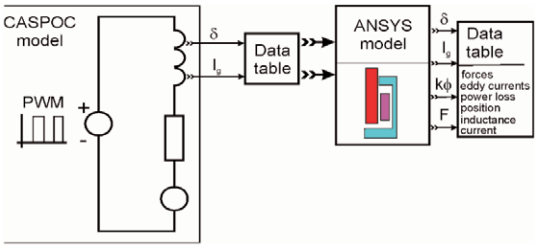

Fig. 4: Block diagram for table data exchange in co-simulation

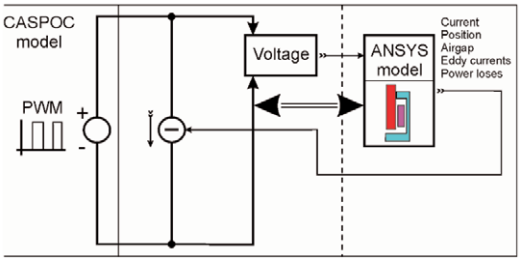

Fig. 5: Block scheme for full dynamic co-simulation (dynamic data exchange)

III. Electromagnetic and mathematical model of solenoid

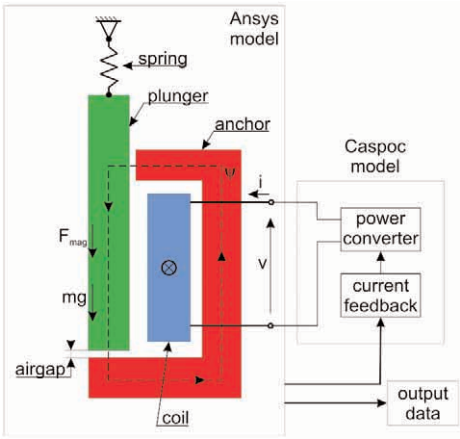

Fig. 6: Co-simulation model design

The principles of feedback current control strategy for solenoid are introduced and a simple electromagnetic actuator is developed. Here an analysis is carried out that calculates the inductance, flux densities, stored magnetic energy and co-energy, magnetic forces, current and power losses. Typical structures for the solenoid are described.

Fig. 6 shows the basic structure of the solenoid with a feedback current controller. Excitation of the windings produces magnetic forces for plunger movement. The plunger is free only in the vertical axis. The current i produces a flux ψ. The flux path is shown by the dotted line in Fig. 6 and 7, and it crosses the air-gap in the vertical direction. The attractive force between the plunger and anchor is function of i and is proportional to the square of i, if the material is not saturated. Under movement conditions, the generated attractive force is higher than the spring force. The spring force is a little bit higher than multiplied plunger weight m with gravity acceleration g. The force command is the sum of spring,

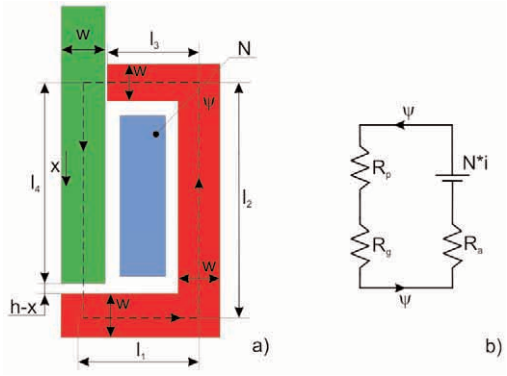

Fig. 7: Solenoid basic dimensions and equivalent magnetic circuit a) and electric circuit b)

gravity and attractive force commands. The spring force is in opposite direction to the gravity and attractive force commands.

The voltage U excites a coil. Let us suppose that the number of turns in the windings is N so that the magneto-motive force (MMF) Ni is produced. Since the permeability in ferromagnetic materials is high, the flux follows the path shown. The flux crosses the air – gap. Note that only one flux path is shown; however, the flux is distributed in the air – gap. The maximum flux density in the air – gap is determined by the coil excitations.

Figure 7 a) shows the model of the solenoid used for simulation. The anchor has the width w. The main flux path is indicated by the doted line. The length of the flux path in the model is defined by l_1, l_2 and l_3. The flux path length in the plunger is l_4. The winding in the coil has N turns. The instantaneous current is i, so that the MMF is Ni. The air-gap length is equal to h at the maximal position. A coordinate position x is defined in plunger position so that the air-gap length is h-x.

Reluctance of magnetic circuit is defined as:

$$R = \frac{l_{fp}}{\mu_{mt} * S} \tag{1}$$

Where:
l_{fp} – Flux path length ($l_{fp} = l_1 + l_2 + l_3 + l_4$)
μ^{mt} – Permeability of the material
S – Cross – section area of the flux path

Permeance is inverse function of magnetic reluctances:

$$P_a = \frac{\mu_{mt} * S}{l_{fp}} \tag{2}$$

Figure 7 b) shows an "electrical" equivalent circuit of the solenoid magnetic circuit. In terms of MMF (voltage), flux (current), reluctances (resistance) and constant (dc) magnetic circuit can be treated in the same way as in the electric circuit. The main difference is that magnetic reluctance is an energy storage component rather than loss component. The "dc voltage" source Ni represents the MMF generated by the winding current. R_p and R_a are the magnetic reluctances in plunger and anchor respectively. R_g represents the magnetic reluctance in the air – gap. These magnetic reluctances are written as:

$$R_a = \frac{l_1 + l_2 + l_3}{\mu_0 \mu_r S} \tag{3}$$

$$R_g = \frac{h - x}{\mu_0 S} \tag{4}$$

$$R_p = \frac{l_4}{\mu_0 \mu_r S} \tag{5}$$

Where:
μ_0 – is the permeability of free space ($\mu_0 = 4\pi * 10^{-7}$)
μ_r – is the relative permeability ($\mu_{mt} = \mu_0 \mu_r$)

The flux ψ is:

$$\psi = \frac{Ni}{2R_g} = \frac{Ni}{2} \frac{\mu_0 S}{h - x} \tag{6}$$

The flux linkage λ_1 of the coil is defined as a number of the turns N multiplied by the flux passing through the coil:

$$\lambda_l = \frac{N^2 i}{2} \frac{\mu_0 S}{h - x} \tag{7}$$

Inductance is defined as flux linkage divided by the current value

$$L = \frac{\lambda_l}{i} = \frac{N^2}{2} \frac{\mu_0 S}{h - x} \tag{8}$$

Stored magnetic energy and co-energy can be determined from the relation between flux linkage λ and current i in the magnetic circuit with ferromagnetic components such as the cores in figure 2. The flux linkage is proportional only to low current values. At high current, the ferromagnetic cores become saturated, producing a nonlinear characteristic. Stored magnetic energy and co-energy is calculated in Ansys with Synergy macro. The stored magnetic energy W_m in a magnetic system is obtained from:

$$W_m = \int_0^{\lambda_0} id\lambda \tag{9}$$

In addition to the magnetic energy, we can introduce the magnetic co-energy W'_m. The magnetic co-energy is defined as:

$$W'_m = \int_0^{\lambda_0} \lambda di \tag{10}$$

The independent variables in a magnetic solenoid system are normally the coil winding current and plunger position. If the system is moved by δ_x then it can be shown that the work done is equal to the change in co-energy of the system. Then, the electromagnetic force F is given as the partial derivative of the magnetic co-energy:

$$F = \frac{\partial W'_m}{\partial x} \tag{11}$$

If the magnetizing characteristic is linear (no saturation) then the magnetic stored energy is equal to magnetic co-energy. Assuming a linear system, where the self-inductance L is constant and $L_i = \lambda$, the magnetic co-energy is derived as:

$$W'_m = \int_0^i Lidi = \frac{1}{2} Li^2 \tag{12}$$

Substituting (8) into (10) yields:

$$F = \frac{\partial L}{\partial x} \frac{i^2}{2} = \frac{L_0}{h} \frac{i^2}{2} \tag{13}$$

The next expression for magnetic force is based on flux density in the air-gap and is well-known as Maxwell stress equation where:

$$F = \frac{B_0^2}{2\mu_0} S \tag{14}$$

S – is defined as the air-gap area and B_0 is nominal flux density. In this electromechanical system the nonlinear characteristic of the material properties are used.

IV. Control circuit model

The control circuit model was created in power electronic and electrical circuit simulation software CASPOC. The full controlled four quadrant inverter is modeled here. Its parameters and values for output signal are described in TABLE 1.

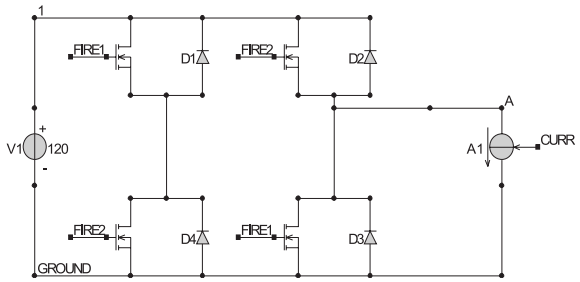

Fig. 8: Single phase full bridge controlled inverter implemented in power electronic circuit simulator.

Inverter parameters and output voltage waveform Table 1

Switching frequency	50 Hz
Input DC voltage	120V
Output voltage	120V
Power	200W
Current	1.2A

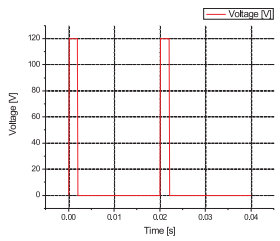

The electric circuit simulator also summarizes the finite element analysis results for value of inductance, power losses, eddy currents and forces and draws their waveforms in scopes. For co-simulation the pre-defined function FROMLF (for receiving data – from open interface) and TOLF (for sending data – to open interface) was used. The block scheme implemented in the power electronic circuit simulator of a single phase full controlled bridge inverter is shown in Fig. 8. This block diagram was prepared for co-simulation (there are co-simulation blocks and all the received data are visualized in the scope). All the received data was also used as an open interface in inverter simulation.

V. Finite element model

Magnetic circuit was created in finite element software ANSYS. There the mechanical and magnetic parts of solenoid were modeled together. Basic dimensions of model and material properties were described.

Basic input dimensions for finite element model Table 2

Model width	15 mm
Model height	35 mm
Material types (nonlinear material properties – BH curves)	Air, Coil, Two ferromagnetic materials
Plunger movement	2.95 mm
Spring constant	1.065e3
Fill factor	0.658
Number of turns	1750
Spring damping	0.05

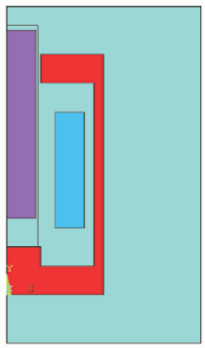

Outputs of this simulation are parameters for impedances, position, power losses, eddy currents and other requested results. These are, e.g., the waveforms for electromagnetic vector potential and magnetic flux density. The basic model dimensions are shown in TABLE 2.

In the finite element model a parameter value is computed and it is used via the open interface in the electric model simula-

Co-simulation possibilities Table 3

Type number	Realization	Description
1st type	One value data exchange without dynamic co-simulation and without saturation effects of electro-magnetic circuit	Exchange of only one value for inductance, Force and Back-EMF from the finite element model. No dynamic interaction between simulation programs.
2nd type	Table data ex-change without dynamic co-simulation, but including saturation effects of the electromagnetic circuit	In this type the data table is used as input into simulation programs. These tables include; for finite element model – values for position and coil current; for power electronics – values for inductances, voltage back-EMF and force.
3rd type	Full dynamic co-simulation considering saturation effects of electromagnetic circuit and transient eddy currents	This simulation is based on full data exchange during simulation. All output values of magnetic and electric circuit simulation are written in the graphs. In this co-simulation finite element model and control power electronic circuit simulator are mutually influenced during computation.

tion (Fig. 8). The electric control circuit computes the input voltage value for the finite element model and also exchanges them via the open interface. These values are used in the next step for each interconnected program. On this basic principle, a loop for co-simulation was created.

VI. Possibilities of co-simulation

For computation, the FEM (finite element method magnetic circuit simulation) and power electronics circuit simulation software are used. In this paper we compare the results for the three different types of co-simulation (TABLE 3 and TABLE 4). The goal is to compare the difference between output values for coil current, inductance, force, air-gap for the mentioned three co-simulation possibilities. They are described below.

VII. 1st Co-simulation type

The basis of this simulation is a simple calculation for one plunger position in the FEM software. For a constant coil current value, from FEM the inductance, force and back-EMF constant (induced voltage) can be obtained. The finite element model provides only one static value for these variables. For one plunger position in FEM the static magnetic vector potential or magnetic flux density can be presented.

The obtained results are used as inputs for power electronic circuit simulation program. The block diagram of this simulation type is shown in Fig.3. The plunger model is presented as output load on inverter DC link and is modeled by a mechanical system, where the plunger can move in one direction. This output load consists of a coil (FEM value of inductance), resistor (FEM value of resistance) and source of EMF (FEM value of induced voltage constant multiplied by plunger speed). From this simulation the waveforms for coil current, forces, and position can be drawn.

VIII. 2nd Co-simulation type

The block diagram of this simulation type is shown in Fig.4. For this co-simulation type the input and output values for inductance, back-EMF and force are in the data table form. The control circuit calculates an initial variable data table for different plunger position, voltage and coil current. This initial variable data table is converted into the finite element software script. This table is written cross the *DIM (defines an array parameter and its dimensions) commands for computation of macro (*DO control for loop computation). In the finite element program these values of voltage and plunger position are read and the FEM program calculates the data table for inductance, back-EMF and force that are needed in its circuit simulation. This data table is written into a text file in column form. The next step is to create the waveform for these values in different software for comparison. Finite element output data can be used in the other control circuit calculation for variable value of inductance and coil current. In these first two co-simulation types only static computing was used in FEM analysis. These programs work separately all the time. These analyses are without dynamic co-simulation and only the second type consid-

Simulation types used in power electronic circuit simulator and finite element analysis Table 4

Type number	Power electronic simulation type	Finite element method simulation type
1st type	Dynamic calculation – In the control circuit the data table, which is used for finite element model static computing is created. After finishing the FEM analysis, the parameters calculated in FEM are used in the transient power electronic simulation.	Static calculation - only one static value computation. For the next step, the model parameters are adjusted based on control circuit data table manually by user.
2nd type	Dynamic calculation – In the control circuit the data table, which is used for finite element model in the static loop computing is created. After finishing the FEM analysis, the table with parameters from the FEM calculation is used in the transient power electronics simulation.	Static calculation together with data loop - based on results of control circuit simulation. A data table is created to model the inputs for the *DIM areas. These are used for changing the model parameters in the *DO loop. The control circuit generates the data table which is used as input for finite element model. Based on this table the finite element model is reconfigured auto-matically and the results are calculated for each position listed in the table.
3rd type	Dynamic calculation - The Power electronic simulator starts the co-simulation. In the first step it computes and sends data for the driving voltage. This data is sent to the FEM program and the simulator waits for the next step. The next step is realized after recalculation of the magnetic circuit in FEM. The whole process is repeated in a loop. After reaching the final simulation end time, the co-simulation process is terminated	Dynamic calculation - in this case the full transients in the magnetic circuit are modeled. The forward movement of the plunger is caused by electro-magnetic force. The backwards movement is caused by a mechanical spring (in the FEM model realized by a spring constant and spring damping) The input value for the driving voltage is obtained from the power electronic circuit simulation. The considered simulation results are values for magnetic vector potential, magnetic intensity, inductance, forces, coil current, speed and back-EMF.

ers saturation of the electromagnetic circuit. Eddy currents are not considered in the first and second type of co-simulation.

IX. 3rd Co-simulation type

This co-simulation is based on full data exchange during simulation. The block diagram of this simulation type is shown in Fig. 5. All the data is exchanged between both programs at each time step in the simulation. The Power electronic simulation software continuously reads this data and in the same time computes the next voltage and position value for FEM software. The results are drawn into the oscilloscopes.

The interconnection between programs is realized inside power electronic and FEM software. In the power electronic software are the co-simulation blocks for data reading and writing (TOLF and FROMFL). The program creates for this purpose two different data sets. The first set for reading FEM results data and the second for writing the output voltage value for finite element software. The name of these datasets, co-simulation time and number of sub-steps can be set in power electronic software. In FEM analysis these data sets are used, where the first data set is used for data writing and second data set for input voltage reading. In this case the co-simulation includes the saturation of magnetic circuit and influence of eddy currents. During the saturation of magnetic circuit there are no changes for the material properties in this simulation set up. These properties are assigned with the assistance of BH curve. There are changes only in current values and inductance.

After finishing the co-simulation the waveforms for all the computed variable values are shown in graphs (Fig. 9 and 10). Transient FEM results are given as animations, variable data table and nonlinear model characteristics are given for magnetic vector potential and magnetic flux density. Some of the results are shown in the next section.

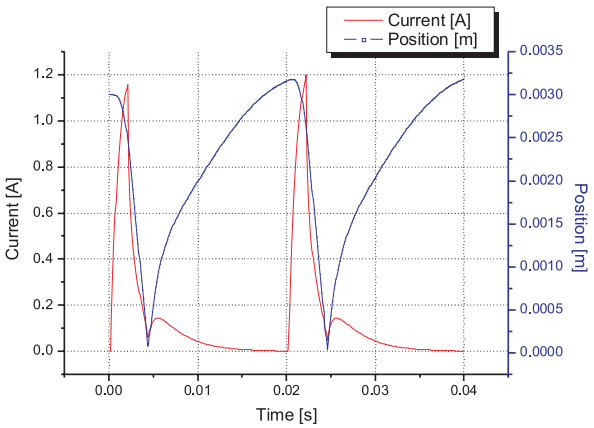

Fig. 9: Dynamic co-simulation results for air-gap and current waveforms (full dynamic co-simulation).

X. Comparison of the results

Different criterions for comparison of these three co-simulation methods are used. The first criterion is for time and hardware requirements. The first method uses not many system requirements, but if we need more results for different plunger position the user must change parameters before the next computation manually. The second method uses a variable data table. The computation is realized for many positions in one step, but not in the real interaction between programs. Control circuit computation is not time consuming, but the finite element calculation takes a long time and is dependent on the variable data table.

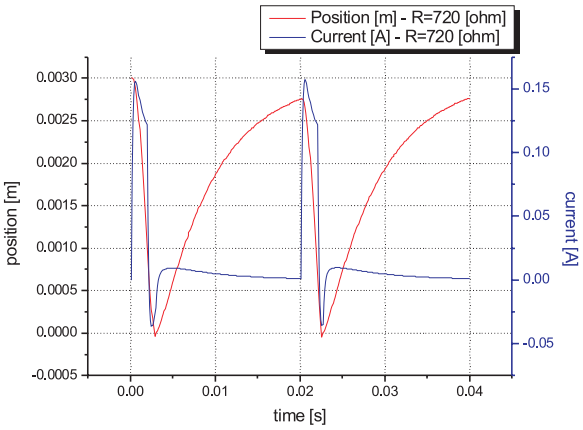

Fig. 10: Power electronic simulator results for air-gap and current (bases for this calculation is variable data table which was computed in static finite element analysis).

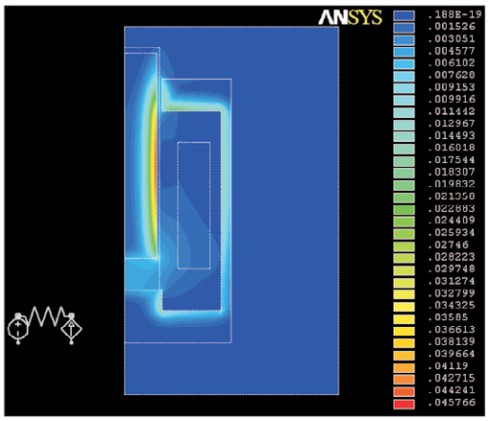

Fig. 11: Magnetic flux density at the maximum air gap (lg = 0.3).

The last co-simulation method is comparable with the second method with respect to the computing time (electric and magnetic model needed the same time for computing), but the results are different due to simplification made in the first two models (Figs. 3 and 4).

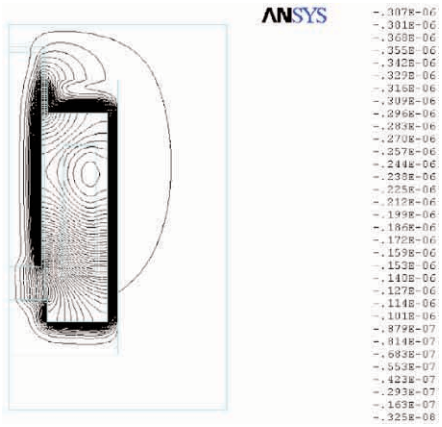

Fig. 12: Magnetic vector potential for maximum air gap (lg = 0.3).

The next criterion is the comparison of the acquired results. We can compare values of inductance, coil current, plunger position and forces. Values of these variables can be written in one graph. The output waveforms for current and position are shown in Figs. 9, 10, 13 and 14.

In Fig. 9 the full dynamic co-simulation results are presented (full cooperation between FEM analysis and power electronic simulation). The coil current (red) and plunger position (blue) are compared there. After starting the co-simulation, the coil current increases as long as there is a driving voltage. At the same time the plunger starts its movement to the zero position. After removing the driving voltage, the current decreases as long as the plunger position is zero. After reaching the zero position and sufficient current drop the backward movement is started. (Spring force is higher than electromagnetic force). Continuously, there is a small peak in the current waveform. It's the effect of induced voltage (back-EMF) and eddy currents. After this state the current is progressively decreasing to zero and air-gap is increasing to maximal position. In Fig. 10 are the same waveforms (red – plunger position, blue – coil current) for 2nd type of co-simulation.

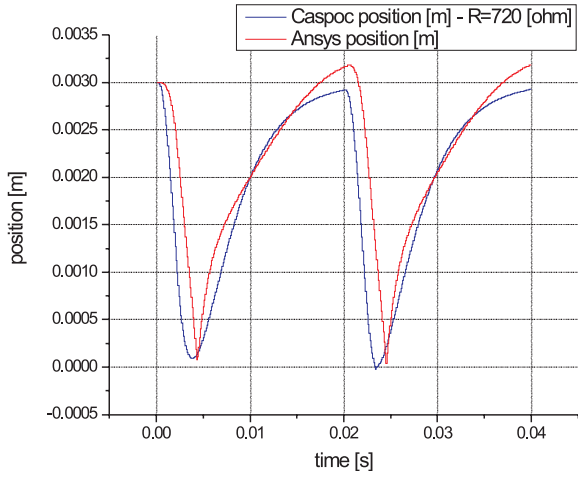

Fig. 13: Comparison of air-gap waveforms for two periods.

Figs. 11, 12, 15 and 16 show value for magnetic vector potential and magnetic flux densities during co-simulation for the maximum and minimum values of air-gap. The results of co-simulation are values for storage magnetic energy and co-energy, inductance, power losses, eddy current and coil current. These results were summarized during co-simulation in power electronic software. Their waveforms are presented in the figures below.

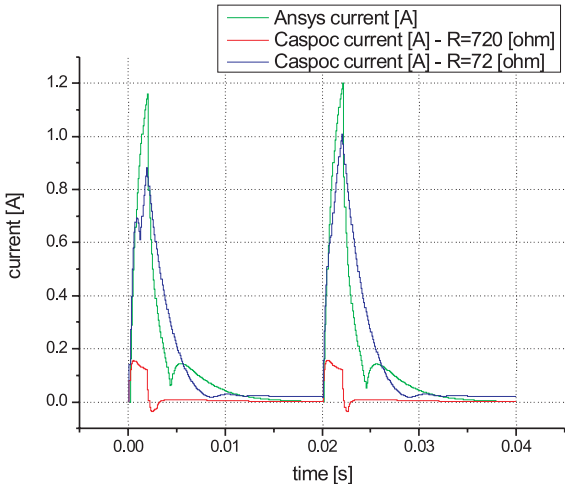

Fig. 14: Comparison of current waveforms for two periods.

In Figs. 13 and 14 is comparison between 2nd and 3rd co-simulation type in position and current. Fig. 13 shows the confrontation between plunger positions (noted as Ansys position – 3rd co-simulation type, noted as Caspoc position – 2nd co-simulation type). The basic difference is in velocity of air-gap reduction and in backward movement; where the third co-simulation result is above the maximum air-gap and the results from second co-simulation are bellow the maximum air-gap. In Fig. 14 the comparison between currents waveforms are presented (Ansys current – 3rd co-simulation type, Caspoc current – 2nd co-simulation type with different model resistance).

The current increases until the input voltage is connected. After removing the driving voltage the current value decreases until the plunger position is equal to zero. When the plunger starts the backwards movement, the current rises a bit. After this situation, the current decreases to zero continuously.

XI. Experimental validation

In measurement the solenoid current waveforms for different size of duty cycle were obtained (Fig. 19). In these current waveforms it is possible to see the effect of the local current minimum. It is the result of mechanical movement of an inductor through a magnetic field. This phenomenon has very important diagnostic implications. Usually the circuit will have about 20 percent to 40 percent more current than is necessary to pull in the coil so it is possible to see about 2/3 to 3/4 of the way up the ramp. The size

and distinction are directly related to the amount of movement. The actual mechanical movement in the fuel injector takes place in about 0,5 millisecond.

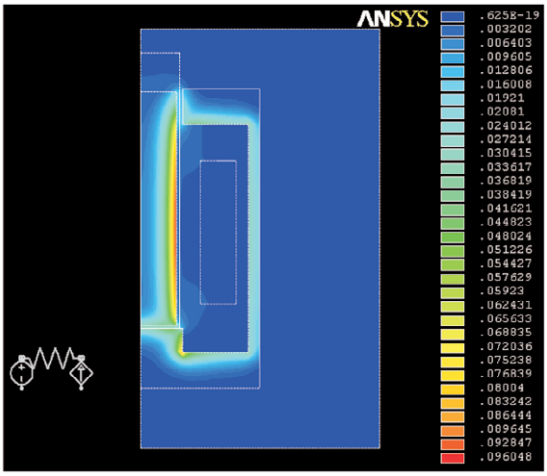

Fig. 15. Magnetic flux density at the minimum air gap (lg = 0).

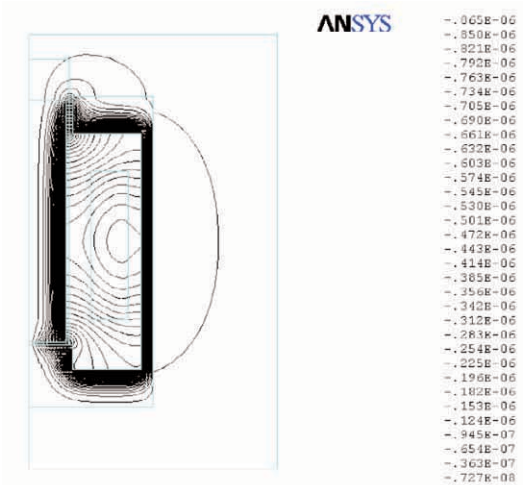

Fig. 16. Magnetic vector potential and magnetic flux density at the minimum air gap (lg = 0).

To better illustrate this phenomenon, it is possible to use a simple relay. A relay coil has a multitude of windings that electrons must pass through before completing a circuit. Magnetic lines of force are created around the conductor. The lines cut across the adjacent windings causing their electrons to move in opposition to the main flow. This is called back-EMF or Counter Electromotive Force (CEMF).

When an inductor is placed in the core of a coil, the magnetic lines of force are attracted to the inductor; as current flows, they concentrate on it causing more CEMF and slow current build-up in the coil. Then as the magnetic field builds enough strength to pull in the inductor, a fluctuation occurs causing the current flow to lessen momentarily as the inductor moves through its travel to a stop. After that it is possible to see the decreasing of current which is in literature presented as a Gull Effect. After saturation of the coil, the current will gradually reach the peak.

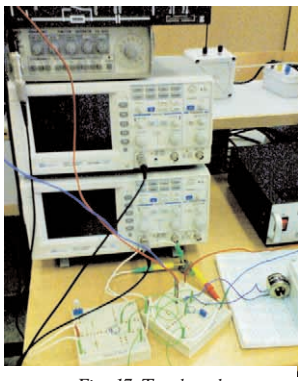

Fig. 17. Test bench

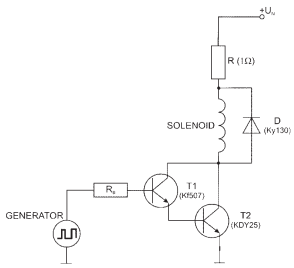

Fig. 18. Basic circuit for solenoid current measurement

In Fig. 18 a simple electronic circuit for solenoid current measurement is presented. The current is calculated with Ohm's law from measured voltage on a precise resistor R. The solenoid voltage was 90V and maximum current value was 136 mA.

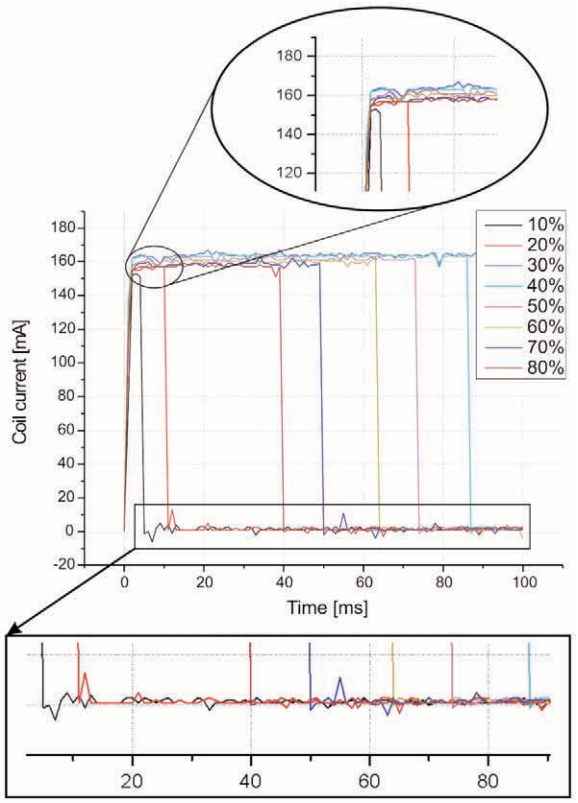

Fig. 19. Comparison of current waveforms for one period and different duty cycle

Fig. 19 shows the solenoid current reading consistently throughout its range up to 80 percent duty cycle along with the voltage signals. At 100 percent duty cycle there would be a 100ms pulse. In presented waveforms it is possible to see the gull effect in the beginning. After finish of voltage pulse the current is decreasing. Near the zero value the current increases a little bit and after that it drops to zero.

XII. Conclusions

A full dynamic co-simulation for an electromechanical system in power electronic circuit simulator and finite element analysis is presented in this paper. In the FEM program ANSYS the magnetic part of solenoid model was computed. In power electronic simulator CASPOC the control circuit values were calculated. The two programs exchange data during the co-simulation and exact values and dynamical simulation are achieved. Both subsystems (electrical and electromechanical) are simulated in full detail. Such a co-simulation allows achieving more precise simulation results and, which is most important; it can include the transient behavior in the magnetic material such as eddy currents. Finally, the output values for current and position were compared and the measurement of a real solenoid current waveform was presented.

References

[1] ANSYS 9.0, www.ansys.com

[2] Caspoc 2005, www.caspoc.com

[3] CHIBA, A., FUKAO, T., ICHIKAVA, O., OSHIMA, M., DORRELL, G. D.: *Magnetic Bearings and Bearingless Drives*, an print of Elsevier, ISBN 07506557278

[4] REEVE, J. M., POLLOCK, C.: *Dynamic simulation model for two-phase mutually coupled reluctance machines, Industry Applications Conference,* 2001. Thirty-Sixth IAS Annual Meeting. Conference Record of the 2001 IEEE,Volume 1, 30 Sept.-4 Oct. 2001, pp. 40–47, vol. 1, Digital Object Identifier 10.1109/IAS.2001.955390

[5] SUN, H.; LU, P.; ZHANG, P.; CHEN, H.: *Dynamic analysis of AT-cut quartz resonators with ANSYS, Sensors,* 2004. Proceedings of IEEE, 24-27 Oct. 2004, pp. 95–98, vol. 1, Digital Object Identifier 10.1109/ICSENS.2004.1426108

[6] SUN, H.; LU, P.; ZHANG, P.; CHEN, H.: *3D ANSYS quench simulation of cosine theta Nb/sub 3/Sn high field dipole magnets*, *Applied Superconductivity,* IEEE Transactions on, 2/2004, pp. 291–294, Digital Object Identifier 10.1109/TASC.2004.829088

[7] ZHIQIANG MENG; ZHONGDONG WANG.: The analysis of mechanical strength of HV winding using finite element method. Part I Calculation of electromagnetic forces, Universities Power Engineering Conference, 2004. UPEC 2004. 39th International,.Vol. 1, 6-8 Sept. 2004, pp. 170–174

[8] SITAR, J., BAUER, P.: *Detailed analysis of Electronics for Solenoid Actuator with FEM and Circuit Simulator,* Power Electronic Intelligent Motion Power Quality, May 30 - June 1, 2006, Nurenberg, Germany, pp. 124–135.

[9] MAGA, D., HARTANSKY, R.: *Numerical solution,* 1. issue, Brno, University of defense, 2006, p. 174 – ISBN 80-7231-130-1.

Péter Korondi – Péter Zsíros – Fetah Kolonic *

HUMANOID TYPE HAND MOVED BY SHAPE MEMORY ALLOY

The main contribution of this paper is a practical application of generalised neural networks for a dextrous hand moved by Shape Memory Alloys (SMA). Since SMA have highly non-linear characteristics and their parameters depend on the environment (mainly on temperature) so the robot hand is controlled by a generalised neural network, which can learn the actual non-linear characteristics of the robot hand. The experimental setup consists of a 20 degree of freedom hand moved by SMA string used as artificial muscle. A video camera is used to detect the position of joints. The position is then sent to the visual display computer via the Internet, which displays the hand in 3D using OpenGl.

1. Introduction

Telemanipulation present an process where the operator has some task done at the far environment where he/she cannot be present physically. Goertz developed the first modern master-slave system teleoperator at Argonne National Laboratory in 1945. Telemanipulation is divided into two strongly coupled processes. One process is the interaction between the operator and the master device, the other is the interaction between the slave device and the far environment contact. The master device represents the far environment at the operator site, and the slave device represents the operator at the remote site. The information flow between the operator and remote site can be seen in Fig. 1, where only three types of information are fed back: visual, audio and sense of touch. Human beings get six types of sensing from the environment surrounding them but only some of these sensings are used during telemanipulation.

Telemanipulation is the extension of human manipulation to a remote location. By providing appropriate feedback, the telemanipulation can be well utilised in dangerous or otherwise unreachable environment. Human operators perform their tasks mostly by hand, so the master and slave devices must fit the operator's hand. In the field of telemanipulation, many haptic devices have been developed.

The glove type master device allows the most complex and dextrous manipulation. The human hand is the most widely used tool. The final goal is to make a device with which the operator can feel as if the function of his whole hand would expanded. There are several commercial sensor gloves without force feedback on the market. The paper [7] proposed a sensor glove with force feedback to the all 20 joints of the operator's hand. If the human hand is covered with these commercial devices, some certain difficult tasks can be done at the remote site, but commercial hand type slave devices are not available. This paper proposes a hand type slave device for precise telemanipulation. Until this point no force feedback has been implemented in this system, thus the actual set up is more simplified than the general one in Fig. 1. The system used is shown in Fig. 2.

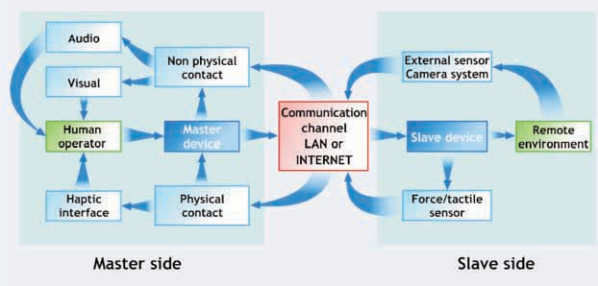

Fig. 1 Information streams of the Telemanipulation

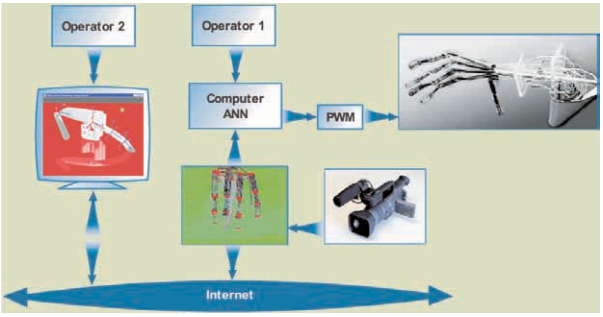

Fig. 2 Data flow of the proposed system

2. The artificial hand description

The hand is primarily used for manipulating activities requiring very fine movement incorporating a wide variety of hand and finger postures. Consequently, there is interplay between the wrist joint positions and efficiency of finger actions. The hand region

* **Péter Korondi[1], Péter Zsíros[1], Fetah Kolonic[2]**
[1]Deptartment of Automation and Applied Informatics Budapest University of Technology and Economics, P.O.Box 91, H-1521, Budapest, Hungary, E-mail: korondi@elektro.get.bme.hu
[2]Faculty of Electrical Engineering and Computing, University of Zagreb, Unska 3, HR-10000 Zagreb, Croatia, fetah.kolonic@fer.hr

has many stable, yet very mobile segments, with very complex muscle and joint actions.

A robotic hand is made similar to the human hand, theoretically it can realise all the twenty freedoms of movement, but this time only eight of them are used. We do not want to control the movement of the most upper knuckle (DIP – Distal Interphalangeal Predominant (arthritis)) separately, because that movement can not be well controlled on a human hand either. Only the upper knuckle is pulled, and across the rubber it will pull up the middle knuckle too. The structure of the hand is shown in Fig. 3.

Fig. 3 Photo of the artificial hand

3. Generalised neural network

A generalised neural network is used to control the hand. The difference between a classical and a generalised neuron is that real numbers are used for the weights of a classical neuron, but the weights are fuzzy functions in the case of generalised neurons. A simple neuron is shown in Fig. 4 and a multi-layer generalised neural network will be discussed in Fig 8.

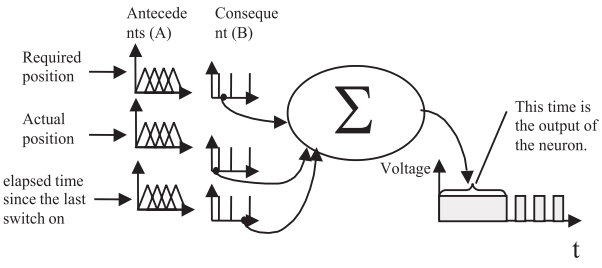

Fig. 4 Neuron model

For each input of a neuron there is a *B* set, which can be fired by an antecedent set *A*. Each antecedent set corresponds to a consequent set *B*, which is a singleton set in our case, as shown in Fig. 5. If input X_0 arrives to the input *X* of the system, it will cut two or more antecedents (depending on the type of antecedent function, triangular sets are assumed here). The *B* values belonging to the antecedents are weighed and the mass point is then calculated.

The value of the mass-point will go into the summation part of the neuron, see in Fig 4. The system can be trained by changing the consequent sets (i.e. B values).

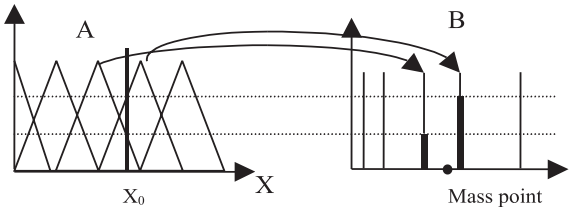

Fig. 5 Calculation of the neurons weight

If we draw the antecedent *A* and the consequent *B* values to the two axes of a co-ordinate system, it will be clearer what is happening. Most functions (which are interesting for engineers) can be approximated by fuzzy functions. The positions of antecedent sets determine the sampling points of the approximated function. The *B* values are the sampled values. The shapes of the antecedent membership functions determine the characteristics of the interpolation between the sampling points. If the triangles as antecedent sets are used, then the approximation will be piecewise linear, as shown in Fig. 6.

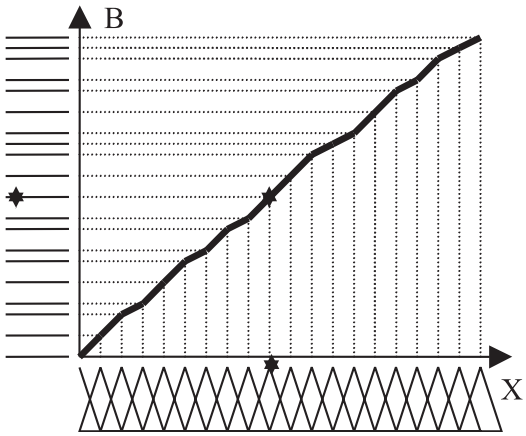

Fig. 6 Approximation of a function by the antecedent and consequent sets

So while in the case of normal neural networks there is the same non-linear function for all the inputs, in the case of this generalised neural network there are different non-linear functions for all inputs. Also by changing the B values one can easily modify these non-linear functions. From the mathematical point of view, the original neuron gives a *non-linear function of* the *linear combination* of its inputs. The generalised neuron gives the *linear com-*

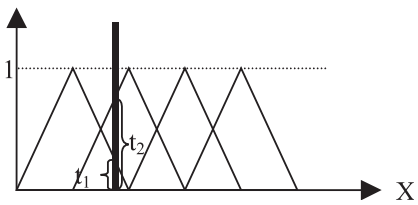

Fig. 7 Ruspini partition

bination of the *non- linear functions* of its inputs. The antecedents of the neurons are triangular functions, because they require the least computation. The antecedents are forming Ruspini partition, which means that the sum of the membership values at any X is equal to 1. This partition is shown in Fig. 7.

$t_1 + t_2 = 1$ at any X.

4. Training of the generalised neural network

A generalised neural network is shown in Fig. 8. Using the notation introduced in this figure, the outputs of the neural network can be calculated in the following way:

$$Y_j = \sum_i \sum_t A_{i,t}^{(2)}(X_i) \cdot B_{i,j,t}^{(2)}, \tag{1}$$

where X_i is the output i-th neuron of the 1-st layer, $A_{i,t}^{(2)}$ is the t-th antecedent of i-th input in the second layer. Each antecedent set corresponds to all neurons. $B_{i,j,t}^{(2)}$ is the consequent set of the j-th neuron fired by $A_{i,t}^{(2)}$.

The output Y_i is calculated as

$$Y_i = \sum_k \sum_t A_{k,t}^{(2)}(P_k) \cdot B_{k,i,t}^{(2)}, \tag{2}$$

where k is the number of inputs, t is the number of antecedents, P_k is the k-th input.

The question is how to modify the $B_{k,i,t}$ -th weight, if the error is h?

$$\frac{\partial h^2}{\partial B_{k,i,t}} = ? \tag{3}$$

The error can not be derived directly according to $B_{k,i,t}$, and therefore the chain rule has to be used as in the back propagation algorithm. The error h can be derived according to the output Y, the output can be derived according to the input X, and finally the input can be derived according to the required B. Then, h^2 can be calculated as:

$$\frac{\partial h^2}{\partial B_{k,i,t}} = \sum_j \frac{\partial h^2}{\partial Y_j} \cdot \frac{\partial Y_j}{\partial X_i} \cdot \frac{\partial X_i}{\partial B_{k,i,t}} =$$

$$= \frac{\partial (h_1^2 + h_2^2 + ... + h_n^2)}{\partial Y_j} \cdot \frac{\partial Y_j}{\partial X_i} \cdot \frac{\partial X_i}{\partial B_{k,i,t}} \tag{4}$$

$$\frac{\partial h_j^2}{\partial Y_j} = \frac{\partial (d_j - Y_j)^2}{\partial Y_j} = -2 \cdot (d_j - Y_j) = -2 \cdot h_j \tag{5}$$

$$\frac{\partial Y_j}{\partial X_i} = \frac{\partial \left(\sum_i \sum_t A_{i,t}(X_i) \cdot B_{i,j,t} \right)}{\partial X_i} = \sum_t A_{i,t}^{\prime(1)}(X_i) \cdot B_{i,j,t} \tag{6}$$

$$\frac{\partial X_i}{\partial B_{k,i,t}} = \frac{\partial \left(\sum_k \sum_t A_{k,t}^{(2)}(P_k) \cdot B_{k,i,t} \right)}{\partial B_{k,i,t}} = A_{k,t}^{(2)}(P_k) \tag{7}$$

$$\frac{\partial h^2}{\partial B_{k,i,t}} = \sum_j \left[-2 \cdot h_j \cdot \left(\sum_t A_{i,t}^{\prime(2)}(Xi) \cdot B_{i,j,t} \right) \right] \cdot A_{k,t}^{(1)}(P_k) \tag{8}$$

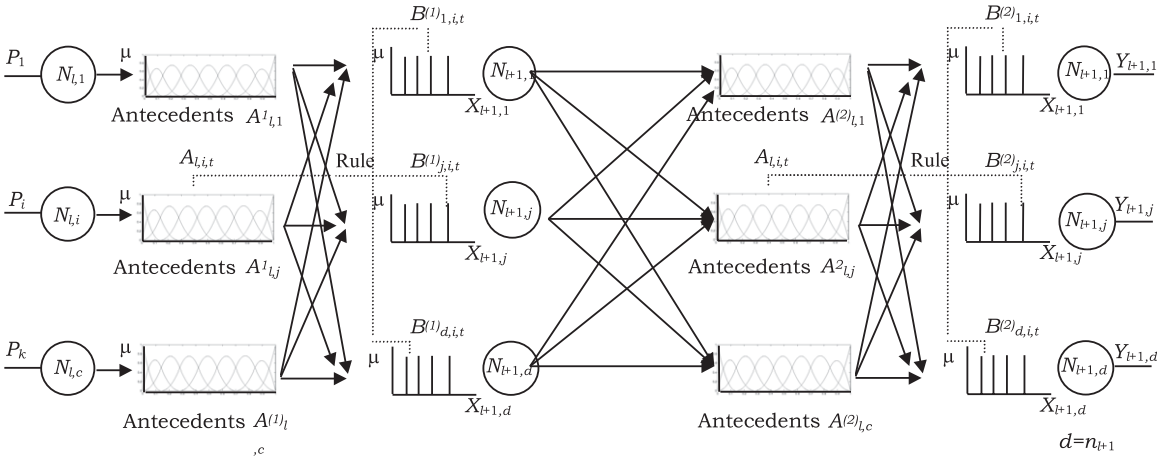

Fig. 8 The generalised neural network

In general, if the errors in the layer n are $h_j^{(n)}$, then the error of the neurons in layer $n-1$ can be calculated in the following way:

$$h_i^{(n-1)} = \sum_j h_j^{(n)} \cdot \left(\sum_t A_{i,t}^{\prime(n)}(X_t) \cdot B_{i,j,t}^{(n)} \right). \tag{9}$$

The weight modification is given as:

$$B_{i,j,t}^{(n)new} = B_{i,j,t}^{(n)old} + 2 \cdot p \cdot h_j^{(n)} \cdot A_{i,j}^{(n)}(X_i). \tag{10}$$

5. Control of the hand

Pulse width modulation is applied to control the movement of the hand. Two different duty rations are used, one to move a certain part of the hand and one to hold it at a certain position (see Fig. 9 and 10). When the operator changes the reference position, the

neural network calculates how long the voltage should be switched across the wire to move a finger into the new reference point as shown in Figs. 9 and 10. Since the condition (mainly the temperature) of the environment has a great influence on the characteristic of SMA wires, the neural network must be retuned continuously.

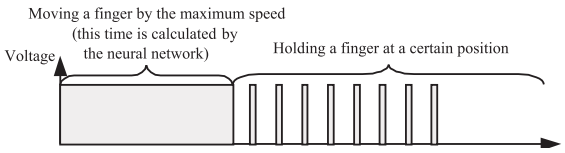

Fig. 9 Moving a finger with maximum speed

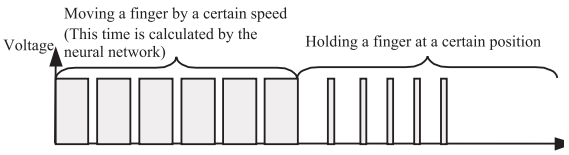

Fig. 10 Moving a finger with less than the maximal speed

The experimental results show good repeatability performance, where desired finger tip angle control is achieved in region from 10 to 90 degrees, Fig. 11

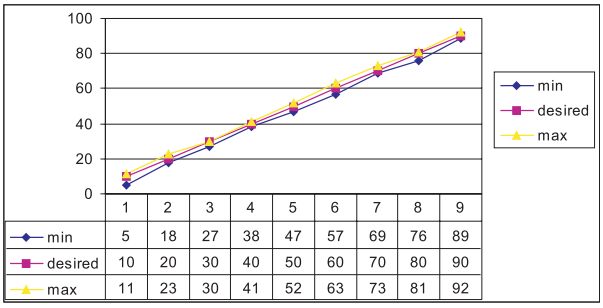

	1	2	3	4	5	6	7	8	9
min	5	18	27	38	47	57	69	76	89
desired	10	20	30	40	50	60	70	80	90
max	11	23	30	41	52	63	73	81	92

Fig. 11 Experimental results (The desired angle is changing from 10 to 20 degree. The measurement is carried out 10 times. The minimal and maximal measured angles are shown)

6. Complexity reduction of the generalized algorithm

One of the main problems of applying fuzzy or neural techniques is calculation complexity. Engineers have to face this problem in complex systems or especially in the field of information retrieval, where extremely large information maps of whole libraries or Internet have to be processed at each user's request. These applications apply the generalized type neural networks. Let us have a brief introduction to the results of complexity theorem.

Lemma 1. *The calculation complexity grows proportionally with the number of parallel layers and the neurons.*

Omitting the computational effort of added operation but considering the product operation, the computational requirement is characterised as:

$$P_c = \sum_{i=1}^{n_l} m_{i,j} \cdot n_{l+1} + P_\mu . \tag{11}$$

P_μ indicates the calculation of the membership functions:

$$P_\mu = s \sum_{i=1}^{n_l} m_{i,j} , \tag{12}$$

where s indicates the calculation of one membership value of one antecedent set.

The main objectives of this section are to propose an algorithm that is capable of filtering out common linear combinations and reducing the number of antecedent sets based on the transformation of the weighting functions. One of the main advantages of the proposed method is that the effectiveness of the compression is controlled by the help of a given error threshold.

Theorem 2. *Equation (4) can always be transformed into the following form:*

$$y_{l+1,j} = \sum_{z=1}^{n^r_{l+1}} a_{l,j,z} \sum_{i=1}^{n_l} \sum_{t=1}^{m^r_{l,i}} \mu_{A^r_{l,i,t}}(y_{l,i}) b^r_{l,z,i,t} , \tag{13}$$

where "r" denotes "reduced", further $n^r_{l+1} \le n_{l+1}$ *and* $\forall i : m^r_{l,i} \le m_{l,i}$.

The reduced form is represented as neural network in Fig 12. The further proofs of this technique are discussed in [9, 10].

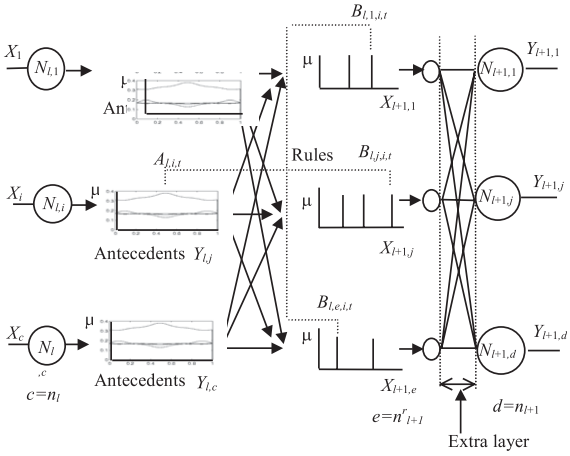

Fig. 12 Reduced neural network

7. Feedback

For finding the joints in the picture of the camera by the computer, the joints were painted red. This colour is chosen because out of the three primary colours (red, green, blue), red colour is the most characteristic.

Unfortunately, the hand is made of copper, which has a quite high red colour content too so the hand had to be painted green. Green has been chosen, because this is another primary colour, and it is used in movie techniques (in spite of the name of the technique, which is blue box, the blue colour had been used only until about 10 years ago, when it was changed to green, because that has better characteristics for cameras). Because there are a lot of red objects in the laboratory so a full green box around the hand is used. We use a Sony Handycam with a Genius Video Wonder II TV card. The computer is a Pentium-166 with 40 Mbyte RAM and with Windows 98 operating system. This is because the programming of the TV card is quite easy under windows, there are drivers for it from the producer, and we simply have to use the routines provided by them. The program is written in Borland Delphi 4. The video-capturing program (eac401) was downloaded from the Internet ("Delphi Superpage"), and modified it to fit the requirements.

The size of the picture is chosen to be 160 times 120 points, because this is the smallest standard size. Even in this case the required computation power can be quite high. In this program different camera options can be set, for example brightness, contrast or saturation. By adjusting these options we could get much better pictures. The phases of the correction of the picture are shown in Figs. 15–18.

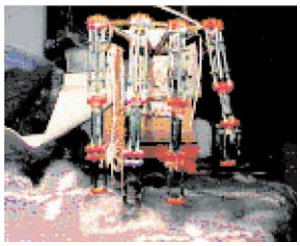

Fig. 13 The normal video picture

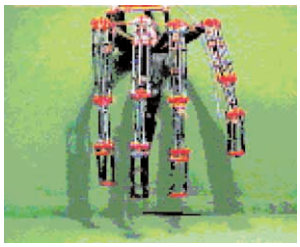

Fig. 14 The picture when the green box is used

Fig. 15 The picture after decreasing the contrast from 128 to 10

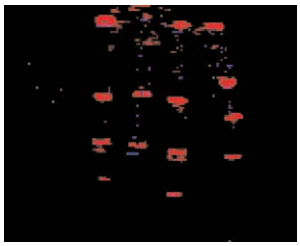

Fig. 16 The picture after decreasing the brightness from 128 to 16

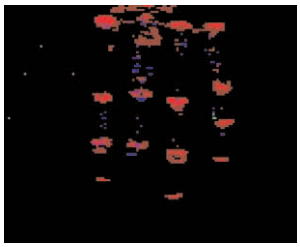

Fig. 17 The picture after increasing the saturation from 128 to 255

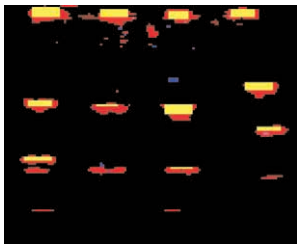

Fig. 18 The picture after the enlargement and recognition of joints

8. Visual interface

The software was developed to give visual feedback of a general hand in telemanipulation. Visual feedback is aimed at giving a quite real representation of the environment, and although at the moment this environment is far from complete, the program enables the user to wander in full three-dimensional space.

The program was designed to run either locally in full simulation mode or over TCP/IP connection, such as Internet or Local Area Network. In simulation mode, the program can be used to represent all the motions of the human hand. To accomplish it, both anatomical and mathematical models were built up, and these models were implemented in OpenGL (Open Graphics Language). The mathematical deduction uses the Denavit-Hartenberg notation, because it can be quite well applied both for hands and in OpenGL. The model uses several basic assumptions:

- The base coordinate frame is the same for all fingers. This is used for having a completely general case, where the fingertip coordinates are calculated with respect to a common frame, for instance to the wrist. This common frame is considered to be at joint 0. This joint is used in order to have the possibility to extend the model at a later time if needed.
- One finger contains three joints, the first has two degrees of freedom, and the other two have only one, which means a planar rotation. The position of the first joint is determined by a variable l_0, which is the distance between the first, common coordinate frame and the first joint.
- Along one finger, the value of d_i is 0, which means that the common normal line on the same line.
- Along one finger the value of a_i is the length of the link.
- The twist angle is taken into account only at the base coordinate frame and at the first joint, since lateral movement of the finger is also considered.

It is important that coordinate frame 0 is the same for all fingers, and is a common reference to the whole hand. The individual θ_i angles and l_0 variables determine the exact position and orientation of the next frame of the next joint in each finger. Between the two frames d_i is just equal to the length of the link, l_0. Since the joint 0 is of the revolute type, q_0 is θ_1 the relationship between the two joints is

$$X = A_1^0 X_1 . \tag{14}$$

In (14) A_1^0 is the 4 × 4-transformation matrix between the two adjacent joints and X^s are position vectors in the respective coordinate frames. Detailed form of (14) is shown in (15) and (16).

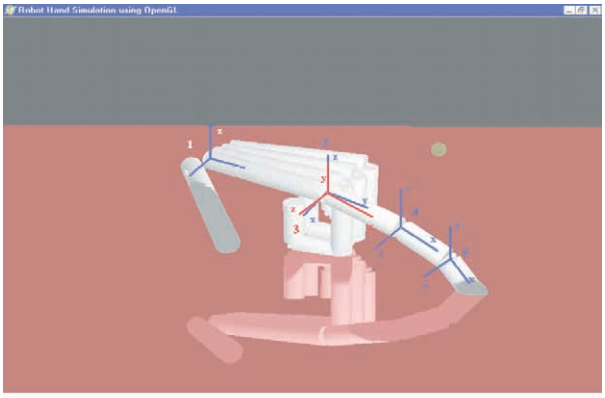

Fig. 19 Computer animation of the robot hand with the coordinate system

$$A_1^0 = \begin{bmatrix} cos\theta_1 & -sin\theta_1\, cos\alpha_1 & sin\theta_1\, sin\alpha_1 & a_0\, cos\theta_1 \\ sin\theta_1 & cos\theta_1\, cos\alpha_1 & -cos\theta_1\, cos\alpha_1 & a_0\, sin\theta_1 \\ 0 & sin\alpha_1 & sin\alpha_0 & d_0 \\ 0 & 0 & 0 & 1 \end{bmatrix} \quad (15)$$

$$\begin{bmatrix} x_0 \\ y_0 \\ z_0 \\ 1 \end{bmatrix} = \begin{bmatrix} cos\theta_1 & -sin\theta_1\, cos\alpha_1 & sin\theta_1\, sin\alpha_1 & a_0\, cos\theta_1 \\ sin\theta_1 & cos\theta_1\, cos\alpha_1 & -cos\theta_1\, cos\alpha_1 & a_0\, sin\theta_1 \\ 0 & sin\alpha_1 & sin\alpha_0 & d_0 \\ 0 & 0 & 0 & 1 \end{bmatrix} \begin{bmatrix} x_1 \\ y_1 \\ z_1 \\ 1 \end{bmatrix}. \quad (16)$$

As it was stated, in this case α is 0°, which means that its cosine is equal to 1 and its sine is 0. For the two joints d is taken to be 0 and a is the length of the link. Substituting these values simplifies the previous equation and yields to

$$\begin{bmatrix} x_0 \\ y_0 \\ z_0 \\ 1 \end{bmatrix} = \begin{bmatrix} cos\theta_1 & sin\theta_1 & 0 & l_0\, cos\theta_1 \\ sin\theta_1 & cos\theta_1 & 0 & l_0\, sin\theta_1 \\ 0 & 0 & 1 & 0 \\ 0 & 0 & 0 & 1 \end{bmatrix} \begin{bmatrix} x_1 \\ y_1 \\ z_1 \\ 1 \end{bmatrix}. \quad (17)$$

Now the position and the orientation of the coordinate frame at joint 1 is received, further transformations can be carried out.

Now, there is a general formula for calculating the position of the fingertip with reference to the common base coordinate frame. (5) shows this, and it is very similar to (14). Matrix T

$$T = A_1^0(q_1)\, A_2^1(q_2)\, A_3^2(q_3)\, A_4^3(q_4)\, A_5^4(q_5) \quad (18)$$

contains the position and orientation of the tip in the base coordinate system.

It is useful to state that joint 2 has two transformation matrices and frames because of the two possible axes of rotation

$$P_1 = T_1 \quad X^{15}, \quad (19)$$

where X^{15} is the position vector of the fingertip in its local co-ordinate frame.

The position and orientation of all the fingertips with respect to the common base frame (the wrist), is given by (20) as a function of joint angles

$$P = [f(\theta_{11}, \theta_{12}, \theta_{13}, \theta_{14}, \theta_{15}) f(\theta_{21}, \theta_{22}, \theta_{23}, \theta_{24}, \theta_{25}) \\ f(\theta_{31}, \theta_{32}, \theta_{33}, \theta_{34}, \theta_{35}) f(\theta_{41}, \theta_{42}, \theta_{43}, \theta_{44}, \theta_{45})]. \quad (20)$$

The computer-aided animation of the robot hand is shown in Fig. 19.

9. Conclusion

This paper demonstrates a dextrous hand as a slave device for telemanipulation. Using shape memory alloy (SMA) as an "artificial muscle", efficiently increases the degree of freedom, in robot mechanisms offering much more flexibility than widely adopted hands that are mostly driven by pneumatic or electric actuators. The SMA wires have much less weight and size than the conventionally used actuators. The construction is much simpler; also its price is comparable. However, applying SMA actuators leads to a very difficult control problem, as the feature of SMA is strongly non-linear. This paper demonstrated that generalised neural networks are promoting solutions for control problems caused by SMA actuators.

Acknowledgements

The authors wish to thank the National Science Research Fund (OTKA K62836), Control Research Group and János Bolyai Research Scholarship of Hungarian Academy of Science for their financial support and the support stemming from the Intergovernmental S & T Cooperation Program.

References

[1] ROJAS, R.: *Neural Networks, A Systematic Introduction*, Springer-Verlag, Berlin, 1996

[2] HORNIK, K., STINCHCOMBE, M., WHITE, H.: *Multi-layer Feedforward Networks are Universal Approximators*, Neural Networks 2., 1998, pp. 359–366

[3] BARANYI, P, YAM, Y., HASHIMOTO, H., KORONDI, P., MICHELBERGER, P.: *Approximation and Complexity Reduction of the Generalized Neural Network*, Submitted to IEEE Trans. on Fuzzy Systems, 2000
[4] BARANYI, P., KÓCZY, L. T., GEDEON, T. D.: *Improved Fuzzy and Neural Network Algorithms for word frequency Prediction in Document Filtering*, Journal of Advanced Computational Intelligence Vol. 2 No. 3, 1998, pp. 88–95
[5] MIZUMOTO M.: *Fuzzy Controls by Product-sum-gravity Method*, Advancement of Fuzzy Theory and Systems in China and Japan, Eds. Liu and Mizumoto, International Academic Publishers, c1.1-c1.4, 1990
[6] ZAM, Y., BARANYI, P., YANG, C. T.: *Reduction of Fuzzy Rule Base Via Singular Value Decomposition*, IEEE Trans. on Fuzzy Systems. Vol.: 7, No. 2, 2000, ISSN 1063-6706, pp. 120–131
[7] HASIMOTO, H., KORONDI, P, SZEMES, P. T.: *Human Interfaces for Telemanipulation*, Invited plenary paper for EPE-PEMC Conference, 2000, Kosice, Slovakia
[8] SHERIDAN, T. B.: *Telerobotics,* Automatica, Vol. 25, No. 4, 1989, pp. 487–507
[9] BARANYI, P., LEI, K. F., YAM, Y.: *Complexity Reduction of Singleton Based Neuro-fuzzy Algorithm,* IEEE Conference on Systems Man and Cybernetics (IEEE SMC'2000), submitted
[10] LEI, K. F., BARANYI, P., YAM, Y.: *Complexity Reduction of Non-singleton Based Neuro-fuzzy Algorithm,* IEEE Conference on Systems Man and Cybernetics (IEEE SMC'2000), submitted.

R. Filka – P. Balazovic – B. Dobrucky *

A SENSORLESS PM SYNCHRONOUS MOTOR DRIVE FOR ELECTRIC WASHERS

This paper presents a complex solution for whole speed range sensorless control of interior permanent magnet synchronous motor drives. To cover an entire speed range of IPMSM without position transducer, different sensorless techniques must be employed. Design and implementation of sensorless techniques for different operating speeds are described in this paper. Presented application has been implemented including the high frequency (hf) injection method and extended back EMF state observer on a single chip solution of DSC56F8300 series without any additional supportive circuitry. The extended back EMF algorithm with angular speed and position observer is suitable for sensorless control drive. It is also transferable for other motor types, e.g. synchronous reluctance- or synchronous one with 'smooth' rotor. The presented sensorless control has been proved in electric washer drive with very good operating properties.

I. Introduction

An important factor for using sensorless control in the drive applications is to optimize the total cost performance ratio of the overall drive cost. The systems should be less noisy, more efficient, smaller and lighter, more advanced in function and accurate in control with a low cost. To achieve efficient control of AC machines, knowledge of rotor position is essential. Different types of mechanical position transducers can be used to measure rotor position directly, but since solution with such transducer introduces additional cost alternative means of obtaining rotor position is highly desirable.

Sensorless control of AC machines has become a frequently discussed topic at engineering conferences. Many researchers and scientists have published papers on this topic but there are only a few articles that discuss complex implementation of the algorithms into a single application covering all operating conditions. Classical solution with six step commutation control (brushless DC motor) has several drawbacks; such as low efficiency, higher audible noise and lower developed torque when compared to sinusoidal control of PMSM. To increase efficiency of the drive, sinusoidal control is needed [1]. Here, all three phases of the inverter are constantly conducting current making observation of back-EMF zero crossing impossible. Therefore more complex sensorless algorithms must be employed.

Sensorless algorithms for sinusoidal control of AC machines can be broadly divided into two major groups; 1) those that utilize magnetic saliency for tracking rotor position [2]–[12] and 2) those that estimate rotor position from calculated motor model [8], [13]. The later, requires accurate knowledge of phase voltages and current for proper functionality. At low speeds, phase voltage reference and measured phase current are low, making it very difficult to separate from noise. Also distortion by inverter non-linearities and model parameter deviation becomes significant with decreasing speed. Therefore methods based on motor model are not suitable for low rotor speeds.

For start-up and low speeds, additional carrier signal superimposed to the main excitation is required. This carrier signal adds needed excitation to the motor at low and zero speed, and its back analysis can provide a viable means of obtaining information about rotor position. The carrier injection methods however, require a certain amount of saliency present in the motor [3]. In IPMSM this saliency results from inductance variation [1] as is explained later in the paper. On the other hand, at high speeds the amplitude of back EMF is big enough for motor model and angle tracking observer to work properly, therefore no additional signal is required. In fact, additional hf signal deteriorates tracking accuracy of the angle tracking observer. Therefore injection of hf signal is not desired for high speed operation. It is obvious that in order to achieve full speed range sensorless operation of IPMSM, both techniques have to be employed, each covering different operational speed ranges. This requires algorithm that will ensure seamless blending of the estimates throughout the entire speed range.

The proposed solution is based on field oriented control of IPMSM with implemented speed control loop. This includes inner current control loop with implemented decoupling of cross-coupled variables achieving good torque control performance. To maximize converter efficiency and minimize its rating, current loop is designed with maximum torque/ampere criteria [1].

* **R. Filka[1], P. Balazovic[1], B. Dobrucky[2]**
[1] Freescale Semiconductor, 1. Maje 1009, Roznov p. Radhostem, Czech Republic, Roman.Filka@freescale.com
[2] University of Zilina, Faculty of Electrical Engineering, Univerzitná 1, 010 26 Žilina, Slovakia

II. IPMSM Characterization

A. Motor Description

Mathematical model of IPM synchronous motor in synchronous reference frame is described as follows

$$\begin{bmatrix} u_d \\ u_q \end{bmatrix} = r_s \begin{bmatrix} i_d \\ i_q \end{bmatrix} + \begin{bmatrix} L_d s & L_q \omega_r \\ -L_d \omega_r & L_q s \end{bmatrix} \begin{bmatrix} i_d \\ i_q \end{bmatrix} + \psi_{PM} \omega_r \begin{bmatrix} 0 \\ 1 \end{bmatrix} \quad (1)$$

where

s – differential operator;
u_{dq} – stator voltages in synchronous reference frame;
i_{dq} – stator currents in synchronous reference frame;
L_{dq} – direct and quadrature inductances;
ω_r – rotor speed;
ψ_{PM} – permanent magnet flux;

Torque developed by the IPM synchronous motors as described by (2), can be divided into two components. First component of the torque is created by contribution of the ψ_{PM} field and is called synchronous torque. Second component, referred to as reluctance torque, arises due to rotor saliency, where the rotor tends to align with the minimum reluctance.

$$T_e = \frac{3}{2} p(\psi_{PM} i_q + (L_d - L_q) i_d) \quad (2)$$

where

p – number of pole pairs

IPM motors have the permanent magnets buried inside the rotor, which makes them salient pole machines with small effective air-gap. Reluctance in q-axis direction is smaller than that one in d-axis, resulting in q-axis inductance bigger than d-axis; $L_d < L_q$. Therefore, in order to develop maximal torque according to (2), reluctance torque should be utilized, i.e. i_d current has to be adjusted to negative values, weakening the resulting magnetic field. On the other hand, the armature reaction effects are dominant, due to small effective air-gap, resulting in saturation of q-axis inductance according to the level of applied load. This phenomenon is particularly important, because magnetic saliency decreases proportionally with saturated inductance and disappears completely at certain load level. Furthermore, under load the torque current in q-axis winding creates a term $\psi_{PM} i_q$ causing air-gap flux distribution to move towards direction of q-axis. Since the HF signal injection sensorless algorithm estimates the position of saliency rather than the position of rotor itself, this phenomenon has to be accounted for in the final application.

B. High Frequency Impedance

In order to verify presence of magnetic saliency at high frequencies (*hf*), *hf* impedance measurements were carried out [4]. In these measurements, the rotor is mechanically locked to prevent current signals distortion. *HF* signal of 50V/500Hz is injected in d_m – axis of the measurement $d_m - q_m$ reference frame. This frame is shifted from the actual rotor $d-q$ frame by *angle_offset*. Offsetting the measurement frame will ensure correct alignment of the frames any time the measurement is repeated. Injection of *hf* voltage $u_{hf} = U_m \sin(\omega_{hf} t)$ into d_m – axis, will result in i_{dm} current as described by (3).

$$i_{dm} = I_{dm\_max} \sin(\omega_{hf} t + \varphi) \quad (3)$$

$$= I_{dm\_max} \cos(\varphi) \sin(\omega_{hf} t) + I_{dm\_max} \sin(\varphi) \cos(\omega_{hf} t) \quad (4)$$

Multiplying by $\sin(\omega_{hf} t)$ and $\cos(\omega_{hf} t)$ respectively will result in spectral separation of low and high frequency components. This allows removing of *hf* component by simple low pass filtering of both products, resulting in (5), (6).

$$i_{dm\_a} = LPF\,[i_{dm} * \sin(\omega_{hf} t)] = \frac{1}{2} I_{dm} \cos(\varphi) \quad (5)$$

$$i_{dm\_b} = LPF\,[i_{dm} * \cos(\omega_{hf} t)] = \frac{1}{2} I_{dm} \sin(\varphi) \quad (6)$$

In order to extract amplitude I_{dm} from (5), and (6), sine and cosine functions have to be eliminated. This can be easily done by squaring i_{dm_a} and i_{dm_b} components respectively and subsequent addition (7). Then the amplitude I_{dm} is calculated as in (8).

$$I_{dm}^2 = 4 * ((i_{dm\_a})^2 + (i_{dm\_b})^2) \quad (7)$$

$$Z_{dm} = \frac{U_m}{I_{dm}} \quad (8)$$

The algorithm as described by eq. (3)–(7) is implemented on 16-bit Freescale Semiconductor digital signal controller (DSC). Output of the algorithm is the square value of I_{dm}. Calculation of square root value of I_{dm} from is done externally together with subsequent calculation of *hf* impedance (8).

Since *angle_offset* is varied ± 180 deg. electrical, at 90 deg. i_{dm} will correspond to i_{qm}. Therefore, to suppress DC offset of the i_{dm} current under load, 1s^t order high pass filter with cut-off frequency 10Hz is used. Block diagram showing the *hf* impedance measurement algorithm as implemented in DSC is depicted on Fig. 1.

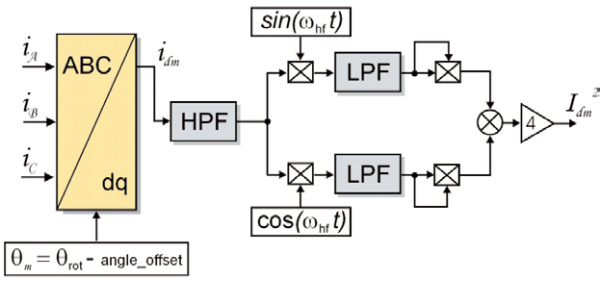

Fig. 1 Block diagram of HF impedance measurement

The obtained measurement results are shown on Fig. 2, where resulting impedance is plotted as a function of *angle_offset* and load level. It can be seen from Fig. 2 that the saliency moves towards the direction of q-axis and disappears with increasing load level as assumed in section II. A. Saliency disappearing with increasing load will cause eventual failure of sensorless algorithm based on

saliency tracking. This can be avoided by proper compensation action in d-axis current [4], which however will introduce additional losses in the motor and decrease the efficiency of the control loop.

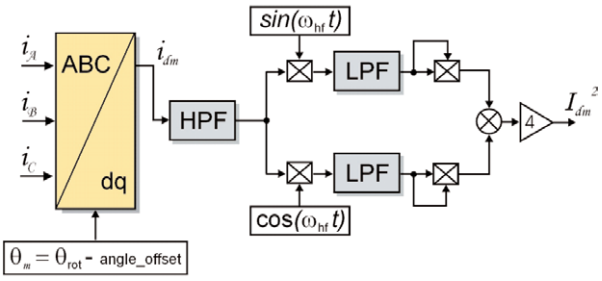

Fig. 2 High Frequency impedances as a function of difference between measurement and actual rotor reference frames and applied load.

III. Design of sensorless control for IPMSM

A. Initial Position Detection

As with any other synchronous motor, the first problem to overcome in FOC is the motor start-up. In contrast with the AC induction motor where the rotor flux is basically created from the stator, in the IPM motor the rotor flux is created by permanent magnets present in the rotor. In order to be able to use FOC, position of this rotor flux has to be known prior to any control action. In conventional IPM control with an encoder as a position transducer, an initial position is set by applying DC voltage in one motor phase, which creates a magnetic pole attracting the opposite pole of rotor magnets (alignment process). This process unavoidably generates often unwanted rotor movements. The sensorless algorithm based on injection of pulsating HF signal in the synchronous frame can be used to estimate the position of rotor at start-up. This sensorless approach is physically based on property of d and q axes flux being decoupled [3]. Therefore, if an estimated $\hat{d}-\hat{q}$ reference frame is defined and not precisely aligned with a real rotor $d-q$ reference frame, then by applying flux vector at known carrier frequency, for example, in the $\hat{d}$ axis, current at carrier frequency can be observed in the $\hat{q}$ axis. This current is directly proportional to the misalignment angle of the estimated and rotor reference frame. Therefore, changing the position of the estimated frame such that this $\hat{q}$ axis current is zero or minimal, will allow for tracking the real rotor, i.e. saliency position.

Considering high frequency signals, the motor model from (1) can be rewritten into an estimated reference frame (9). In this *hf* IPMSM model, voltage drop across the stator resistance and back-EMF components can be neglected.

$$\begin{bmatrix}\hat{u}_d\\ \hat{u}_q\end{bmatrix}=\begin{bmatrix}Z_1+\Delta Z\cos(2\theta_{err}) & -\Delta Z\sin(2\theta_{err})\\ -\Delta Z\sin(2\theta_{err}) & Z_1-\Delta Z\cos(2\theta_{err})\end{bmatrix}\begin{bmatrix}\hat{I}_d\\ \hat{I}_q\end{bmatrix} \quad (9)$$

where

$$Z_1=\frac{Z_d+Z_q}{2},\ \frac{\Delta Z=Z_d-Z_q}{2},\ \theta_{err}=\theta_{rot}-\theta_{est} \quad (10)$$

$\hat{u}_{dq}$ – stator voltages in estimated frame;
$\hat{I}_{dq}$ – stator currents in estimated frame;
θ_{rot} – rotor position;
θ_{est} – estimated position;
θ_{err} – position error;

Applying high frequency signal $u_{hf}=U_m\sin(\omega_{hf}t)$ in d-axis of *hf* model of (9), will result in high frequency currents

$$\begin{bmatrix}\hat{I}_d\\ \hat{I}_q\end{bmatrix}=-\frac{U_m}{\omega_{hf}Z_dZ_q}\cos(\omega_{hf}t)\begin{bmatrix}Z_1-\Delta Z\cos(2\theta_{err})\\ -\Delta Z\sin(2\theta_{err})\end{bmatrix} \quad (11)$$

After filtering and demodulation, $\hat{I}_q$ current is described as

$$\hat{I}_q=-\frac{U_m\Delta Z}{2\omega_{hf}Z_dZ_q}\sin(2\theta_{err}) \quad (12)$$

Fig. 3 depicts the $\hat{I}_q$ current in dependency on the rotor position θ_{rot}. In this measurement the estimated position θ_{est} is kept zero in order to see variations in $\hat{I}_q$ current.

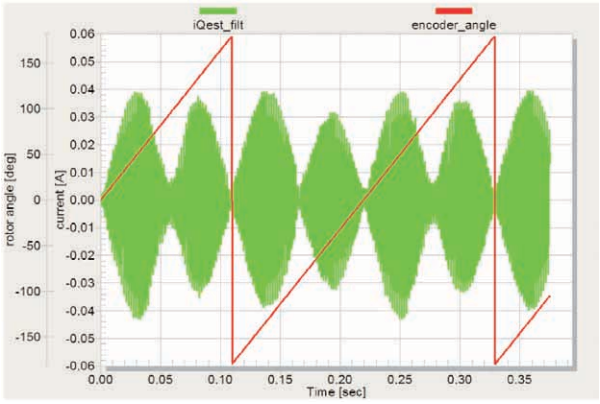

Fig. 3 Estimated quadrature axis current as a function of rotor position when estimated angle = 0

The relationship between $\hat{I}_q$ and estimated position error from suggest to use a controller capable of driving its output such that $\hat{I}_q$ current will remain zero.

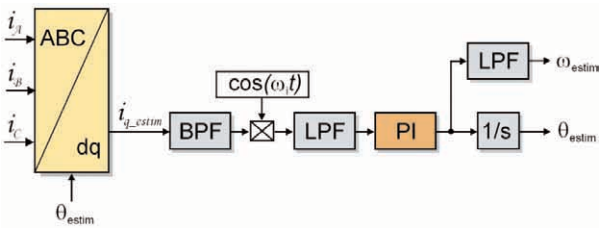

Fig. 4 Saliency tracking observer, as used for rotor position estimation at zero and low speeds

The controller output represents the estimated speed, thus its integration yields position of the estimated reference frame. Such structure acts as a phase locked loop and its schematic block diagram is depicted in Fig. 4. Fig. 5 demonstrates experimental results of the initial Saliency Tracking Observer (STO) alignment, which is used for the start-up rotor position detection. The experiment is carried out with the rotor manually rotated to an arbitrary position and then running STO alignment process.

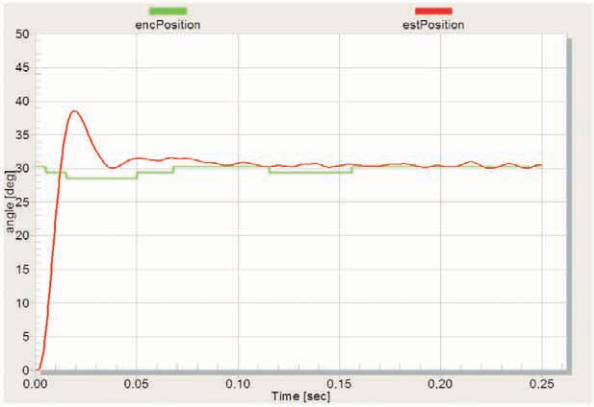

Fig. 5 Saliency tracking observer; initial position alignment

B. Low Speed Sensorless Control

The saliency tracking observer, as shown in Fig. 4, is used for start-up as well as for low speed sensorless control. A standard PI type controller is used, assuring zero position error in steady state. The saliency tracking loop is a non-linear structure but linearization around operation point $\theta_{esto.p.} = \theta rot$ allows approximation of the loop by

$$\theta_{est}\backslash\theta_{rot} = \frac{K_p s + K_I}{s^2 + K_p s + K_I} \qquad (13)$$

A standard PI type controller is considered in equation (13). Since the filtering and demodulation is done in the synchronous reference frame, the band pass filter (BPF) from Fig. 4, does not distort the phase of the estimated signal. Phase distortion is introduced by the low pass filter (LPF). Therefore, LPF affects the dynamics of the tracking loop and has to be accounted for in the loop tuning. Tuning of the saliency tracking loop is performed using *hf* IPMSM model from , as shown on Fig. 6.

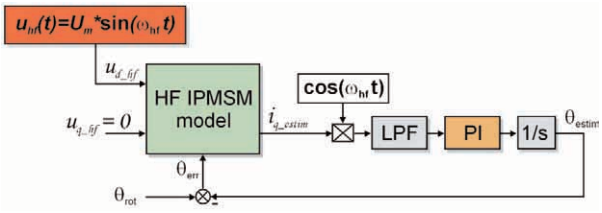

Fig. 6 Block diagram for tuning saliency tracking observer

It has to be noted however, that the carrier frequency limits STO bandwidth. Therefore, the PI controller should be designed so that STO will exhibit sufficient rejection capabilities at the carrier frequency.

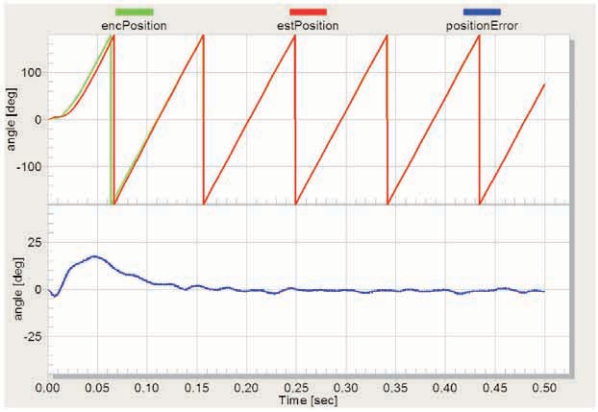

Fig. 7 Saliency tracking observer behaviour in open loop control during voltage transient (0 - ~ 45[rpm])

Fig. 7 shows the behaviour of STO in the open loop low speed tracking mode, during input voltage transient. Here the q-axis voltage command is changed in step 0–10 % of DC bus voltage, resulting in a sharp change in the rotor speed. Transient change generates the transient error in estimated position of ~18 deg electrical. Steady state estimation error of 3 deg. electrical has been achieved. The rotor speed settled at ~45 rpm.

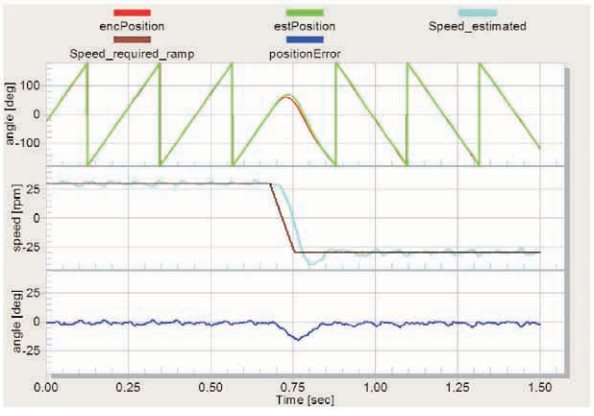

Fig. 8 Position error during reversal at 30rpm, IPMSM operated in full sensorless speed FOC

Position error during speed reversal at 30 rpm is depicted on Fig. 8. Here the motor is operated in speed FOC with position and speed feedback provided by STO, i.e. full sensorless mode. The rotor position from encoder is used only for comparison with the estimated position.

Experimental results of low speed full sensorless control with speed reversal under different load conditions are shown on Figs. 9 and 10. Rotor position information from encoder is not used in these experiments.

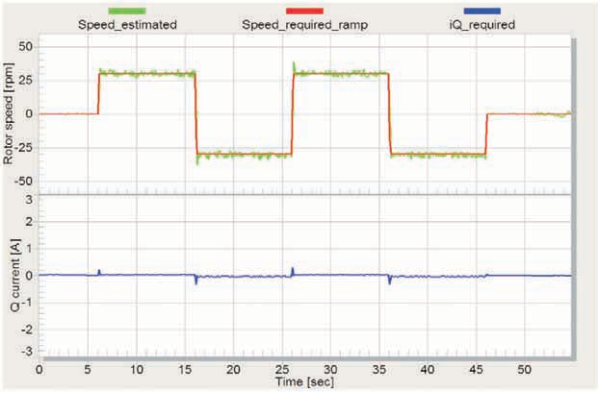

Fig. 9 Low speed full sensorless FOC, with speed reversal ±30 rpm under no load

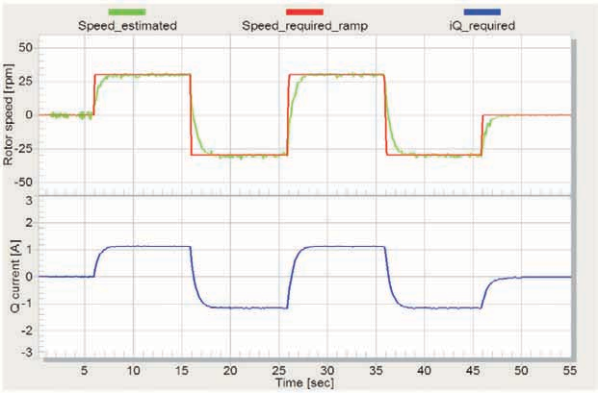

Fig. 10 Low speed full sensorless FOC, with speed reversal ±30 rpm under load (20 % nominal).

C. High Speed Sensorless Control

There have been proposed many sensorless control methods for surface permanent-magnet synchronous motors based on estimation of electromotive force in which the electrical position information of machine is encoded.

Fundamentally, these estimation methods for the position and velocity are based on the motor mathematical model. However, mentioned methods cannot be directly applied to an interior permanent-magnet synchronous motor, because the position information is contained not only in the conventionally defined back electro-motive force (EMF) but also in the definition of stator inductance as shown in (14).

Now the stator voltage u_s is interpreted as a sum of four voltage vectors u_R (voltage drop), u_L (inductance drop) and conventional u_E (back EMF), and u_{REL} (reluctance EMF). The last term of equation known as generated reluctance voltage is caused by motor saliency.

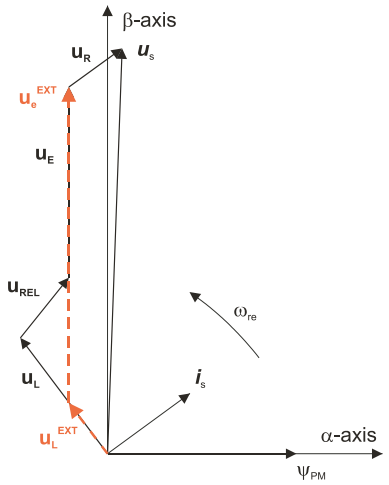

Fig. 11 Vector diagram of salient-pole machine.

The vector representation of given equation is displayed in Fig. 11. Unfortunately, the computation of position dependent information which is contained in two unknown voltage vectors conventional u_E, and u_{REL} makes difficulties to assess it. However, there has been proposed [] a simple way to resolve this problem by eliminating the $2\theta e$ term in (14) using a purely mathematical method.

Here is described a mathematical model of the interior PMSM motor which is based on an extended electro-motive force function [13]. This extended electro-motive force (EEMF) model includes both position information from the conventionally defined EMF and the stator inductance as well. Then, it makes possible to obtain

$$\underbrace{\begin{bmatrix} u_\alpha \\ u_\beta \end{bmatrix}}_{u_s} = \underbrace{R_s \cdot \begin{bmatrix} i_\alpha \\ i_\beta \end{bmatrix}}_{u_R} + \underbrace{pL_0 \cdot \begin{bmatrix} i_\alpha \\ i_\beta \end{bmatrix}}_{u_L} + \underbrace{k_e \cdot \omega_e \cdot \begin{bmatrix} -\sin(\theta_e) \\ \cos(\theta_e) \end{bmatrix}}_{u_E} + \underbrace{2 \cdot \omega_e \cdot \Delta L \cdot \begin{bmatrix} -\sin(2\theta_e) & \cos(2\theta_e) \\ \cos(2\theta_e) & \sin(2\theta_e) \end{bmatrix} \cdot \begin{bmatrix} i_\alpha \\ i_\beta \end{bmatrix}}_{u_{REL}} \tag{14}$$

$$\underbrace{\begin{bmatrix} u_\alpha \\ u_\beta \end{bmatrix}}_{u_s} = \underbrace{R \cdot \begin{bmatrix} i_\alpha \\ i_\beta \end{bmatrix}}_{u_R} + \underbrace{\begin{bmatrix} pL_d & (L_d - L_q) \cdot \omega_e \\ -(L_d - L_q) \cdot \omega_e & pL_d \end{bmatrix} \cdot \begin{bmatrix} i_\alpha \\ i_\beta \end{bmatrix}}_{u_L^{EXT}} + \underbrace{\{(L_d - L_q)(\omega_e i_d - i'_q) + k_e \cdot \omega_e\} \cdot \begin{bmatrix} -\sin(\theta_e) \\ \cos(\theta_e) \end{bmatrix}}_{u_E^{EXT}} \tag{15}$$

the rotor position and velocity information by estimating the extended EMF only.

In this equation (15) there is no $2\theta_e$ dependent term comparing to the conventionally defined IPMSM machine model (14). The second term u_L^{EXT} and third term u_E^{EXT} on the right side of equation (15) are depicted in Fig. 11 as vectors in dashed yellow lines. The u_L^{EXT} vector term in equation (15) can be explained as extension of conventional inductance voltage drop, and second vector term u_E^{EXT} is considered as an extension of conventional back EMF term. It is obvious that extended inductance voltage drop u_L^{EXT} has no position dependent information and only extended back EMF term u_E^{EXT} possesses position depen ent information. This rewritten mathematical model of interior PMSM motor makes possible to express the extended back EMF term u_E^{EXT} to be simply estimated using standard estimation approach of the surface-mounted PMSM motor.

$$\begin{bmatrix} u_{e\alpha} \\ u_{e\beta} \end{bmatrix} = [(L_d - L_q)(\omega_e i_d - i'_q) + k_e \cdot \omega_e] \cdot \begin{bmatrix} -\sin(\theta_e) \\ \cos(\theta_e) \end{bmatrix} \quad (16)$$

In this term (16), besides the conventionally defined EMF generated by the permanent magnet, there is a kind of voltage related to the saliency of the interior PMSM motor. It includes the position information from both the EMF and the stator inductance. It is a general form of mathematical model for all the synchronous motors [13].

D. State Observer of Extended Back EMF

In this section the described state observer is applied to the interior PMSM motor with an estimator model excluding the extended EMF term. Then the extended EMF term can be estimated using the state observer as depicted in Fig. 12, which utilizes a simple observer of IPM motor stator current. Here presented state observer is realized within stationary reference frame ($\alpha\beta$). The estimator of α-axis consists of the stator current observer based on *RL* motor circuit with estimated motor parameters. This current observer is fed by the sum of the actual applied motor voltage (u_α), cross-coupled rotational term which corresponds to the motor saliency ΔL and compensator $F_{c\_}(s)$ corrective output. Since the extended term of back EMF is not included in the interior PMSM motor observer model, the compensator $F_{c\_}(s)$ corrective output shown in Fig. 12 supplies the not modeled extended back EMF [14], [15]. The estimate of extended EMF term in α-axis can be derived as follows

$$\hat{E}_\alpha(s) = F_c(s) \cdot [I_\alpha(s) - \hat{I}_\alpha(s)] \quad (17)$$

It is obvious that the accuracy of the back EMF estimates is determined by the correctness of used motor parameters (R, L) by fidelity of the reference stator voltage and by quality of compensator such as bandwidth, phase lag and so on. It is obvious from the extended EMF transfer function that even if the motor parameters are precisely matched, the estimates are limited by the compensator quality. This implies that the state observer bandwidth and its corresponding phase lag constraints the performance of used method. The same consequences apply for estimate of the extended EMF in β-axis.

If assumed a perfect match between motor parameters and its estimated counterparts, then the transfer function is given as

$$\hat{E}_\alpha(s) = -E_\alpha(s) \cdot \left[\frac{F_c(s)}{s\hat{L}_d + \hat{R}_s + F_c(s)} \right] \quad (18)$$

and this yields the parameter insensitivity within the bandwidth. This clearly implies that the state observer bandwidth determines the performance of this method. The angle tracking observer [16] shown in Fig. 12 is widely used for the estimation of the rotor angle. By employing the tracking observer, noise on the position estimate can be filtered out without adding lag to the estimate within its bandwidth [14], [16]. Note that mathematical expression of the tracking observer error is well known as the formula of the difference of two angles

$$\sin(\theta_e - \hat{\theta}_e) = \sin(\theta)\cos(\hat{\theta}) - \cos(\theta)\sin(\hat{\theta}) \quad (19)$$

and this denotes an observer error. In the case of minimal deviations out of the estimated rotor angle compared to the actual rotor angle, the observer error may be expressed in the following form

$$\theta_e - \hat{\theta}_e = \sin(\theta_e - \hat{\theta}_e) \quad (20)$$

The primary benefit of the angle tracking observer utilization, in comparison with the trigonometric method, is its smoothing capability [17]. This filtering is achieved by the integrator and PI controller, which are connected in series and closed by a unit feedback loop

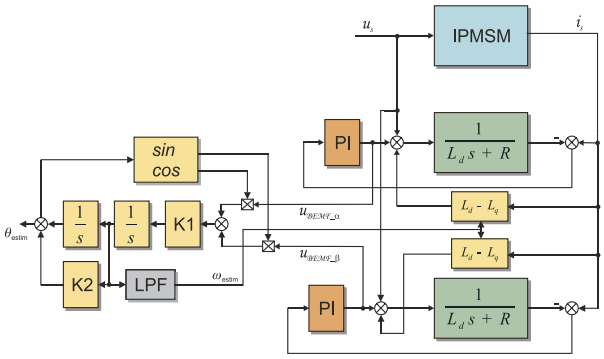

Fig. 12 Block diagram of state observer of extended back EMF

E. Experimetal Results of Extended Back EMF State Observer

The extended back EMF state observer was implemented using a digital signal controller of Freescale's 56F8300 series with interior PMSM. The motor with parameters summarized in Table IV was used for these experiments.

First, the experiments in tracking mode are presented, where field oriented control with operation of speed closed loop is used and the encoder transducer is used as position and speed feedback.

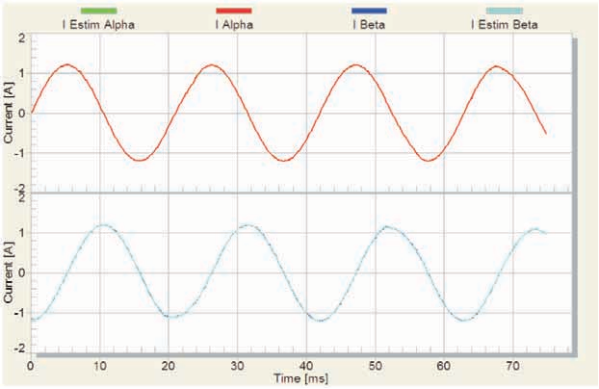

Fig. 13 Estimated αβ currents by state observer at 300 [rad.sec^{-1}]

Electrical rotor position and speed are fed back from the encoder transducer, and are granted as reference to estimated values of the rotor electrical position θ_{estim} and angular speed ω_{estim}. This motor drive operation allows to evaluate the quality of sensorless algorithm. The observer tracking capability of phase stator currents expressed in a stationary reference frame are evaluated as shown in Fig. 13. It is apparent that there is very good signal fidelity between actual measured current of motor and estimated current value calculated by back EMF observer.

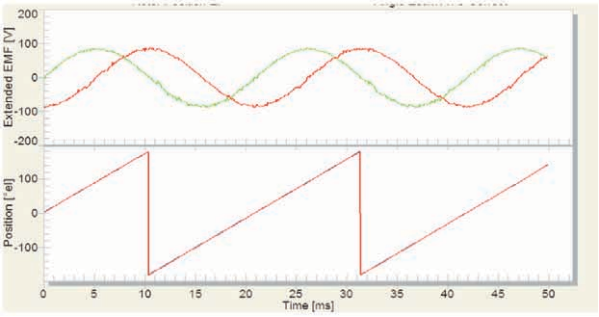

Fig. 14 Estimated extended EMF by state observer at 300 [rad.sec^{-1}] and estimated electrical position by angle tracking observer

The interior PMSM motor under test operated in a tracking mode where speed control attained position and speed the from encoder, and estimation algorithm tracks the actual rotor position. As can be seen from Fig. 14, the estimation of speed and position have very good accuracy and apparently the encoder position feedback can be replaced by these estimates from the extended back EMF state filter.

The controller output, which corrects motor phase currents, is supplying not modelled part of motor state the extended back EMF. Fig. 14 shows the estimated extended back EMF at 300 [rad.sec^{-1}].

If the interior PMSM motor drive operates in a sensorless mode where the electrical position required for vector transformation is attained from sensorless algorithm and the feedback speed control loop is formed by state observer estimate. A satisfactory sensorless operation was achieved under different operation condition. As it can be seen from Fig. 14 there is a very high correspondence between the estimated rotor position (red) and encoder measurement of electrical position (blue). The exact knowledge of rotor position is very critical to the IPM motor stable operation and it is seen that in a sensorless mode the interior PMSM motor functions with minimum sensitivity to a motor load having very high agreement of the measured position from encoder and state filter estimate.

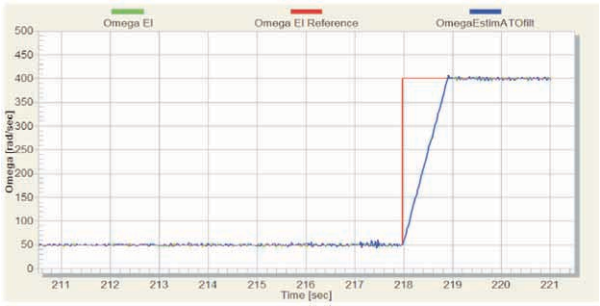

Fig. 15 Speed control with ramp acceleration under load condition

Since the state observer sensorless algorithm operates reliable from 50 [rad.sec^{-1}], the speed command is demanded from this limit. A speed acceleration Fig. 15 from 50 [rad.sec^{-1}] up to 400 [rad.sec^{-1}] is tested with achieving almost identical behaviour of estimated and encoder speed.

The operation of sensorless IPM motor drive was tested under a variable load condition as shown in Fig. 16. The developed speed and position estimation algorithm demonstrates very good and stable speed estimation performance.

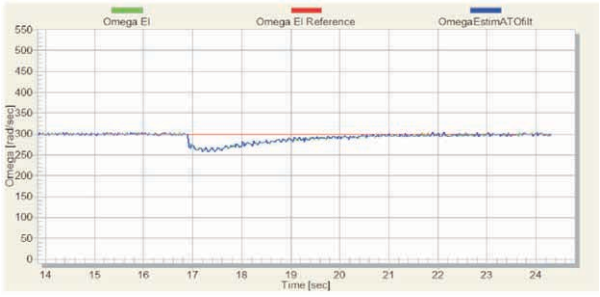

Fig. 16 Sensorless speed control at step change in load

A step change in the motor load was generated to verify dynamic performance of speed estimation and sensorless speed control, it can be seen in Fig. 15. Very stable drive operation during unexpected loading was observed. This makes this approach adequately robust to motor loading.

F. Whole Speed Sensorless Control

In order to fully control IPMSM throughout the entire speed range, estimates from low and high speed sensorless algorithms have to be evaluated and merged. The proposed merging algorithm is based on cross-over functions, assuring smooth transition between algorithms. Moreover using cross-over functions allows completely switching off the algorithm currently not used [8], thus minimizing losses due to *hf* injection at high speeds. Fig. 17 shows block diagram of algorithms for the whole speed sensorless control of IPMSM.

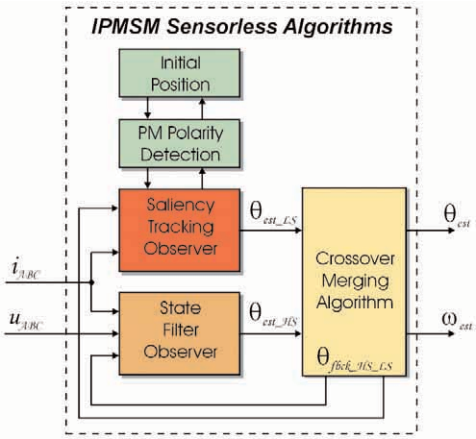

Fig. 17 Block diagram of IPMSM sensorless algorithms for entire speed range

Fig 18 shows experimental results of full IPMSM sensorless control obtained from experimental setup according to Fig. 19. In this experiment IPMSM is operated in speed FOC with estimated position/speed provided by merging algorithm. Parameters of the IPMSM synchronous motor are given in Tab. I.

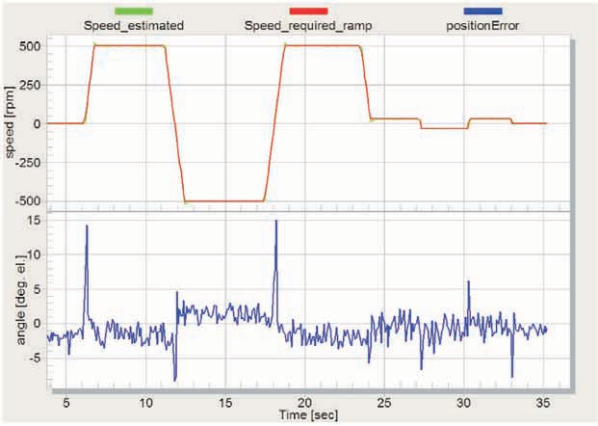

Fig. 18 Whole speed range full sensorless control with speed reversal

MOTOR PARAMETERS TABLE I.

Motor Parameter	Value
Number of poles	20
Rated speed	600 [rpm]
Phase voltage max.	AC 200 [V]
Phase current max	8A p-p
Ke	0.255 [V.sec/rad]
Rs	7.5 [Ω]
Ld	0.081 [H]
Lq	0.095 [H]

The overall structure of IPMSM sensorless drive for an electric washer is depicted on Fig. 19. IPMSM operated in speed sensorless FOC Position error is calculated with respect to the position obtained from the encoder. The encoder is used only for comparisons.

IV. Conclusion

Sensorless field oriented control of IPMSM covering the entire speed range is presented. The merging algorithm based on a cross-over function was designed in order to perform a smooth transition between two different sensorless algorithms. The approach presented in this paper is based on hf signal injection method for low speed operation and on the estimation of an extended EMF in the stationary reference frame using a state filter for high speed operation. The spatial information obtained from the estimates of extended EMF is used in an angle tracking observer to estimate the rotor electrical position. The extended EMF model includes both position information from the conventionally defined EMF and the stator inductance. This makes it possible to obtain the rotor position and velocity information by estimating the extended EMF only. Whole implementation of the transient injection method and extended back EMF state filter was achieved on a single chip solution of DSC56F8300 series without any additional supportive circuitry.

Acknowledgement

The authors wish to thank for the financial support to the Scientific Grant Agency of the Slovak Republic for project No. 1/3086/06 *"Research of the new methods of modeling-, control and simulation of mechatronic systems".*

References

[1] BOSE, B.: *Modern Power Electronics and AC Drives,* Prentice Hall PTR, 2002.

[2] VADSTRUP, P., LORENZ, R. D.: *Robust Estimator Design for Signal Injection-Based IPM Synchronous Machine Drives,* Trans. of IEEE-IAS, 2004, pp. 957–963.

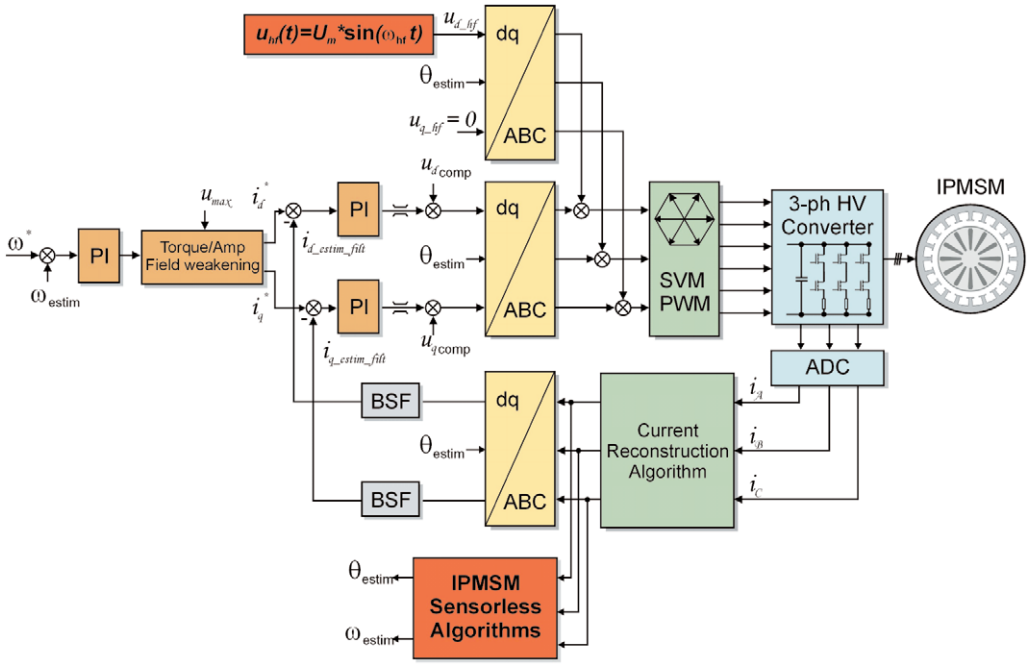

Fig. 19 Overall structure of IPMSM sensorless drive for electric washer

[3] HA, J., SUL, S. K., IDE, K., MUROKITA, I., SAWAMURA, K.: *Physical Understanding of High Frequency Injection Method to Sensorless Drives of an IM,* Trans. of IEEE, 2000, pp. 1802–1808.

[4] HA, J., IDE, K., SAWA, T., SUL, S. K.: *Sensorless Position Control and Initial Position Estimation of an Interior Permanent Magnet Motor,* Trans. of IEEE-IAS, 2001, pp. 2607–2613.

[5] JEONG, Y., LORENZ, R. D., JAHNS, T. M., SUL, S. K.: *Initial Rotor Position Estimation of an Interior Permanent-Magnet Synchronous Machine Using Carrier-Frequency Injection Methods, IEEE Trans.* on IA, vol. 41, 1/2005, pp. 38–45.

[6] KIM, H., HUH, K. K., LORENZ, R. D., JAHNS, T. M.: *A Novel Method for Initial Rotor Position Estimation for IPM Synchronous Machine Drives,* Proc. of IEEE, 2003, pp. 1173–1180.

[7] OGASAWARA, S., AKAGI, H.: *An Approach to Real-Time Position Estimation at Zero and Low Speed for a PM Motor Based on Saliency, IEEE Trans.* on IA, 1/1998, pp. 163–168.

[8] KIM, H., YI, S., KIM, N., LORENZ, R. D.: *Using Low Resolution Sensors in Bumpless Estimation Methods for Low Cost PMSM Drives,* Trans. of IEEE-IAS, 2005, pp. 2518–2525.

[9] KIM, J. M., SUL, S. K.: *Speed Control of Interior Permanent Magnet Synchronous Motor Drive for the Flux Weakening Operation,* Trans. of IEEE, 1/1997, pp. 43–48.

[10] IDE K., HA, J., M. SAWAMURA, IURA, H. AND YAMAMOTO, Y.: *HF Injection Method Improved by Flux Observer for Sensorless Control of an IM,* in Proc. of PCC-Osaka, 2002, pp. 516–521.

[11] DOBRUCKÝ, B., BALAŽOVIČ, P., FILKA, R., ABDALMULA M.A.R.: *Robotic Servo-System with Sensorless Measurement of Initial Position of PMSM Motor Using PC&ADSP21062 Control,* in Proc. of RAAD'01 Conf., Vienna (AT), May 2001

[12] ABDALMULA, M.A.R., DOBRUCKÝ, B., PAVELKA, P.: *Combined Method for Position Determination of PMSM in Zero- and Low Range of the Speed,* Proc. of EDPE'03 Conference, Sep. 2003

[13] CHEN, Z, TOMITA, M., DOKI, S., OKUMA, S.: *An extended electromotive force model for sensorless control of interior permanent-magnet synchronous motors,* IEEE Trans. on Industrial Electronics, 4/2003, pp. 288–295.

[14] DOČAR, M., BUDAY, J.: *Control System and Drives of OJ-10 Robotic operation Unit (in Slovak),* Výkonová elektronika, zborník ZTS-EVÚ, N. Dubnica, 3/1983, pp. 3–9.

[15] LORENZ, R. D.: *Observers and state filters in drives and power electronics,* Conf. Rec. of the IEEE IAS OPTIM, May 2002.

[16] MIENKINA, M., PEKAREK, P., DOBES, F.: *56F80x resolver driver and hardware interface, Application Note AN1942,* Freescale Semiconductor Inc., 2005.

[17] FILKA, R., BALAZOVIC, P.: *Intelligent sensorless control of AC permanent magnet motors,* Embedded Control Europe, October 2005, pp. 17–19.

[18] FRANKLIN, G. F., POWELL, J. D., EMAMI-NAEINI, A.: *Feedback Control of Dynamical System,* 4th edition, Prentice-Hall, 2002.

Eva Belicová *

MODELLING OF THERMAL TRANSIENT PHENOMENA IN AXIAL FLUX PERMANENT MAGNET MACHINE BASED ON COUPLING OF TWO SEPARETED MODELS – ELECTRICAL AND THERMAL MODELS

The paper deals with transient thermal modelling of air cooled axial flux permanent magnet machine. It has a rotor with permanent magnets placed on the rotor surface situated between two stators. The simulation model consists of two equivalent circuits - electrical equivalent circuit and thermal equivalent circuit to cover various machine operations. This model can be very useful mainly in mechatronic applications in order to be sure that applied machine will manage with requirements put by operation conditions and environment roughness.

1. Introduction

With the coming of automobile industry to the Slovak Republic, an interest in mechatronic has increased and mechatronic applications have been under the greater investigation of many researchers, too.

Synchronous machines with permanent magnets have been more and more popular in the field of electrical drives in the last decades. They have many advantages in comparison with classical synchronous machines with d. c. excitation. Of course, they have some disadvantages, especially impossibility of controlling by varying types of excitation. In the past, prime interest was given to radial flux permanent magnet machines (RFPM). Recently, greater development of axial flux permanent magnet machines has been introduced to industry. In general, it is known that AFPM feature analogous operation behavior as RFPM but their geometrical dimensions and small moment of inertia are major profits. This could be very useful in mechatronic applications.

Mechatronic applications are characterized by short time multiple overloading of an applied machine. This overloading can lead to degradation and faster ageing of construction materials, thus decreasing machine lifetime. Therefore, it is very important to know the thermal behavior of machine in order to prevent early failure of the machine.

During operation of the machine, different types of losses are generated, namely losses in the stator yoke, losses in the stator teeth, losses in permanent magnets (PM), mechanical losses (they can be neglected in the case of a low speed machine) and Joule losses, which present dominant heat source. In the case of AFPM, the winding losses are organized to outer and inner endwinding losses and losses in the slot part of winding.

The paper focuses on finding a suitable simulation model in order to find limits for overloading permitted to prevent the machine failure due to overheating.

2. Simulation model

The simulation model was developed for air naturally cooled AFPM with construction stator-rotor-stator, see Fig. 1, with the following nameplate: P_N = 5000 W; T_N = 159 Nm; V_N = 230 V, winding connected to star; f = 30 Hz; I_N = 8.4 A; $2p$ = 12; n = 300 rpm, Br = 1.05 T. This model is mainly oriented to investigate how Joule losses affect the heating of the machine during operation.

Previously, the steady state thermal model of the investigated motor was developed in [1]. The thermal model of AFPM was extended with thermal capacitances to cover the transient thermal analysis. The thermal model was also made by electrical equivalent circuit up to gain a possibility of the different operation duties investigation.

The overall simulation model involves an electrical equivalent circuit based on equations of general theory of AC machines transformed to d, q, 0 reference frame. Equations for AFPM do not differ from equations validated for RFPM which may be found in many publications, for example [2], [3], [4] and others.

The system of equations, used to describe the electrical equivalent circuit, can be summarized as follows:

$$u_d = R_s i_d + L_d \frac{di_d}{dt} - \omega L_q i_q \qquad (1)$$

* **Eva Belicová**
Nuclear Power Plant Research Institute (VUJE), Okruzna 5, 918 64 Trnava, Slovakia, E-mail: eva.belicova@gmail.com

$$u_q = R_s\, i_q + L_q \frac{di_q}{dt} + \omega L_d\, i_d + \omega \psi_{PM} \tag{2}$$

$$m_e = p[(L_d\, i_d + \psi_{PM})iq - (L_q\, i_q)i_d] \tag{3}$$

$$J \frac{d\omega}{dt} = p(m_e - m_L) \tag{4}$$

$$\vartheta_r = \int \omega_r\, dt \tag{5}$$

Where $u_{d(q)}$, $i_{d(q)}$, $L_{d(q)}$, R_s, ω, m_e, p, J, m_L, ϑ_r, ω_r are voltages, currents and synchronous inductance in d (q) axis, phase resistance, electromagnetic torque, number of pole pairs, moment of inertia, load torque, rotor position angle and mechanical rotor speed, respectively. Voltages in d (q) axis are given by Park's transformation of phase voltage waveforms. To keep an invariance principle of powers, transformation constants were chosen as $k_{d(q)} = \sqrt{2/3}$.

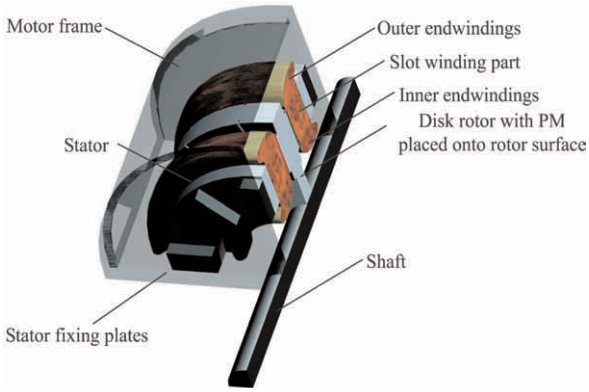

Fig. 1 Slit of analyzed AFPM

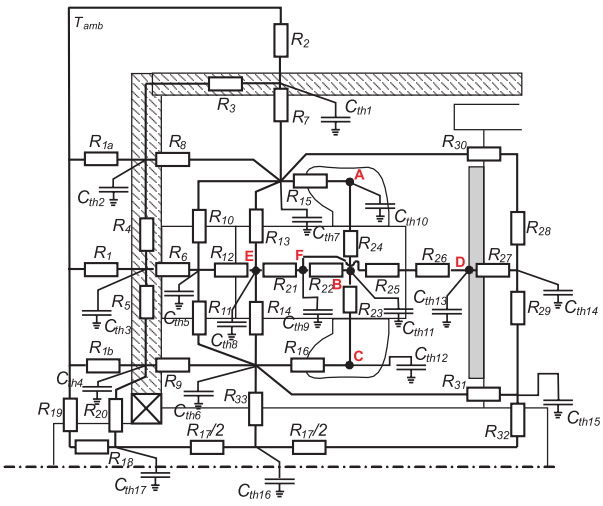

Fig. 2 Simplified thermal network of analyzed AFPM

A – Outer endwinding; B – Slot part of winding; C – Inner endwinding
D – Permanent magnets; E – Stator yoke; F – Stator teeth

The phase current waveform is gained by using the backward Park's transformation from the system mentioned above. Consequently the root-mean-square value of the stator current IRMS was evaluated to determine the Joule losses in the stator winding which denote the dominant heat source. These losses are dependent on the temperature rise because the value of stator resistance alters with the temperature and affects size of Joule losses, too.

The thermal network of AFPM is shown in Fig. 2. This thermal network model consists of thermal resistances that are determined based on the type of heat transfer and thermal properties of used construction material; see [5]. All the analyzed nodes have assigned the thermal capacitances, which present stored energy. The letters A-F show where individual losses input into the thermal model as the heat sources, see Fig. 2.

The transient thermal simulation was realized by using the following differential equation:

$$\frac{d}{dt}(\Delta\vartheta) = C^{-1}(\Delta P_d - G(\Delta\vartheta)) \tag{6}$$

Where $\Delta\vartheta$, ΔP_d, C^{-1}, $G(\Delta\vartheta)$ are a temperature rise vector, vector of the dissipated losses, an inverse matrix to a capacitance matrix and a thermal conductance matrix, respectively. Elements of the capacitance matrix are equal to zero except main diagonal where particular thermal capacitances are located. The elements of the main diagonal of the conductance matrix were assigned with a sum of the thermal conductances that are connected to the particular nodes. The other components are defined by the thermal conductance located between the corresponding nodes.

The principal block diagram of the overall simulation model is shown in Fig.3. It is very clearly seen from the figure how temperature affects individual components of the simulation model. Some of the thermal resistances, mainly the thermal resistances of parts filled by air, are dependent on the temperature and they must be regularly updated. In the figure, there is also shown feedback loop from the thermal equivalent circuit to the electrical equivalent circuit to update the value of the stator resistance, and so it is provided, the correct value of the stator resistance is taken into account. Based on this mutual affecting, the changes of the model parameters that appeared in the machine during operation are more precisely included during simulation. In this way, it is possible to involve changes of the thermal equivalent circuit as well as of the electrical equivalent circuit with quite a good accuracy.

3. Simulation results

The simulation model was built in Simulink. One operation duty cycle was selected to verify the model's accuracy. Both simulation models were running at the same time. The machine was started up and loaded with the nominal torque after the 1.5 s, see Fig. 4a). The root-mean-square current was gained from electrical model. The Joule losses were calculated for the current temperature in every simulation step by the current value (see Fig. 4b)) as well as by the value of stator resistance, see Fig. 4c).

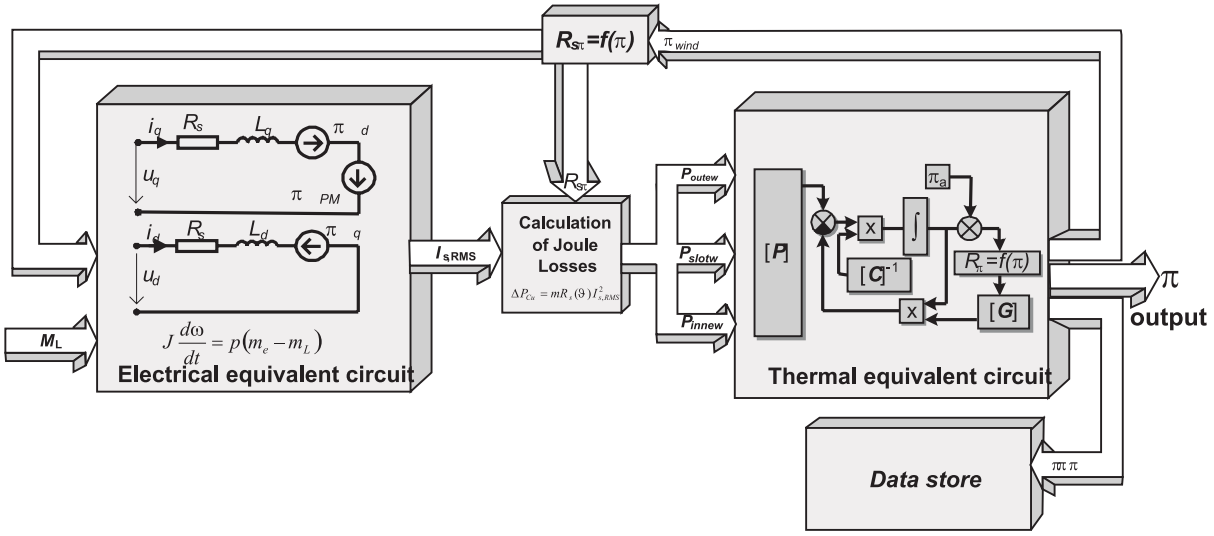

Fig. 3 Block diagram of the simulation model

The total Joule losses were divided into three parts; outer and inner endwinding Joule losses as well as slot part of winding losses, in a ratio which corresponds to the resistance values of the individual winding parts, see Fig. 4d). Other losses generated inside the machine were kept constant during the whole simulation because their variation was not so notable. Here must be noted that all the values of thermal capacitances were also kept constant in every node.

The simulation had been running till the stable values of the temperature were reached. As it is seen in Fig. 4b) the root-mean-square value of the current was risen by temperature increase which

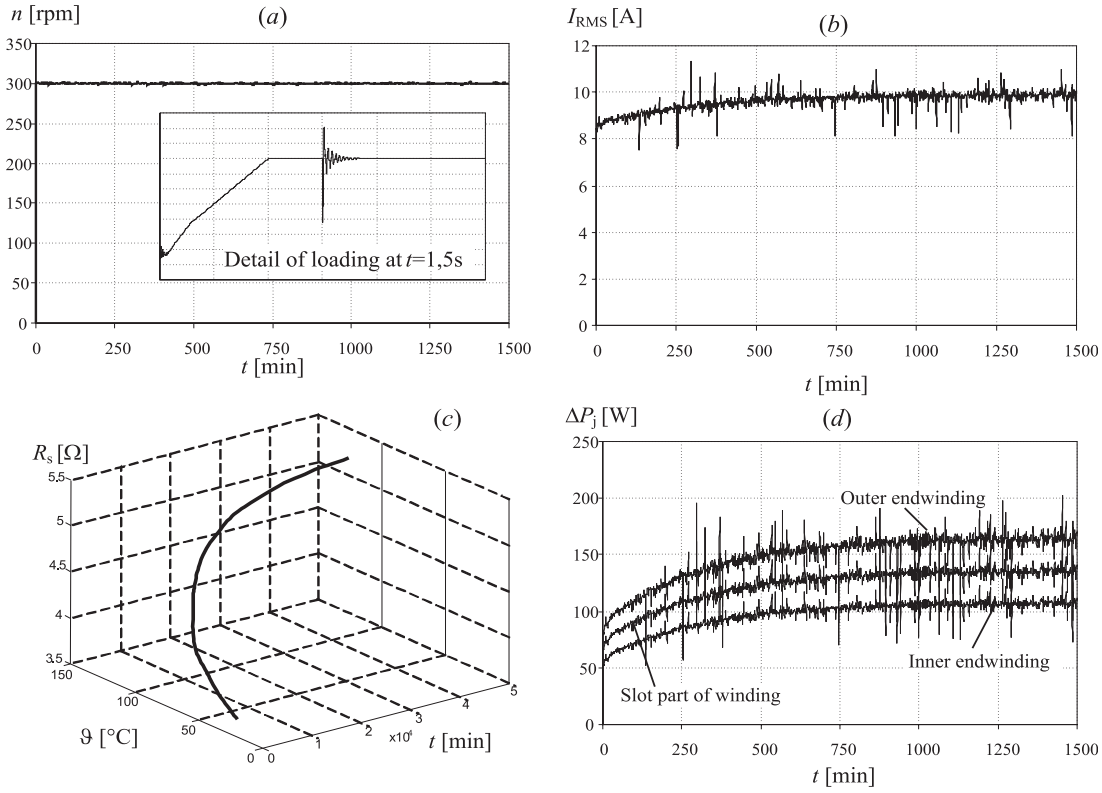

Fig. 4 Simulated waveforms of (a) revolutions with a detail of loading; (b) root-mean-square phase current (c) stator resistance versus temperature at given time (d) Joule losses in outer and inner endwinding and in slot part of winding

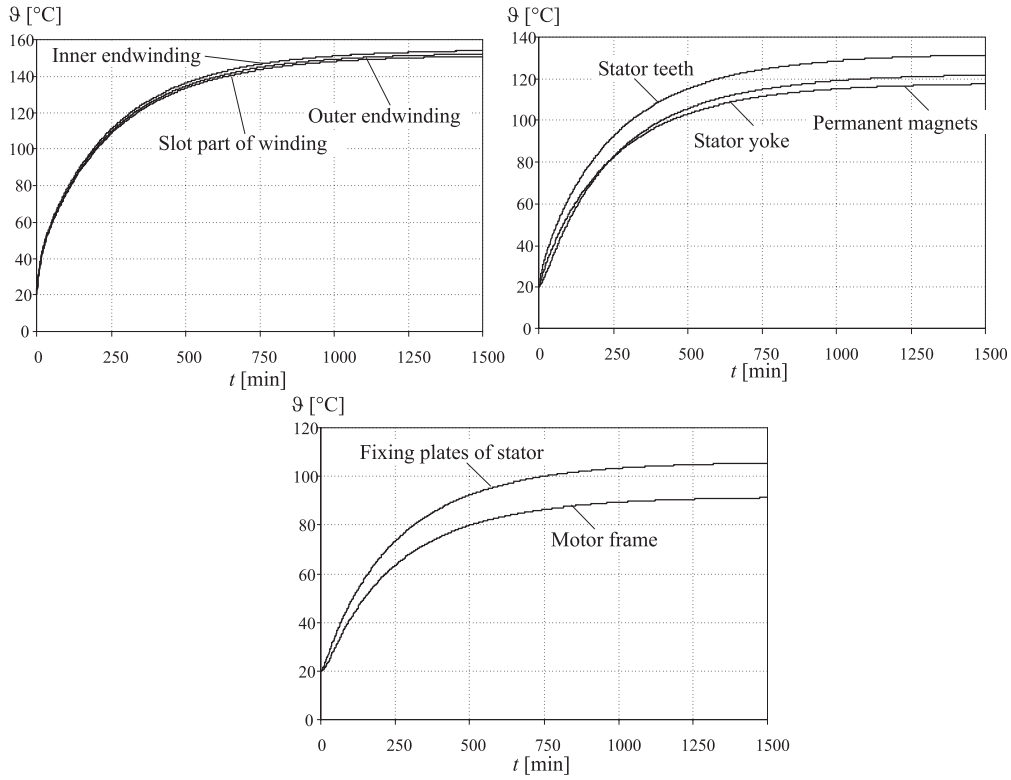

Fig. 5 Temperature curves of individual analyzed nodes of AFPM

was caused by the Joule losses rise. While it was requested to have a constant output power on the shaft, and the machine was supplied from a constant voltage source, the input power had to be increased by varying the input current value. The existence of peaks in the current and the Joule losses waveforms could be caused by sensitivity of the electrical simulation model to the resistance changes.

The simulation time was set up to 25 hours of continuous machine operation under the full load. The simulation of the given operation period consumed 23 hours of the real time on the computer with 2.8 GHz processor and 2 GB RAM.

In Fig.5 temperature curves of analyzed nodes are shown. As it is seen from the figure, the machine was operating under conditions which did not affect its lifetime. The insulation used in the machine belongs to the thermal-insulation of B class, which has the upper limit temperature about 170 °C if air-cooling of the machine is considered. The operation temperature of PMs used in the investigated machine is 150 °C. This value does not present risk of their properties degradation if an ambient temperature was considered about 20 °C.

The prime advantage of such a simulation model is a possibility to investigate different operation modes. Mainly, when the simulation model is used to investigate period overloading or starting up, which are typical operations of mechatronic applications.

The thermal network model could be replaced by a finite element model of analyzed machine, which can bring a more precise solution. In this way it will be possible to create a direct online solution. This interconnection of the electrical equivalent circuit and finite element model will be done in the future.

4. Conclusion

The paper deals with the transient thermal analysis of AFPM based on coupling two equivalent circuits, electrical and thermal. This approach will be suitable if operation conditions are not defined exactly.

The simulation model was built in Simulink on the base of differential equations to obtain the stator current waveform. The RMS value of the stator current was determined from the stator current waveform and this value was used to find out Joule's losses in the stator winding which were used as heat sources for a thermal network model of AFPM. The stator resistance variation caused by winding temperature changes was taken into account.

In this manner it is possible to find suitable use of machine in the mechatronic field. Moreover, it will be useful to get optimal operation of the machine to prevent reducing the machine lifetime.

Acknowledgement

This work was supported by Science and research Assistance Agency under the contract No. APVT-20-039602 and by the Scientific Grant Agency of the Ministry of Education of SR and the Slovak Academy of Science under contract No. VEGA 1/2052/05 and No. VEGA 1/3086/06.

References

[1] PARVIAINEN, A.: *Design of Axial-Flux Permanent-Magnet Low-Speed Machine and Performance Comparison between Radial-Flux and Axial-Flux Machines,* Dissertation Thesis, Lappeenranta University of Technology, 2005

[2] HRABOVCOVÁ, V., JANOUŠEK, L., RAFAJDUS, P., LIČKO, M.: *Modern electrical machines (in Slovak)*, EDIS, Zilina, 2001

[3] HRABOVCOVÁ, V., BRŠLICA, V.: *Disk Synchronous Machine with Permanent Magnets - Electric and Thermal Equivalent Circuits,* Proc. of Electrical Drives Symposium, Capri, Italy 1990, p. 163-169

[4] HRABOVCOVÁ, V., RAFAJDUS, P., FRANKO, M., HUDÁK, P.: *Measurement and modelling of electrical machines (in Slovak)*, EDIS, Zilina, 2004

[5] INCROPERA, F. P., DE WITT, D. P.: *Fundamentals of Heat and Mass Transfer,* USA, 2002.

Tomáš Michulek – Vojtech Šimák – Ján Capák *

SIX LEGGED WALKING ROBOT SIMULATION AND CONTROL

The authors present the first results of their scientific work related to design and development of the walking robot control systems in virtual reality. Six-legged walking robot was created along with its virtual counterpart simulated in virtual environment. A control system was created and tested on virtual model. This control system was then directly used to control real robotic construction. Differences between real and virtual robot behavior were analyzed.

1. Introduction

Autonomous mobile robots have become more and more important during last years. They are able to solve problems to dangerous for human beings. Special types of mobile robots are walking robots. This includes robots that locomote without wheels, or use walking wheels [9]. Their ability to cope with rough terrain makes them the best choice for many applications where standard wheeled vehicles are useless. Many different constructions were created. Most popular are biped [13], quadruped [2] and six legged constructions. Robots are often inspired by various life forms [11].

Two main approaches can be used to control walking robot. First one is based on precise joint angle control. This approach is based on direct control of every DOF of the robot. The second is based on passive dynamics of the robot construction. In this case,

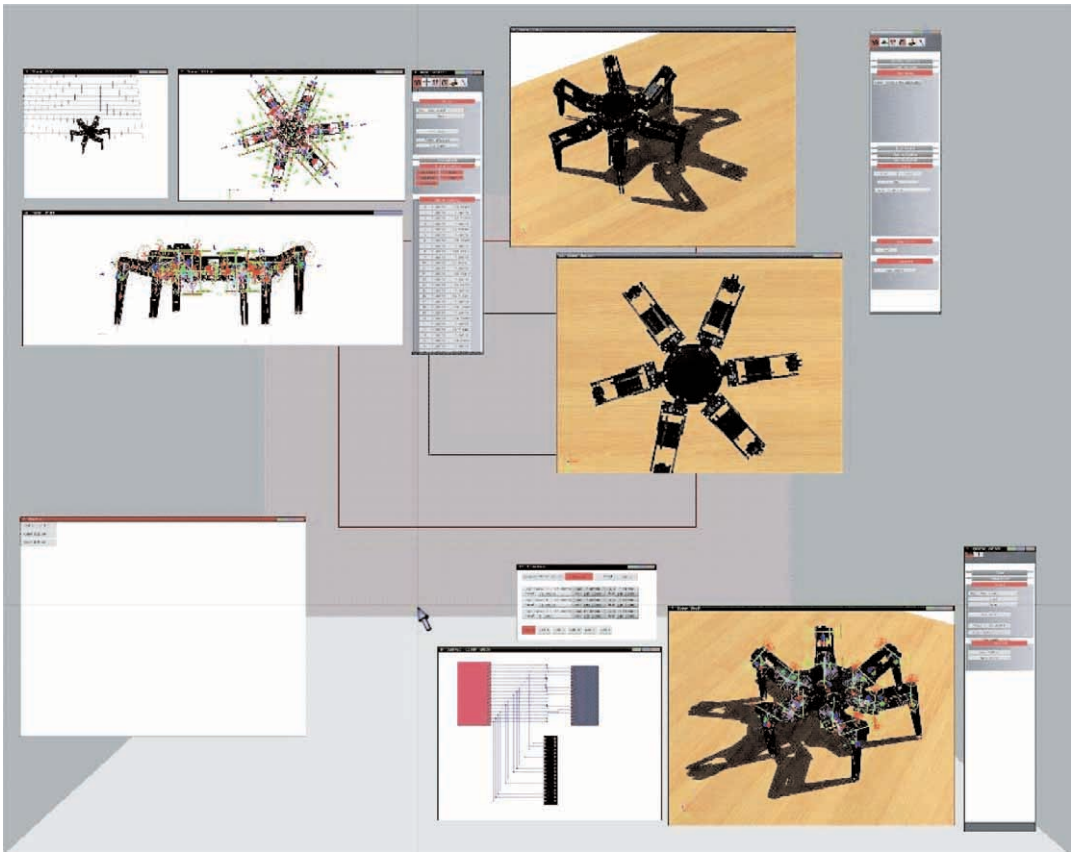

Fig. 1 Basic application interface

* **Tomáš Michulek, Vojtech Šimák, Ján Capák**
Faculty of Electrotechnical Engineering, University of Žilina, Slovakia,
E-mail: Tomas.Michulek@fel.utc.sk, Vojtech.Simak@fel.utc.sk, jan.capak@gmail.com

part of the walk control problem is solved by robot construction. A precise joint control approach was used to control our robot.

Many software solutions were created to simulate walking robots. Examples can by found in [3] [6] [8] [10]. Simulation is being used to speed up the development of the robot construction and to optimize its control system. The evolution of computing hardware has enabled more p1recise simulation of complicated robotic construction during last few years.

In this paper, we present the results of our development of a six legged walking robot, along with its virtual counterpart. A control system developed to control these robots is also described.

2. Simulation software

Since no existing software package was able to fulfill all our current and future requirements, our own software development environment was created. The basic interface is shown in Fig. 1. The program has been created in C++ and GLSL programming languages and it uses OpenGL and SDL libraries. It works under Linux operating system (Fedora Core 6 distribution).

Simulation of a robot body is based on rigid body dynamics. The model consists of rigid segments connected together via flexible joints. Segments are defined by their geometric shape, mass and inertia matrix. Every rigid part is affected by various forces. These forces are generated in joints in order to preserve the model's geometric configuration. Another group of forces is generated as a result of a robot versus environment interaction. All these forces are then applied to a corresponding segment.

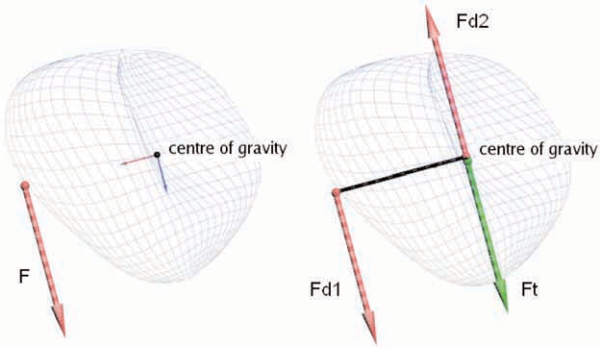

Fig. 2 Force transformation

After transformation displayed in Fig. 2. every force $\vec{F}_i$ is transformed to $\vec{Ft}_i$, $\vec{Fd}1_i$ and $\vec{Fd}2_i$ parts. $\vec{Ft}_i$ affects movement of the segment.

Resulting force is given by an expression:

$$\vec{F}_t = \sum_{i=0}^{n} \vec{F}_{ti} \tag{1}$$

Acceleration $\vec{a}$, speed $\vec{v}$ and position $\vec{c}$ of segments centre of gravity are then given by:

$$\vec{a} = \frac{\vec{F}}{m} \tag{2}$$

$$\vec{v} = \vec{v}_0 + \int_0^T \vec{a}\,dt \tag{3}$$

$$\vec{c} = \vec{c}_0 + \int_0^T \vec{v}\,dt \tag{4}$$

where T is actual time of simulation, $\vec{c}_0$ is position and $\vec{v}_0$ speed of the segment at the moment of a simulation start.

$\vec{Fd}1_i$ with $\vec{Fd}2_i$ forces affect rotation of the segment (Fig. 3.).

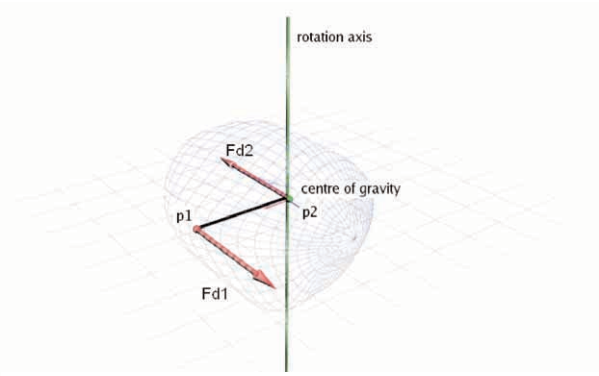

Fig. 3 Segment rotation

The resulting torque $\vec{M}_i$ is given by an expression:

$$\vec{M}_i = \vec{Fd}1_i \times (\vec{p}_1 - \vec{p}_2) \tag{5}$$

The torque $\vec{M}$ affecting the segment is then computed by:

$$\vec{M} = \sum_{i=0}^{n} \vec{M}_i \tag{6}$$

Angular speed of the segment can be computed from the torque $\vec{M}$.

Control system commands are not directly affecting forces generated in joints. Various preprocessing algorithms are used to simulate real world motors. The model of six legged robot contains virtual servo motors. Only an expected angle of the joint supplied to this servos and simple regulator generates appropriate forces. This way the behaviour of the simulated model can be externally affected. Simulation is being used for development and testing of control systems. Therefore, flawless behaviour from the physics point of view is not required. Only a decent degree of similarity between reactions of real and virtual model is needed.

Peripheral devices communication interface is a fundamental element of the application. It allows image acquiring from exter-

nal video camera using Video4Linux2 communication interface. Real robot models can be controlled via RS232 protocol. When a lower bit-rate is acceptable, the wireless data-transfer modules can be used. If necessary, the software can communicate via Internet using TCP/IP protocol too.

3. Created robots

For the purpose of practical tests we have constructed the real 6-legged walking robot. It is built from komatex plastic. We used six Hitec HS805BB and twelve Hitec HS645MG servos in the robot. Each leg is being moved by 3 of them. Whole construction has 18 DOF. The micro-controller AT Mega 16 which is placed inside the robot body receives information about a desired position of each servo via RS232 interface. Then it encodes information to PWM for the servos.

Every servo motor contains integrated analog regulator, which rotates joint to angle encoded in the PWM signal. This regulator is acting similarly to its virtual counterpart integrated in virtual servo motors.

Current supply of the robot is provided by PC-ATX power supply. Servos and micro-controller are operating with voltage +5 V. The current consumption is up to 20 A. The real robot is shown in Fig. 4.

When construction of the real robot had been finished, its virtual copy was created. Geometric parameters of real and virtual robot are nearly identical. Parameters of virtual servo motors can be changed in order to improve its performance and speed up work. The virtual model is shown in Fig. 1.

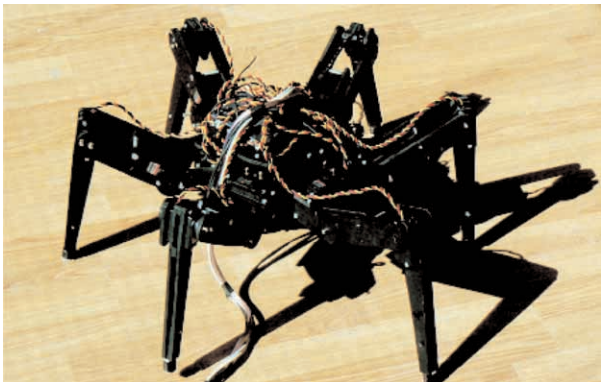

Fig. 4 Real robot

4. Control system

In order to test the behaviour of robots, a control system was developed (Fig. 5.). It allows the robot to walk in any direction, rotate and change distance between its body and a surface. The control system is divided into three cooperating blocks:

- Central control
- 6 individual leg controllers
- Inverse kinematics solver

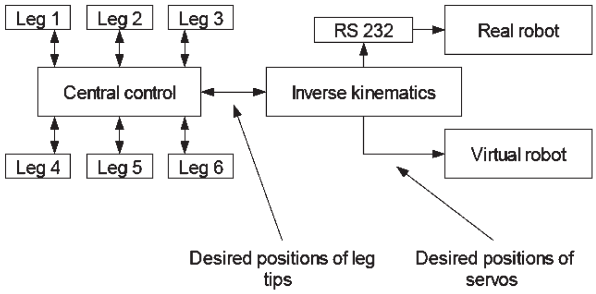

Fig. 5 Testing control system

The central control block coordinates steps of legs and its primary duty is to keep the robot balanced. At least three legs must be on the ground to ensure stability during walking. The individual leg controller must request permission from the central control before it can lift the leg from the ground. If the request of the leg controller is rejected, movement of the robot body is stopped until sufficient number of other legs is placed on the ground.

The individual leg controller generates vector $\vec{w}_i$, that defines direction in which the leg sole is supposed to move, relatively to the robot body. For example, if an expected movement of the robot body is $\vec{m}$ and the leg is on the ground, then $\vec{w}_i$ is given by an expression:

$$\vec{w}_i = -\vec{m} \tag{7}$$

The actual position of the sole $\vec{s}_i$ is then given by:

$$\vec{s}_i(T) = \vec{s}_i(0) + \int_0^T \vec{w}_i(t)dt \tag{8}$$

Leg controller acts as a simple state machine. Its states are UP, LAYING, DOWN and LIFTING. The state DOWN is the only one of the four that grants support for the robot body. Leg controller must request permission from central control block, to leave the DOWN state.

The size of the leg movement vector $\vec{w}$ varies, depending on the current state of the leg . Lifting of the leg is faster than laying and the leg on the ground moves slower than lifted one.

Each leg has its own boundaries were its tip can be moved. These boundaries depend on geometric configuration of the leg. When the leg lying on the ground is about to leave its boundaries, it is lifted and moved in opposite direction. Initially, cylindrical boundaries were chosen in order to simplify control system creation. More complex shape will increase future algorithm performance.

Inverse kinematics block transforms expected positions of the leg tips to expected angles of the joints. A simple algebraic solution is used for this purpose. This prevents any unwanted oscillations. Expected angles are used to control the motors directly. This approach allows us to change geometric configuration of the robot without the need to change any part the control system except inverse kinematics solver.

5. Experimental results

The initial tests and optimizations of the control system were made exclusively on the virtual model. Then, without further changes, the control system was connected to the real robot. During this test, the response of the real robot was very similar to the response previously observed in virtual reality. Only minor differences in specific situations were observed. This fact made doing changes of the control unit very easy, because no intensive testing on the real model was needed. When both robots were simultaneously connected to the same control system, difference between positions of their bodies became visually recognizable after 20–25 seconds. Simultaneous control was used to find hardware and software errors. For example, when power supply of one servo was partially unplugged, the behaviour of the real robot changed, but the virtual model behaviour remained the same. This directed us to a possible hardware problem, rather than a control system inconsistency. When the behaviour of both robots changed in a wrong way, the control system was checked first.

Resulting speed of the robot walking is given by expression:

$$v = \frac{l_s}{t_u + t_d + \frac{l_s}{v_f} + \frac{l_s}{v_b} + t_s} \tag{9}$$

Where is speed of the robot body movement, l_s is length of each step, t^u is time needed to lift leg from the ground, t_d is time needed to lay leg on the ground, v_f is speed of body supporting leg tip, v_b is speed of the lifted leg tip, t_s is additional time depending on current leg synchronization state. When the robot is walking straight in one direction, synchronized walking is possible and three legs move simultaneously. But when robot is moving and rotating at the same time, synchronization is lost and resulting movement is slower. This issue will be hopefully fixed during further control system optimization. Maximum walking speed achieved during our experiments was 1 m/s.

6. Conclusions

In this paper we demonstrated possibilities of using virtual reality for walking robot control system development and a simple walk control solution. Our results can be used for further research in the field of walking robot control system development. In our further work a combination of recently achieved results with artificial intelligence methods looks promising.

References

[1] LIPSON, H., BONGARD, J., ZYKOV, V., MALONE, E.: *Evolutionary Robotics for Legged Machines: From Simulation to Physical Reality,* Computational Synthesis Lab Cornell University, Ithaca NY 14853, USA

[2] DE LASA, M, BUEHLER, M.: *Dynamic Compliant Walking of a Quadruped Robot: Preliminary Experiments,* Dept. of Electrical Engineering & Dept. of Mechanical Engineering, Center for Intelligent Machines, McGill University Montreal, Canada

[3] HOPLER, R., STELZER, M., VON STRYK, O.: *Object-oriented dynamics modeling for simulation, optimization and control of walking robots,* Proc. 18th Symposium on Simulation Technique, ASIM, Erlangen, September 12-15, 2005

[4] BUSCH, J., ZIEGLER, J., AUE, C., ROSS, A., SAWITZKI, D., BANZHAF, W.: *Automatic Generation of Control Programs for Walking Robots Using Genetic Programming,* Univ. of Dortmund, Dept. of Computer Science, Chair of Systems Analysis (LSXI) Dortmund, Germany

[5] BILLARD, A., IJSPEERT, A. J.: *Biologically inspired neural controllers for motor control in a quadruped robot,* Robotics Laboratory, University of Southern California, U.S.A

[6] HAAVISTO, O., HYÖTYNIEMI, H.: *Simulation tool of a biped walking robot model, Helsinki Univ. of Technology,* Control Engineering Laboratory, Finland In Espoo, 2004, Report 138

[7] PORTA, J. M., CELAYA, E.: *Body and leg coordination for omnidirectional walking in rough terrain,* Inst. de Robotika i Informatica Industrial (UPC-CSIC), Barcelona, Spain

[8] MICHEL, O: WebotsTM: *Professional Mobile Robot Simulation,* Swiss Federal Inst. of Technology in Lausanne, BIRG & SWIS research groups

[9] HALME, A., LEPPÄNEN, I., SALMI, S., YLÖNEN, S.: *Hybrid locomotion of a wheel-legged machine,* Automation Technology Laboratory Helsinki University of Technology, Finland

[10] Aarnio, P., Koskinen, K., Salmi, S.: *Simulation of the Hybtor Robot, Information and Computer Systems in Automation,* Helsinki Univ. of Technology, Finland

[11] KINGSLEY, D. A., QUINN, R. D., RITZMANN, R. E.: *A Cockroach Inspired Robot With Artificial Muscles,* Case Western Reserve University Cleveland, USA,

[12] CHANDANA, P., BONGARD, J. C.: *The Road Less Travelled: Morphology in the Optimization of Biped Robot Locomotion,* Artificial Intelligence Laboratory, Univ. of Zurich, Switzerland
[13] COLLINS, S. H., RUINA, A.: *A Bipedal Walking Robot with Efficient and Human-Like Gait,* Dept. of Mechanical Engineering, Univ. of Michigan, Theoretical and Applied Mechanics, Cornell University
[13] MACEKA, J.: *Mobile autonomous line robot (in Slovak),* diploma thesis, Electrotechnická fakulta Žilinská univerzita, Žilina, 2005.
[14] Page of the OpenGL library http://www.opengl.org.
[15] MICHULEK, T.: *Development and graphical simulation of a mobile robot control system (in Slovak)*, diploma thesis, Elektrotechnická fakulta, Žilinská univerzita, Žilina 2005.
[16] ÚŘEDNÍČEK, Z., BUDAY, J., PLECHLO, M.: *Inductive - and Deductive Approach to Identification of Kinematic Model for the OJ-10 Robotic Operation Unit (in Czech)*, Výkonová elektronika, zborník ZTS-EVÚ, N. Dubnica, roč. 25/1990, pp. 1–5.

Fedor Kállay – Peter Peniak *

THE COMMUNICATION IN MECHATRONIC SYSTEMS

The paper deals with mechatronic systems and communication among mechatronic modules. This article proposes possible solution of usage open CAL protocol above CAN bus, which is independent from any manufacturers and can be widely accepted themselves. The main attention is paid to open CAN/CAL protocols including the viewpoint of their implementation, essential functions and potential integration within the vehicle control system. The required communication functions, communication models, communication objects (PDO, SDO) and applied profiles are being described in the CAL protocol. As an example a double bus CAN system is shown as a typical CAN/CAL solution for mechatronic systems in automotive industry.

1. Introduction

Mechatronics is the cooperation of mechanical engineering ("mecha" for mechanisms), electronic engineering ("tronics" for electronics), and software engineering. The purpose of this interdisciplinary engineering field is the study of automats from an engineering perspective and serves to view the control of advanced hybrid systems (Wikipedia), see Figure 1. The distributed control production system utilises CAN (*Controller Area Networks*) and VAN (*Vehicle Area Networks*) to link and integrate autonomous mechatronic modules.

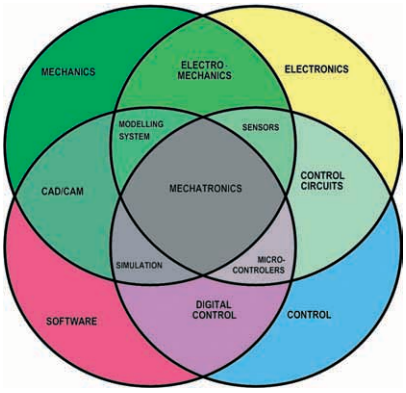

Fig. 1 Mechatronic -interdisciplinary conjuction

Automotive industry was one of the first areas where bus (fieldbus) networks for the communication of mechatronic systems in vehicles and cars was apllied. The standard CAN (*Controller Area Networks*), developed by Bosh and standardized by ISO is still the most popular fieldbus system. There are typically two different types of CAN buses used in cars that differ from each other with available network bandwidth to provide redundancy and to meet the different requirements for end devices. The first bus has a speed of 500kbps and is used for communication between main

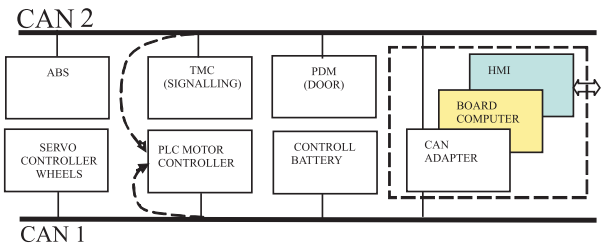

Fig. 2 Example of CAN network application in automotive industry

devices (servomotors, switches, etc.) and the second one with 125 kbps is applied as a communication system for the interconnection of the control subsystems. CAN is used mainly as

- machine control (control of batteries, servomotors of wheels, etc.),
- interconnection bus for various mechatronic systems (ABS, PDM, TMC),
- communication system for system diagnostic.

2. Communication requirements

The networks that are applied in mechatronic systems differ in many ways from standard networks covering needs of typical information systems. Some applications of different network nodes could be introduced in contrast to standard networks, prevailing communication between the machines and control units whereby the accent is put on the communication requirements of mechatronic modules. Different requirements are, therefore, focused on architecture and network protocols. Generally, the specific aspects could be sumarized into considerations:

1. *Deterministic communication* is important to provide communication in real time. It is derived from necessity to control all subsystems in real time. Therefore, each node must have the access to the bus within a defined time window that has to be assigned with access method to bus (media).

* **Fedor Kállay[1], Peter Peniak[2]**
[1] Dept. of Mechatronic and Electronic, Faculty of Electrotechnical Engineering, University of Zilina, E-mail: Fedor.Kallay@fel.utc.sk
[2] Peter Peniak, Continental Matador, Puchov, Slovakia

High noise-resistance and fault tolerance in communication. The network must eliminate influence of noise and industrial disturbance so the communication can be able to achieve functions and information without any damage. The network protocols have to allow communication in real time. It is derived from the necessity to control all subsystems in real time. Therefore, each node must have the access to the bus within a defined time window that has to be assigned with a bus access method. The network protocols have to include mechanisms for the communication correction, fail-safe behaviour and auto configuration.

2. *Peer-to-Peer/ Master-slave communication.* The network must support a typical communication for central control (Master-slave/Pooling), see Fig. 3c,b in a cyclic mode, but also provide peer-to-peer communication among mechatronics systems too, so they can cooperate with each other (Fig. 3d) according to real needs. To provide a better utilization and time response, there are also optional communication modes available for communication on-demand such as Change-of-State (Fig. 3a) or Producer-Consumer well known in industrial networks.

3. *Priority communication.* The control process requires communication distributed into hierarchical levels among groups of nodes according to rate of importance and functional classification. For communication in real time the network has to support a division of nodes to the hierarchical levels with defined priority and communication ability.

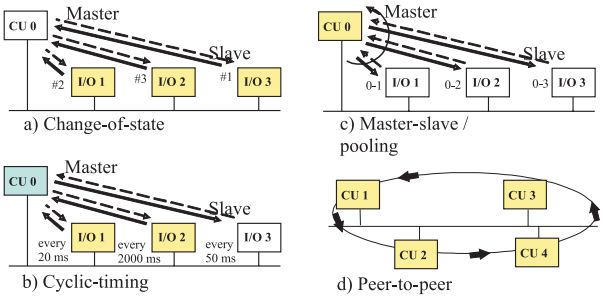

Fig.3. The used communication models for mechatronic modules

3. CAL/CAN Protocols

The application layer of CAN networks has to provide a wide stack of configurational and transfer functions for reliable interactions, including control functions and device profiles. Nowadays, there are several protocols available for CAN networks. Let's enumerate the most used:

- ***CAL/CAN** open (CAN Open Application Layer)* defined by ***CiA*** organization,
- ***CIP** (Common Industrial Protocol)* from ***ODVA*** organization *(Device Net)*,
- ***SDS** (Smart Distributed Sensors)* from ***Honeywell*** company.

The main point of this article is to concentrate on the CAL protocol (***CAN Open Application Layer***) that was developed by the ***CiA*** organization (***CAN in Automation***) in 1993 as a result of the EU research programme. The CiA dealt with open communication of heterogeneous systems via CAN bus. CAL provides applicative, independent, object oriented background for production of distributed mechatronic systems. The CAN/CAL protocol stack according to the ISO model with sub protocols is shown in Table 1.

CAL protocol stack Tab. 1

LAYER	PROTOCOL			
Profile equipment	Profile A	Profile B	Profile C	.....
7	CAL/CAN open (CiA)			
	NMT	DBT	LMT	CMS
-				
2	CAN 2.0			
1	CAN ISO 11898			

- ***LMT** (Layer Management)* – management of particular layers CAN,
- ***NMT** (Network Management)* – management and control of CAN network and net devices,
- ***DBT** (Distributor)* – assignment and distribution of identificators for network nodes,
- ***CMS** (CAN Message Specification)* – message format and protocol CAN.

The protocol defines several methods for message transfer and communication objects. There are 4 main messages used in CAL communication:

- ***AM** (Administration Messages)* – for initialisation and configuration of network nodes, assignment of CAN identificators by using sub protocols (LMT, NM, DBT)
- ***SDM/SDOs** (Service Data Messages/Objects)* – to transfer service data above 8B. These messages are also used during device configuration and for copying data buffers with lower priority.
- ***PDM/PDO** (Process Data Messages/Objects)* – defined for communication process in real time via data messages up to 8B size. The messages have high priority and could be applied for cyclic and non-cyclic communication according to the model *"producer-consumer"*.
- ***PM** (Pre-defined Messages)* – messages for auxiliary purposes like communication by way using ***"Sync Object", "Time Stamp"*** objects, and service messages like *"Emergency"*.

SDO object utilizes the supporting protocol ***"CAL Multiplexed Domain Protocol"*** to create a service channel for peer-to-peer communication of network nodes. An *"Initiate Domain Request"* procedure serves for transfering the messages up to 4B (without fragmentation). The first three octets contain an index (16b) and a sub-index (8b) that refer to the object/item ***CMO** (CMS Object)* in the object dictionary. The protocol enables reading and writing to the dictionary. The transfer of bigger blocks of data is ensured

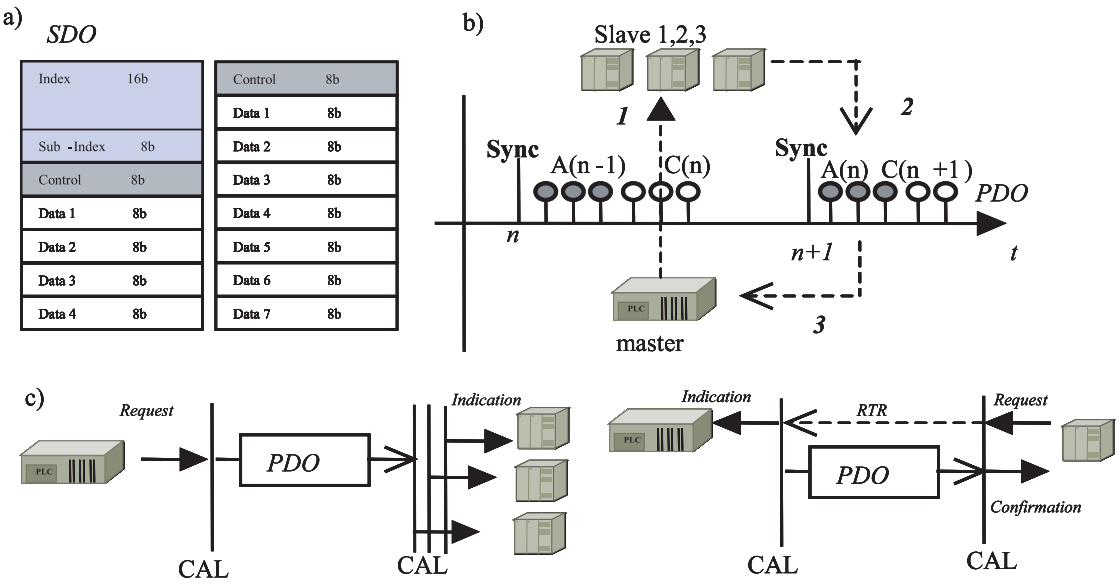

Fig. 4. The communication services of CAL protocol

by the *"Acknowledged **Fragmented Protocol**"* which allows transfer of message's fragments (7B) with acknowledging. Both protocols are shown in Figure 4a. A directory owner acts as SDO server and the remote device has a client role. Each device provides two predefined identifiers that are mapped to the SDO server and used for device configuration from network administrators' tools.

PDO object permits access to **CMO** through *variables, events* and data structures *(domain)*. These are mapped to assigned messages/objects PDO by using *"Index/sub index/data length"* in the device object dictionary. The transfer is always initiated by a client with a *"Store-and-Immediately-Notify-Event/Read-Event protocol"*. PDO objects supports communication via ***"Pooling"*** with the help of link layer services ***"CAN remote request"*** and as well ***Change-of-State*** mode with the *"Event"* object. The Event object is created by the SDO object via a service channel. Therefore, there is no need to transfer additional protocol information together with data transfer. The transfer of data is done synchronously with defined time windows according to ***"PDO-rate"*** parameters, which describe the time to send, continuation a periodically generated message ***"Sync Object"***. Another option for communication is a master-slave mode, the master generates requests for slave devices ***C** (Command Messages)*, and slave devices have to answer in following time window (cycle) by sending their I/O values ***A** (Actual Messages)*, see examples in figure 4b. Figure 4c shows the usage of *"Store-and-Immediately-Notify-Event/Read-Event protocol"*, with PDO message sending from the master. Another option is a request for data sending from the remote node.

4. Assignment of can identifiers, network management and profiles

The assignment of CAN identifiers is one of the most important functions in each CAN network. CAN identifiers are used for priority defining and addressing purposes for filtering messages among nodes. The original concept for an assignment of the identifiers assumed the static approach with predefined identifiers for typical kind of nodes (I/O device, etc.) and applications. Nowadays there is dynamic way of usage an assignment, so that CAN networks could be applied not only for defined application or object, but also for communication of the open systems. CAL protocol maintains a common list of identifiers (Pool). Each node with help of **DMT** protocol may ask for dynamic registration of free identifiers for given object or application. There are 1760 identifiers available in Pool for CMO objects. Only small part is predefined for specific purposes. For example 128 CAN identifiers were specified for monitoring of nodes (Node Guarding).

Network management. NMT server enables the network management and monitoring of the network nodes by the "*NMT Guarding*" function. The server maintains a list of active nodes and pass along "*Guard Request*" message in pooling mode, see Figure 5b. Each object has to answer for this request with the "*Operational State*" message. If a node does not answer in a defined time window NMT server creates error message. The same procedure is applied in the network node. If a "*Guard Request*" message is not received in defined time window then an error message will be generated for running applications.

Device profile is a standard tool for modelling various devices and their communication abilities. CAL defines common directory for all network "***Object Dictionary***" objects, where each object is addressed by 16-bit index and 16-bit sub index. The directory is divided into 4 parts. The first part "*Definition of data types*" is used to define all objects, the second one "*Communication Profile Area*" describes the mapping of application objects to PDO objects and defined SDO channels. The third part "*Standardized Profile Area*" consists of device profiles, for example for I/O modules, converters, engines. The fourth part "*Manufacturer Specific area*", con-

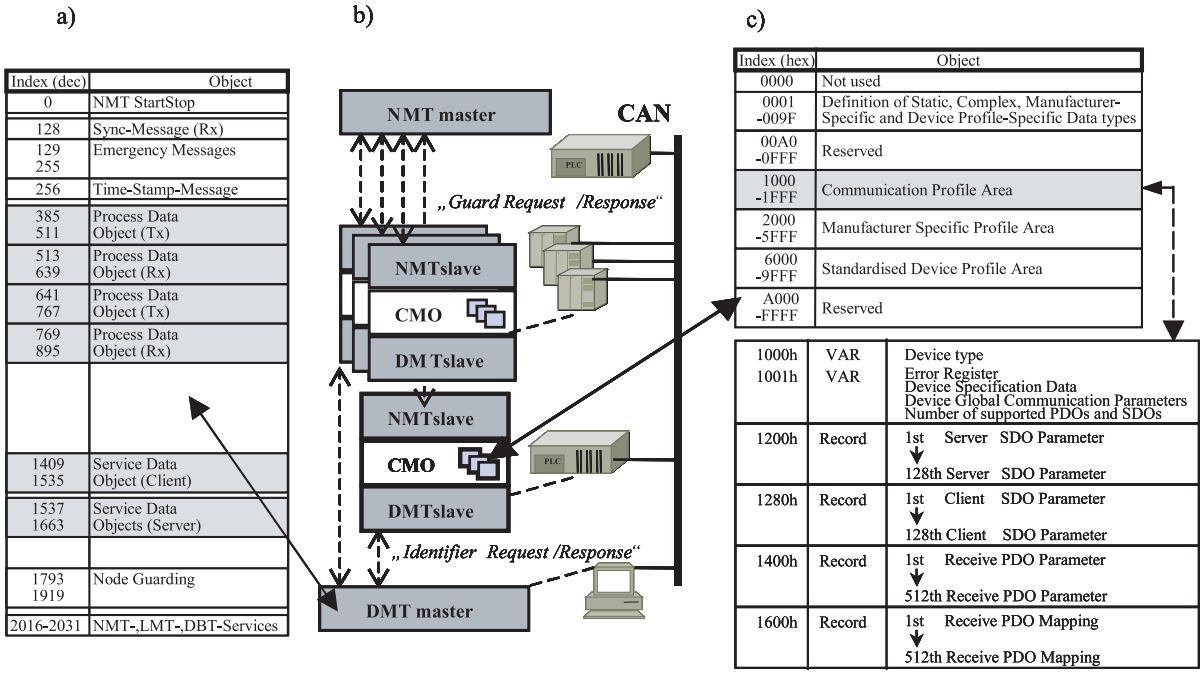

Fig. 5. Supporting services NMT and DBT in CAL protocol

tains profiles of specific manufacturer's devices. The example of CAN communication profiles is shown in Fig. 5c.

Conclusion

This article deals with the specific communication requirements of the mechatronic modules. The main intention was paid on the possible solutions for communication of the open mechatronic systems. The problem is how to design and establish the communication between heterogenic mechatronic subsystems from various producers. Then a question arises regarding the necessary communication interfaces and a way of their integration. This article proposes one of the possible solutions of applying open CAL protocol above CAN bus that is independent on any manufacturers and can be widely accepted themselves. One of typical applications was shown on Figure 2 where CAN double bus enables communication for different machatronic modules via standard CAL protocol with the defined communication objects and device profiles. CAL is the one of the perspective solutions for mechatronic applications and modules not only in automotive industry, but also in manufacturing area (CNC machines, robots, embedded devices).

Acknowledgement:

The authors wish to thank for the financial support to VEGA - Scientific Grant Agency of Slovak Republic for the projects No. 1/3086/06 "Research of the New Methods of Modelling-, Control and Simulation of Mechatronic Systems" and VEGA No.1/3123/06 "Research of Commutation Processes in the Power Transistor Structures and Optimisation of their Control at Soft-Switching Mode".

References

[1] MAHALIK, N. P.: *Fieldbus technology,* Industrial network standard for Real - Time Distributed Control, Springer, 2003
[2] KÁLLAY, F., PENIAK, P.: *Computers networks LAN/MAN/WAN and their applications (in Czech)*, Grada Publishing a.s., 2003
[3] SPALEK, J. et al: *Decision and management with artificial intelligence support (in Slovak)*, EDIS, Žilina, 80-8070-354-X
[4] FRANEKOVÁ, M., JANOTA, A., RÁSTOČNÝ, K.: *Trends in segment of communication safety of industrial networks (in Slovak)*, J. AEEE, 4/2005, pp. 250-253, ISSN 1336-1337
[5] GUTTEN, M., KORENČIAK, D.: *Utilization of neuron networks in monitoring system of power transformers,* Transcom 2003, 5th European Conference of Young Research and Science Workers in Transport and Telecommunications, Section 2, Žilina
[6] http://en.wikipedia.org/wiki/Image:MechatronicsDiagram.svg.

Viliam Fedák – Pavol Bauer *

METHODS IN TEACHING INDUSTRIAL MECHATRONIC SYSTEMS

Explanation in courses from the field of mechatronics is enough difficult due to the complexity and variety of phenomena to be explained. The introduction of computer based learning enables to make the learning easier and visualisation of variables offers a deeper insight in the system behaviour. Moreover, the introduction of e-learning into the teaching praxis makes learning in the courses more attractive for students and easier for the understanding of the presented subject. The paper describes the e-learning support of the study programmes in industrial mechatronic systems. Topics in e-learning modules are structured hierarchically starting from a system level in order to face the students with an increased complexity (top down approach). Introduced interactivity and animations allow the students to acquire a possibly deep insight into the complex and dynamic interactions of a number of parameters in the mechatronic systems.

1. Introduction

Industrial products are becoming more and more sophisticated and more complex. Continuous industrial manufacturing belongs among the most effective technologies. The manufacturing lines present mechatronic systems in industrial environment. Here, the technological operations are performed continuously on the material in form of a strip (of steel, paper, plastic, rubber, etc.), that moves continuously from one working machine to another. The production lines of such types occur in various areas of industry, e.g. in paper making machines (paper strips production), rolling mills (steel strips), production lines in chemical industry (plastic fibres and strips), and in many other industries. In fact, the processed material causes a mechanical coupling of electrical drives driving the working machines which increases complexity of the system and introduces some problems at its control.

Such a mechatronic system requires a concurrent design of mechanical, electronic, and information processing sub-systems in order to reach the cost requirements of the industry. The growing importance of mechatronics requires adequately prepared specialists. Regardless of whether the mechatronics is explicitly mentioned, almost all engineering schools have given serious thoughts and enhanced their programs so that their graduates are ready to successfully face today's industrial challenges and practice mechatronics, as discussed detailed in [1]. Nowadays, when the students incline more to the fields of study of informatics and telecommunications, education in the field of electrical and mechatronic engineering is really troublesome job [2]. The steadily decreasing ratio of the students interested in studying "soft and clean" branches of study like informatics and telecommunications to the students dealing with electrical- and electro-mechanical engineering (considered generally as "hard and muddy" ones) has led to lack of specialists in the field in many European countries.

A mechatronic engineer is an ideal solution to the problem faced by complex industrial environment but there are very few engineers of this type available. This is mainly due to the fact that the students are not encouraged to move into this field. Mechatronic courses need to be marketed in a different way, by making them more attractive, although they are seen to be difficult ones. The students need to be aware of rewards and acquired knowledge and of the fact that manufacturers have difficulty in finding these type of engineers. It is the job of the university teachers to make studying more attractive and easier accessible [3]. Web based learning tools help to contribute to fulfilment of the presented goals.

2. Object of industrial mechatronics curricula

Manufacturing lines equipped with motion control represent industrial mechatronic systems. In Fig. 1, a control structure of tandem hot-mill line is shown, that presents a typical multi-motor drive system with mechanically coupled drives. Appearance of dis-

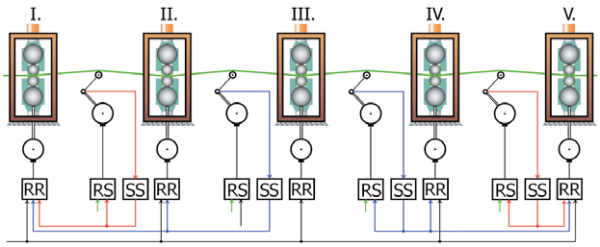

Fig. 1 Control structure of a tandem hot rolling mill as an example of a large industrial mechatronic system (RR – speed controller, RS – looper motor controller, SS – looper position sensor)

* **Viliam Fedák[1], Pavol Bauer[2]**
[1] Faculty of Electrical Engineering and Informatics, Technical University, Košice, Slovakia, E-mail: Viliam.Fedak@tuke.sk
[2] Delft University of Technology, Delft, The Netherlands, E-mail: P.Bauer@tudelft.nl

turbance (caused e.g. by inhomogenity of the processed material) in one section influences the strip tension and thickness of the material elsewhere. Thus it affects the behaviour of the whole group of drives. To eliminate this effect sophisticated control structures and algorithms are used.

A detailed analysis shows that such industrial technologic line has all attributes of a mechatronic system, consisting of mechanical, electrical and control (information processing) parts (Fig. 2a). Control of such a complicated system with many mutual couplings and dependencies requires a deep knowledge from all fields of mechatronics: mechanical, electrical and information engineering.

There are plenty of mechatronic systems of various complexities and ranges. For example, an electrical drive itself can be also considered as a mechatronic system, although a simpler one, that integrates various subsystems and knowledge from mechatronics (Fig. 2b).

When designing controllers for a single electrical drive, influence of the environment is replaced by a load torque. In case of analysed multi-motor drive, a complex multivariable system arises causing difficulties in its control. Knowledge of a graduate in electrical engineering is usually in this case unsatisfactory. The knowledge from mechanical engineering as well as production technology is also required. Without following a specialised course on mechatronics, the specialist is not able to deal with the control of such complex plant as described here.

A general problem in mechatronics is the fact that the explanation deals with rather abstract notions (e.g. for electrical engineering they are current, voltage, resistance, capacitance etc.). It has been found that students who have faced with the principles of fundamental courses (electronics, power electronics, control theory, ...) have problems in understanding the phenomena in complex mechatronic systems where the main feature is a large number of simultaneously occurring variables and changes of various substance, where the variables can vary with time, can be mutually dependent, depend on state of other system variables, etc.

Teachers may clearly discuss all the phenomena involved during lectures. However, even if computer animations are used, the students cannot grasp the details in a short time, since the teacher only once or twice shows examples or animations. There remains a need for repetition and exercises. As a side problem, students tend to get de-motivated by this complexity. This leads to the undesirable situation that increases the discrepancy between the number of students in mechatronic engineering and the demands from industry for engineers in this field. After some considerations it was decided to develop a number of computer animations showing in a systematic and consistent way the interactions of switching states, currents and voltages of different circuits of a mechatronic system.

3. Basic philosophy of e-learning platform for courses on mechatronics

The most important task at beginning of design and development of an e-learning material is its philosophy. This covers the appearance of the screens (environment), mutual linking of the screens (screen flow), introducing animation and simulation tools, introducing interactivity (external change of structure and parameters of the system), and, last but not least, presenting a way of explanation and description of phenomena on the screen and other ideas.

Each good e-learning material for mechatronics should evidently clarify the phenomena and variables that are not directly visible. In fact, nobody sees the current, voltage, mechanical stress, force, etc., but their consequences are apparent. This is why a good e-learning material should contain interactive animations to show the phenomena-component-circuit-system behaviour. The introduced interactivity brings a new dimension into education by showing and evaluating influence of a variable parameter. A possibility to change a circuit and/or system parameter by shifting a slider or inserting the parameter value presents a presumption of the system analysis.

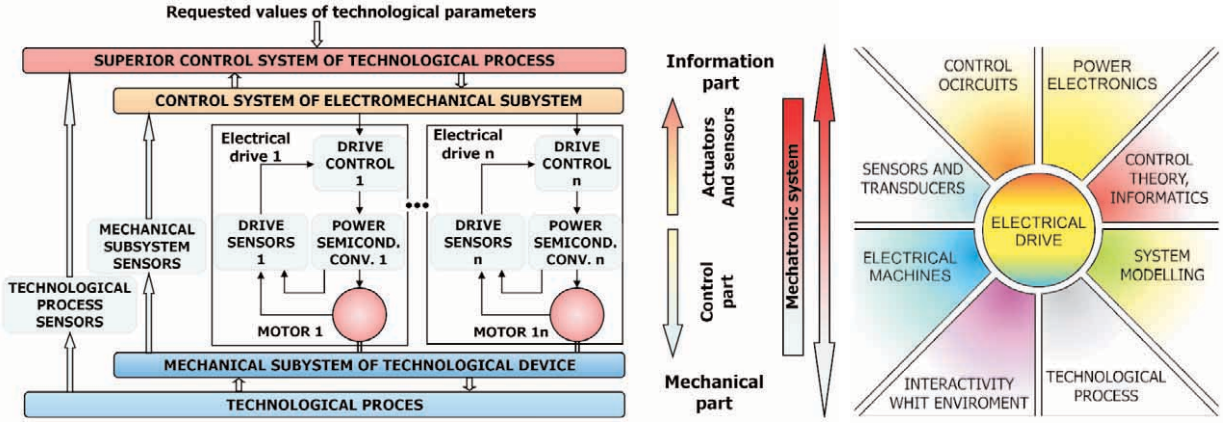

a) *b)*

Fig. 2 Decomposition of mechatronic systems into subsystems: a) multi-motor drive of the hot rolling mill, b) electrical drive

Further key point of a good e-learning material is the way of theoretical explanation. It is not a simple question which amount of textual explanation is necessary to make the basics understanding, but not too much to become boring. This fact depends on a target group – on the audience for whom the e-learning material is prepared. These are the reasons why it is difficult to design a proper e-learning material:

- if the tools are utilized as a complementary part of the lectures at the university, then the theory is mostly explained by the teacher, and the lecture notes, handouts can be used as the main source,
- short explanations in form of flowing windows appearing after any mouse activity (running over the picture, pushing buttons, etc) are usually also enough for the qualified engineers, who would like only to refresh or update their knowledge,
- much deeper theoretical explanations should be provided if the main objective is the distance learning, since the learners are expected to study most of the curriculum alone, after their work or on the weekends.

The wide spectrum of key courses to be studied in the BSc. and MSc. degrees study programmes on mechatronics covers all three fields of the mechatronics: mechanical, electrical and information engineering, mutually penetrating themselves [11].

4. Examples of e-elarning modules

The most important parts which the mechatronic motion systems consist of are the system mechanics, electrical system consisting of integrating power electronic converter, electrical drive, and the information part covering control system with implemented control algorithm. Let's show several typical examples.

4.1 System Mechanics

A large part in the curricula of courses on mechatronics is devoted to explanation of mechanic of more complex systems that in our case are presented by the multi-motor drives. Their behaviour depends on the mutual mechanical coupling properties, in our case on the form and mechanical properties of the processed material. The screen in Fig. 3a shows a simple simulation of a two-motor drive where the student can adjust elasticity and damping of the strip material and to observe their influence to oscillations of the tension in the strip. The parameters are set continuously, by a slider. The students do not learn the properties of the system only from simulation but they have a chance to verify the simulated results on the laboratory model of a technological line (Fig. 3b) that of a coiler and uncoiler, and three driven cylinders transporting the strip. Altogether five drives are mechanically coupled through the strip. In the laboratory model, the tension in the strip in each loop is measured by a position of a simple swinging arm whose force can be separately adjusted. On the right side of the figure a multiprocessor control system is shown.

Fig. 3a shows the full screen with the menu where the buttons enable to control the screen flow and other supported functions (e.g. to get the Contents, Symbols, Index, Help and more information). In order to show the screens in the following figures simpler, the menu is further omitted. The number in the left upper corner of the screens assigns the chapter number of the developed multimedia e-learning module.

4.2 Power Electronics

Power electronic converters are the main actuators of electrical motors in the drive system. When studying a certain power electronic circuit, the first question of the student is always for the different current paths in dependency of the switching states and certain impressed currents and voltages. With traditional teaching a current paths are drawn using different colours into some figures of the power circuit, or the teacher presents slide-shows in the classroom. Here the approach of interactive animations is used.

To illustrate the ideas mentioned above an example is shown here. The square wave generation principle shown in Fig. 4 pre-

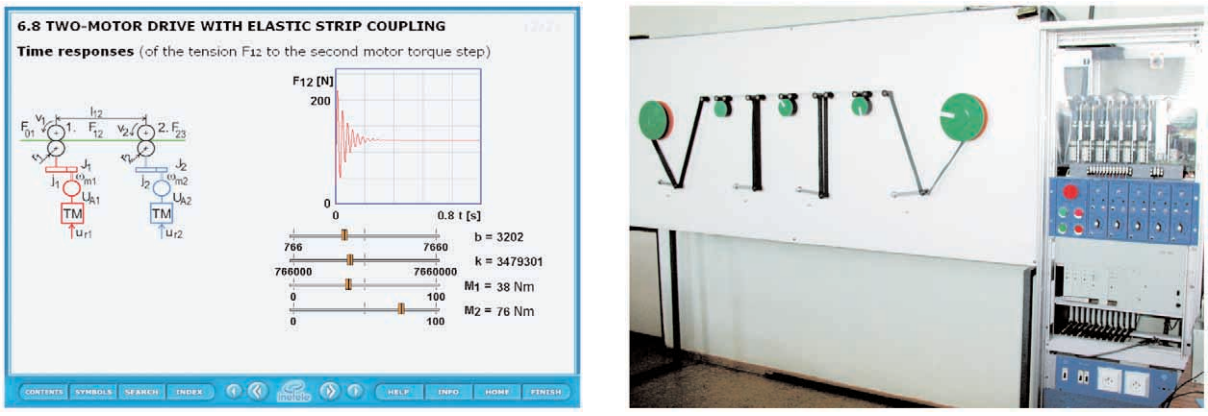

a) *b)*

Fig. 3 A multi-motor drive with mechanical coupling through the strip of the processed material as an example of an industrial mechatronic system: a) block diagram with time response of the strip tension, b) laboratory model

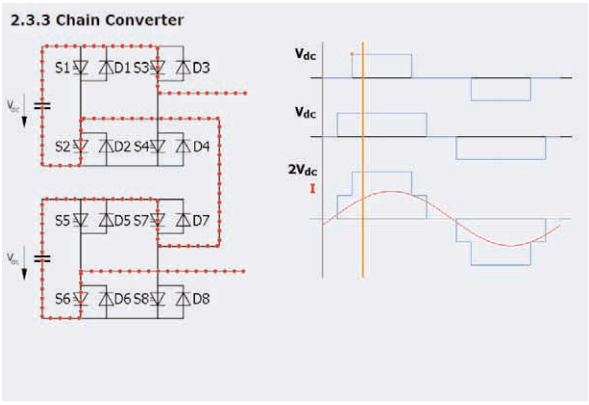

Fig. 4 A single-phase structure of an m-level cascade inverter

sents a basic switching strategy used for high power converters. The continuously running animation was replaced by a static one where the cursor (orange vertical line in the time diagram) can be shifted in time. This solution gives a possibility to explain circuit behaviour given by switching states of the power semiconductor devices in the required time instant. The chain circuit represents a straightforward approach to the realisation of a multi-level converter for use in high power applications without the need for magnetic combining circuitry and complex transformer arrangement. The main advantage of this approach is the well-defined operating environment for each three-level pole within a substantially isolated H-bridge circuit.

4.3 Electrical Drives

In an open-loop drive system, consisting of a power electronic converter and motor, the students learn properties of the drive from time courses of the system typical variables (voltages, currents, magnetic fluxes, motor torque and shaft speed) in the dynamic and steady-state states.

A typical example from the field of AC electrical drives supplied by a voltage-source inverter (VSI) in Fig. 5 shows time courses of the drive typical variables – the phase voltage of the motor, the stator current, the electrical torque and the speed.

The student can set up the frequency of the inverter switching and thus study influence of the six-pulse converter switching on the motor behaviour, separately at low frequencies where the oscillation of the speed occurs and at higher frequencies. The frequency is set by the orange colour slider. The built-in switch enables to demonstrate frequency starting and direct connection of the induction motor to the pre-set frequency. More advanced topics deal with eliminating the torque and speed oscillations by introducing other switching algorithms (different PWM techniques) for the inverter.

4.4 Motion Control

Here, the students learn various motor control structures and a design of motor controllers from the point of view of ensuring performance criteria. The most important is to explain the system behaviour, to show the procedure for controller parameters calculation and to show the time courses of the inner and output drive variables.

To eliminate sensors, the control structures of modern drives involve also observers of inaccessible system variables. Fig. 6 shows an example of a linear state and disturbance observer [10]. Their time courses of observed state variables and disturbance are shown after opening the block of the scope as shown in the Fig. 6b.

Necessary calculations for the observer gains would disturb the attention of the students at explanation of performance the observer. This is the reason why they were put in the secondary screen which is opened after clicking on the "Example" button. The observer parameters are calculated based on the system eigenvalues and observer chosen eigenvalues (i.e. on the desired characteristic polynomial). Based on the procedure, the student can calculate observer parameters for own system.

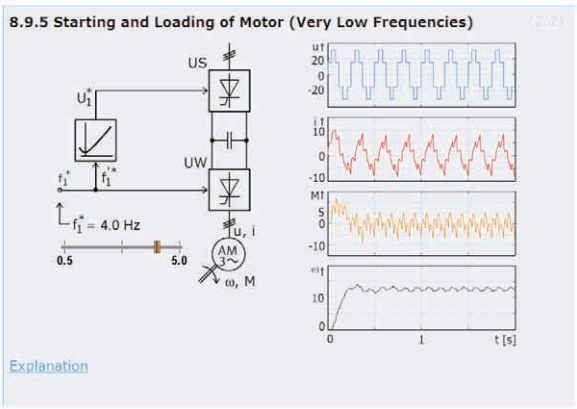

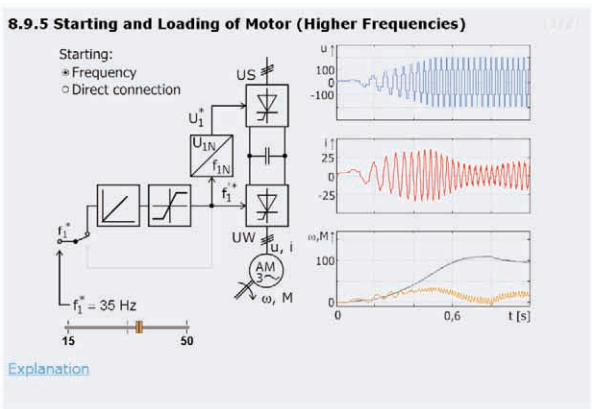

a) *b)*

Fig. 5 AC drive with VSI: animation of drive behaviour in area of low (a) and higher (b) frequencies

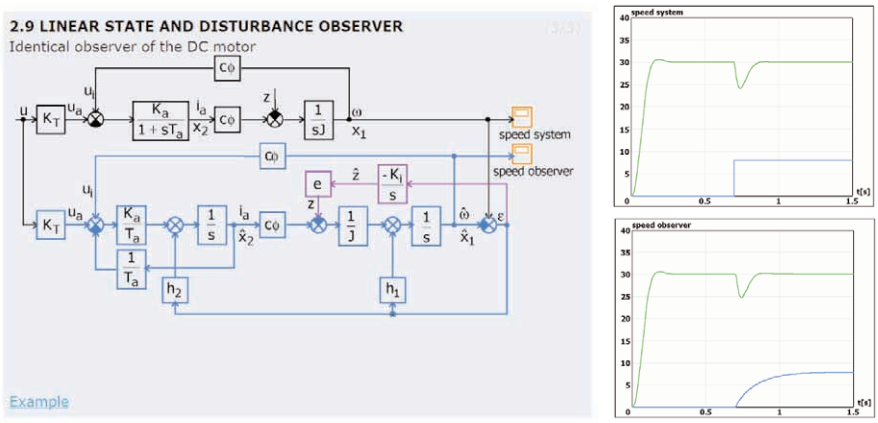

a) *b)*

Fig. 6 a) Block diagram of a DC drive with state and disturbance observer and b) time responses of the actual and observed speed and disturbance (load torque)

5. Conclusions

The paper gives an overview of needs and skills required by the engineers working in the mechatronic system environment. After a brief presentation of the background of the curricula in mechatronics the paper shows philosophy of the web based interactive modules supporting the courses. They were developed not only in order to make education easier but also with the aim to attract the students to follow the accredited courses on mechatronics. On several screens there are some typical results from realised e-learning modules presented, enhancing the used philosophy and ways of visualisation.

The e-learning approach helps to understand coherences in complex mechatronic systems but it presents a part of education only. The training is also supported by a laboratory equipment where the students get practical experience.

The animations in the modules were realised in Macromedia Director environment and finally implemented in the html using Macromedia Dreamweaver. The Macromedia software can develop interactive graphical user interfaces that are easy to use.

References

[1] 2nd IFAC Conference on Mechatronics Systems, Dec. 2002 Berkeley, California, www.unex.berkeley.edu/eng/mech/
[2] BAUER, P., KOLAR, J.: *Teaching Power Electronics in 21 Century, EPE Journal,* vol. 13, Nov.-Dec./2003, ISSN: 0939-8368.
[3] UNDELAND, T. M., MOHAN, N.: *Teaching Electric Machines and Drives: A re-examination for the new millennium,* 11th *Int. Power Electronics and Motion Control Conf. (EPE-PEMC 2002)*, Dubrovnik, Croatia, 2002.
[4] FEDÁK, N., BAUER, P., HÁJEK, V., WEISS, H., DAVAT, B. et al: *Interactive e-Learning in Electrical Engineering, Int. Conf. on Electrical Drives and Power Electronics (EDPE'03)*, The High Tatras, Slovakia, pp. 368–373, 2003, ISBN 80-89114-45-4.
[5] BAUER, P., FEDÁK, V.: *Educational Visualization of Different Aspects for Power Circuits and Electrical Drives, 11th Int. Power Electronics and Motion Control Conf. (EPE-PEMC 2004)*, Riga, 2004, ISBN 9984-32-010-3.
[6] FEDÁK, V., REPISCAK, M., ZBORAY, L.: *Design and Implementation of E-Learning Tool for Courses on Electrical Drives, Int. Conf. on Electrical Drives and Power Electronics (EDPE 2005)*, Dubrovnik, 2005, CD ROM - E05-115, ISBN 953-6037-43-2.
[7] UNDELAND, T. M.: *There is a Need for Changes in PE&ED Education at Universities, EPE Journal,* 1/2002, ISSN: 0939-8368.
[8] FEDÁK, V., FETYKO, J.: *Interactive Solutions Design for E-learning Course on Mechatronics, 3rd Int. Conf. on Emerging Telecommunications Technologies and Applications (ICETA 2004)*, elfa, Košice, 2004, 431-433, ISBN 80-89066-85-2.
[9] HAMAR, J., FUNATO, H., OGASAWARA, S., NAGY, I.: *New E-Learning Tools for DC-DC Converters, 11th Eur. Conf. on Power Electronics and Applications (EPE 2005),* Dresden, ISBN 90-75815-08-5, IEEE Cat. Number: 05EX1132C.
[10] ZBORAY, L.: *Controlled Drives, E-learning module. INETELE,* VUT Brno, 2005, ISBN 80-214-2978-X
[11] FEDÁK, V., FETYKO, J.: *New Courses on Large Industrial Mechatronics Systems at the FEEI TU Kosice, Int. Conf. on Electrical Drives and Power Electronics, EDPE 2005*, Dubrovnik, 26-28 Sept. 2005. CD ROM - E05-114. ISBN 953-6037-43-2.
[12] FEDÁK, V., ĎUROVSKÝ, F., FETYKO, J.: *Web-Based Support of Courses in Industrial and Automotive Mechatronics, 12th Power Electronics and Motion Control Conf. (EPE-PEMC 2006)*, Portorož, 2006. ISBN 1-4244-0121-6. IEEE Cat. Number 06EX1282C, pp. 2118–2123.
[13] SÜTŐ, Z., NAGY, I.: *Nonlinearity in Controlled Electric Drives: Review, IEEE ISEIE 2006*, July 9-12, Montreal, pp. 2069–1076.

Pavel Pavlásek *

E-MECHATRONICS: DIGITAL CONTENT IN TRANSFORMATION OF TEACHING AND LEARNING

This article deals with mechatronics as a one of the leading and fast growing world industrial and economic sectors, for which in educational niche it is critical to provide enriched digital contents through a homogenous training tool. Mechatronics is from now based on historical know-how but truly needs to evolve through enhanced collaboration with various industries: home and office products, transport, automotive, space, etc. Providing the eContent of mechatronics as a common training tool that will help these multidisciplinary collaborations and strength exchanges within these scientific and technological areas eMECHATRONICS will position itself at the junction of mechanics, electronics and software engineering. The article is based on more than 15 years experiences at University of Žilina in mechatronics, and linguistic contribution, as well as in the analysis in the existing digital content, knowledge and know-how available at the educational, professional and public level in these different scientific and technological domains. Such eContent will serve, as described in this article, to propose and enhance web-based training services, providing mechatronics-related knowledge according to the individual level, language competency and needs of its users, may they be students, professionals or individuals.

1. Introduction to eMECHATRONICS

eMECHATRONICS represents a significant role of an amount of training documents, case studies and other relevant materials and tools providing mechatronics added value knowledge [1]. Nevertheless such support truly needs to be enriched, mostly to enable interactions between the mechatronics various scientific and technological areas to be covered. The eMECHATRONICS web-based training solution will then propose enriched digital content according to its user's origin, level of scientific and technological expertise and knowledge as well as of its previous use of the eMECHATRONICS service. eMECHATRONICS will also ensure multilingual and cultural adaptation. eMECHATRONICS work to be carried out will include:

- Search, define and classify existing documents.
- Analyse the user needs and manners of solving problems in order to propose solving problem typologies to be implemented in the user interface,
- Define the user needs in view of constituting the ontologies to improve by means of semantic technology the annotation, enrichment and organisation of existing digital content.
- Construct the tools to search and enrich the existing educating digital documents, the training tool and user-friendly knowledge database interface.
- Constitute the database, implement it within the training tool and test and adapt it after validation by a first end-user group.
- Define the various levels of information and their access (private, common or public information), the intellectual rights and quality survey of the product.
- Implement the tool for profiling, filtering and managing the digital content taking also into account the economic return for each content producer.
- Adapt and implement the tool and content of the learning service to user with various profiles and languages.
- Widely deploy and constantly update the eMECHATRONICS service.
- Implement wide commercial eMECHATRONICS training service.

2. The eContent characteristics

Digital content, in modern eContent, is oriented to university and market programme which aims to support the production, use and distribution of digital content and to promote linguistic and cultural diversity on the global networks. eMECHATRONICS will implement continuous activities devoted to the control and assessment of the progress and results in mechatronics [2], [3], [4]. Indicators and metrics should be defined to achieve such evaluation, among them we can note:

- number and quality of reachable digital documents contained in the knowledge database,
- number of entries of thesaurus, meta-data specifications and domain ontologies and content of multilingual glossary,
- number and quality of training elements and completion and quality of problem solving tools,
- quantity and quality survey with statistics about access count to the database, to the training and decision-helping tools with duration of use and training time.

Digital content and networked applications will support transformative changes in the approach to teaching and learning of mechatronics. In order for these changes to lead to increased educational opportunities for all students, digital content and net-

* **Pavel Pavlásek**
Faculty of Electrical Engineering, University of Zilina, E-mail: Pavel.Pavlasek@fel.utc.sk

worked applications must be independently judged to be of high quality in the terms of science and didactical effectiveness, well-documented, comprehensive and available for all grades heterogeneous groups and have the power to insipre or motivate students. In addition, eContent must be easy to find and access, easy for students and teachers to use. Todays CA.instruments offer tremendous opportunities for creation of powerful eContent by helping students to comprehend difficult to understand mechatronical concepts, helping students to engage in learning, providing students with access to information resources and remote technology. eContent makes better contribution to the students individual needs, and improve the accountability and effeciency of university administration. High speed connection to the Internet had the opportunity to expand and extend eContent previously established learning program. At the time eContent established itself as a leader in mechatronics training in CA.technologies (CAD software), remote access to online hardware units (Rapid Prototyping machines), development and test software (Virtual Labs – Matlab, Simulink, LabView, etc.) and video conferencing as a regularly scheduled master classes, one-to-one teaching sessions, educational and community programs, and professional development programs [5], [6], [7]. The manufacturing lines present mechatronic systems in industrial environment. Elements critical to eMECHATRONICS education – visual imagery, movement, virtual modelling, parameters simulation, and the like are almost completely compromised with the real environment, and although many innovation in technology, the limits of the support are in eContent of mechatronics [8]. In so doing, we will enable a virtual teaching and learning experience that simulates and in many ways enhances the real live experiences. According to actual technology support, we are able to regularly produce eContent and deliver high-quality interactive education programs over network to participants on university level. For example, one of our most innovative and powerful area of eContent application – visualization and simulations improved the complex machine operation in automotive industry (Fig. 1).

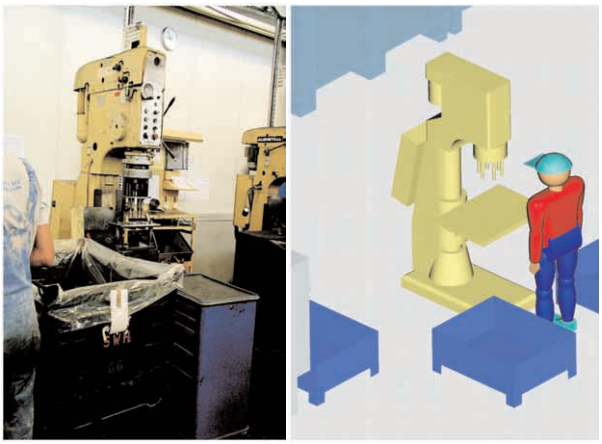

Fig. 1 Imagery (left), movement, virtual modelling and simulation of personel operation (right) in the real environment [5]

The aim of transformation to eMECHATRONICS is to contribute to knowledge economy development by facilitating access and usability of enhanced eContent of mechatronics to all potential users and especially to those from the educational and professional areas. Digital content players in mechatronics are of all sizes, i.e. universities, content creators and owners, packagers and designers, language and customisation players, publishers and distributors, net services companies, rights trading actors, capital market players, experts and market enablers [9]. The main problems encountered in the mechatronics environment are dealing with the integration of several independent well-known techniques from various domains (mechanics, electronics and computing), which, when in synergy, generate easier, more economical, reliable and versatile systems. However their interactions are more difficult to control. Moreover, the mechatronic systems are often critical and their reliability crucial. The educational technology and products are getting more and more complex with immense cost pressure. The mechatronic system requires manifold technology combination of different engineering disciplines, which were traditionally educated separately. It requires new modelling tools and complex systems simulation and standardised software, which facilitate better co-ordination on the development process amongst the various actors. These are classical mechanics and mechanical engineering, material studies, electronics, electrical engineering, drive and control technology, sensor technology, computer science, technical image processing and many more. In engineering education, mechatronics is rapidly expanding, especially in automotive industry, where great successes in the area of robotics, drive technology and automation in vehicle manufacturing have been achieved. In a global and strongly competing industry, mechatronics represents a competitive advantage for the Slovak industry. Universities and productive companies in industries like railway have significant competencies in mechatronic technologies, which already exploit this type of devices (Fig. 2). Market of mechatronic devices in the car industry (sensors, convertors and actuators) already represented nearly 32 billion Euro in 2005 [10]. Mechatronics represented in 2005 nearly 30% of the cost of a vehicle (25% for electronics). The period 2005–2010 will conduct to a stabilisation of this market. An average growth of 0.4% over the period will lead to a 32.7 billion Euro market. Mechatronics in the car industry will represent in

Fig. 2 Virtual art model based on sophisticated technologies for eContent application (designer's model) [12]

2015 a sales turnover close to 39 billion Euro. Those previsions do not include the progressive penetration of hybrid vehicles. Just like the first developments of electric vehicles marked the arrival of mechatronics, vehicle's hybridisation could be a significant catalyst of mechatronics in the car industry. The European car industry is also facing a very dense lawful and normative context. This context exerts a determining influence on the one hand on the development of electronics in the vehicle and on the other hand on the design methodology and industrial processes of manufacturing.

All the directives contributed at the European level to accelerate the evolution of the technologies deployed. Those new materials, new procedures and new devices are requiring more and more adequacy between basic mechatronical technologies – electronics, mechanics and computing (software, hardware). Moreover, they constitute a barrier at the additional entry on the European market in an increasingly intense competing context. The principal stake of mechatronics is to better take into account more complex interfaces of different natures: technological but also human and organisational. This new context requires closer relations between universities, manufacturers, equipment suppliers and other industries.

3. Basic Principles of eMechatronics education

The development of eMECHATRONICS requires educating and training people to a broad panel of technologies. Such professionals will later on assume within their organisation the role of interface between its various development teams. As demonstrated below (Fig. 3, Fig. 4 and Fig. 5), educational activities and eContent materials can come from many different sources, both inside and outside organization (demonstrated shining example of concurrent methodology come out of the R&D company, university, and railways). Organization's eContent strategies were focused on the diversity of eContent offerings – production, professional training, and university education.

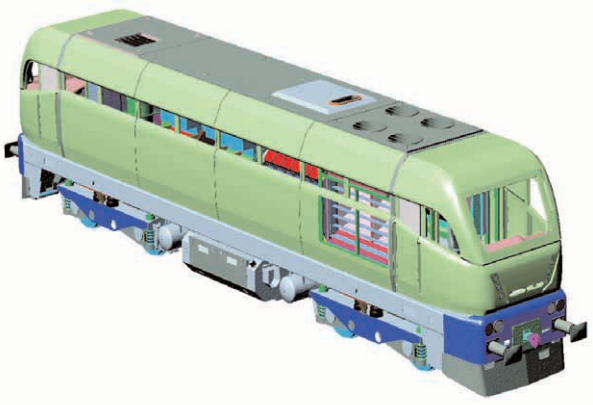

Fig. 3 Virtual parametric model based on sophisticated technologies for eContent application (diesel-electric locomotive in Pro/ENGINEER) [12]

Fig. 4 Standard eContent application (diesel-electric locomotive in Pro/ENGINEER) [12]

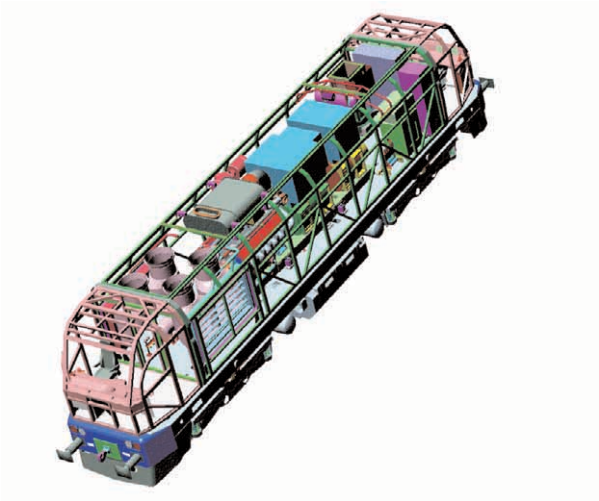

Fig. 5 Virtual parametric model based on modular units for eContent application (diesel-electric locomotive modules in Pro/ENGINEER) [12]

eMECHATRONICS characteristic shows educational needs in a broad spectrum of scientific and technological areas:

- Mechanics,
- Analog and digital electronics,
- Automatic control and algorithmic,
- Networks and associated software (including embedded real-time software),
- Electrotechnics and power electronics, materials and chemistry,
- Design and ergonomics,
- Assembling and packaging,
- Industrial process, etc.

The eContent of mechatronics – documents, case studies and other relevant tools do exist within the universities and faculties, but they truly need to be enhanced and completed for eContent

strategy so a wider range of possible interactions between the mechatronics various scientific and technological areas be covered [1]. One of the eMECHATRONICS main task will be the selection of analysed documents and its high quality indexing so it fit precisely to the user needs may it be student or professional. The results of its search will be very useful according to its origin, level expertise and knowledge as well as previous use of the eMECHATRONICS service [11]. Concerning multilinguism and cultural adaptation, the achieved solution will provide educational eContent according to the user profile in terms of professional qualification and language. In the first step it is bilingual Slovak/English version of eContent.

4. Analysis of the demands on eContent strategy

The results of the eMECHATRONICS based on eContent strategy will be adapted to various educational needs (initial training for students and engineers, on the job training for improving qualification of workers, on demand training and solving problems interface for conception and case study analyse), and level of knowledge, technological backgrounds, languages and cultures [12]. The eContent works as a dynamic factor at providing enriched digital content to be found on a really easy and quick way. For young engineers the proposed eMECHATRONICS platform will be an open training area enabling them to learn from senior engineers inputs and arouse their mechatronics awareness using virtual parametric models. The eMECHATRONICS platform will also help to formalise a large variety of eContent: basic training such as an introduction to mechatronics, up to advanced training on specific mechatronics topics or problems. The eMECHATRONICS concept will also help to facilitate cross-fertilisation between disciplines, sites, and companies, in order to find innovative solutions through the implementation of problem solving libraries and tools [1], [8]. In this way, the eMECHATRONICS platform will help to offer the experts, art designers, engineers and technicians' community a large access to mechatronics best practices and know-how. As a result of eContent strategy, eMECHATRONICS should be a major contribution to improve Slovak economy competitiveness as well as components and products overall quality and safety. The eMECHATRONICs users will mostly be in engineering study program students from the network of universities and technical schools as well as professionals from the industry [12]. The OEMs and customers can also be included among the eMECHATRONICS users to identify common strategies and future requests. Regarding students to be targeted, they are several thousands to be taught mechatronics related contents in universities or specialised schools [13].

5. Description of the objectives and the proposed solution

The actual tasks of the eMECHATRONICS are willing to form a workgroup, which will build up the structure, method and service for an effective deployment of a bilingual learning tool dedicated to students and professionals concerned with mechatronics. The proposed service will target the real needs of those end users, faced with questions in various scientific and technological fields in which they are not educated and or trained. They may just not have a global view or ignore some scientific and technological interactions, for example between material and physical environment of a technical piece, an electronic chipset and embedded program. The eMECHATRONICS service will propose training elements in relation with a specific question asked through the service. It will then contribute to help understand basic and constituting scientific and technological elements as well as provide some clues to solve problems dealing with issues such as conception, design and production of new integrated elements [14], [15].

eMECHATRONICS will be structured so as to adapt eContent to be provided with the scientific and technological level of qualification of the user, its past search and queries, its knowledge in different domains, learning styles and possible interactions analysed by the system [16], [17]. The constituted database and the user interface will also propose a bilingual tool (in Slovak and in English and possibly with other additional languages) in order to propose a wide understanding (the international industrial companies involved in the mechatronics niche in Slovakia have a huge amount of documents in English). The eContent could be classified according to the mechatronic's principal domains (mechanical, electrical, control and computing) with the help of domain ontology classification (Fig. 6).

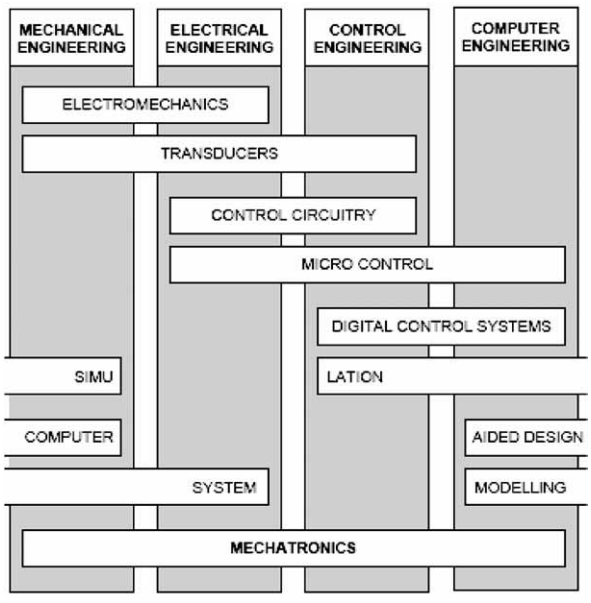

Fig. 6 The eContent classification according to the mechatronic's principal domains [18]

Meta-data on language, region, source type, term classification and text type could also be indicated [18]. To achieve this overall objective, the eMECHATRONICS task will provide:

- knowledge anagement database constituted with existing documents,

- bilingual glossary about mechatronics based on existing ones to be adapted and completed,
- knowledge management base tool aimed to prepare and assist the enrichment, classification and organisation of existing eDocuments in order to make them more accessible, usable and exploitable,
- training database adapted to the training needs of users constituted with existing training tools improved in terms of quality, efficiency and user-friendly characteristics,
- user-friendly interface based on the analysis of user needs, questions, usual queries, problems and habits of searching as well as on the analysis of possible methods of solving their problems so the results be presented in a manner adapted to train them on the basic knowledge needed to solve the problem they are faced with.

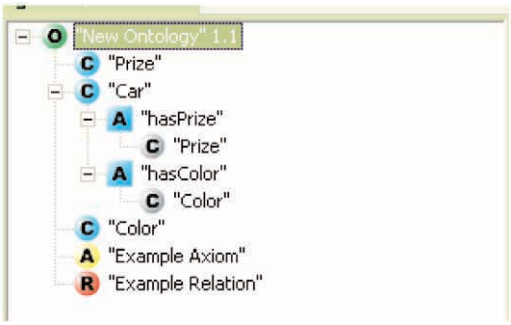

Fig. 7 The integrated ontology editor for editing, browsing and classification for eContent [18]

Therefore, the future work in eContent will carry out the following tasks:

- Search, define and classify existing documents.
- Analyse the user needs and manners of solving problems in order to propose solving problem typologies to be implemented in the user interface,
- Define the user needs in view of constituting the ontologies to improve by means of semantic technology the annotation, enrichment and organisation of existing eContent (Fig.7).
- Construct the tools to search and enrich the existing educating digital documents, the training tool and user-friendly knowledge database interface.
- Constitute the database, implement it within the training tool and test and adapt it after validation by a first end-user group.
- Define various levels of information and their access (private, common or public information), the intellectual rights and quality survey of the product.
- Implement the tool for profiling, filtering and managing the eContent taking also in account the economic return for each content producer.
- Adapt and implement the tools and content of the learning services to user with various profiles and languages.
- Widely deploy and constantly update the eMECHATRONICS services.
- Implement the commercial eMECHATRONICS training services.

At the beginning of the work on the eMECHATRONICS research, development and educational experts, designers, engineers, manufacturing technicians, are daily confronted to:

- choice of design solutions,
- interfaces design and development, test, maintenance, between mechanical parts,
- electronic components and software,
- components manufacturing and maintenance processes and devices.

Through the specific activities, various know-how, return of experience, documents, are available for the benefit of eMECHATRONICS. Concerning complementary existing documents, the searching and indexing system that will be built throughout the transformation to eContent will allow to search on the Internet every other interesting digital content which could enrich the eMECHATRONICS service. So, eContent can be enriched, classified and prepared to be published, brokering services, integrated in the eMECHATRONICS system will support the reusability of any kind of documents.

6. Bilingual and multicultural aspects of the eContent

eMECHATRONICS will use the termontography method, which is a multidisciplinary methodology for development of bilingual terminologies. Language-independent domain ontology is constructed and confronted with textual material in different languages. As a result of this confrontation, the framework gradually evolves in an enriched semantic network, reflecting the differences in language, culture and knowledge. The method and tools have been applied in pilot activities in the field of automotive engineering: the compilation of multilingual terminology of an internal combustion engine. This has enabled to constitute a first base of glossary with no more number of words. For the aim of this article, a platform supporting aspects of multilingual knowledge management were used. The final valorisation of existing eContent and organisation of the data will enable to make it accessible for different types of users and applications in different languages. In an initial phase, expert knowledge is used to identify key categories, concepts and conceptual relations by adaptation of the existing multilingual knowledge. In termontography the classification of domain-specific texts uses the domain ontology of the previous phase. In the next phase of transformation to eContent, a multilingual corpus with relevant textual information will be created. Documents will be classified according to the three domains (mechanics, electronics and computing). Meta-data on language, region, source type, term classification and text type will also be indicated. In a third phase, relevant terminology will be extracted from the domain-specific texts. The terms will be connected to categories and concepts of the categorisation framework. Terms, but also definitions, explanations, examples, legal restrictions will be extracted from the documents. The extracted terms, term descriptions and laws will be displayed in the annotation tree. During the term extraction phase, the categorisation framework will enable further refinement. For example, language and culture-specific concepts could be added to the domain ontology. The termontog-

raphy workbench will also have features to add terminological information to the extracted terms.

7. Expected results from transformation of teaching and learning

As the main expected result of the transformation of mechatronics to the eContent strategy, there will be a tool dedicated to training and problem solving in the field of mechatronics usable both by students and engineers who are in everyday contact with mechatronical problems. Transformation to the eMECHATRONICS platform will be based on the following expected results:

- a bilingual indexing tool for documents (studies, research cases, training documents...), and as result,
- a bilingual knowledge base in the field of mechatronics aimed to training of students and professionals,
- a set of methodologies aimed to solve complex problems of integration in mechatronics.

The diversity of eContent formats described in this article indicates that the online learning landscape is highly varied and in a state of flux. Given the many interesting ways to connect people with learning materials and with each other, there is really no reason to continue with the "page-turning" model of e-learning. At the same time, the design of e-learning has become more complex and requires a new set of instructional design skills. Effective teachers know that eContent, used in its broadest sense as an educational task or experience that has some impact on the learner needs to be placed in context and needs to be adapted to the learning abilities, interests, and level of previous knowledge of the learner.

8. Performance and success indicators

Within the lifetime of the eContent preparing, constant evaluation will be going on in order to measure the progress achieved and if needed bring corrective measure to ensure the highest level of efficiency, among the activities to be carried out one can note:

- The number and the quality of reachable digital documents contained in the eMECHATRONICS knowledge database.
- Number of entries of thesaurus, meta-data specifications and domain ontologies and content of multilingual glossary will also be surveyed.
- Number and quality of training elements and completion and quality of problem solving tool will also be supervised.
- On the user side, quantity and quality survey will be carried out and will include statistics about number of access to the knowledge database, to the training tools and to the decision-helping tool, including duration of document use or of training time (Fig. 8).

The eMECHATRONICS development is answering to a crucial and actual evolution of the Slovak industry and its achievements will help to make aware both the educational and professional environment of the rapidly changing industrial context and of the necessity to reinforce production organisations' personnel knowledge and know-how on a broad spectrum of scientific and technological areas. The eMECHATRONICS system will in addition complementary to indexing and ontologies identify the documents with their origin (author, owner), value (level of interest, complexity and quality) and status (public, restricted, internal, and private). It will then be easy to complete the system with a brokerage system which will help to evaluate the market value of each document by testing document and knowledge exchange within the participating partners. Interested in the implementation of the eMECHATRONICS system in their professional organisation, the project industrial partners will enable a large dissemination of the results through the network, members, clients, subcontractors and peers. Leaning on a well-adapted and high quality product responding to the user-needs, such service will be easy to replicate to similar challenges. As the system and the methodology developed for eMECHATRONICS is intended to be enlarged or adapted to other domains or fields of interest.

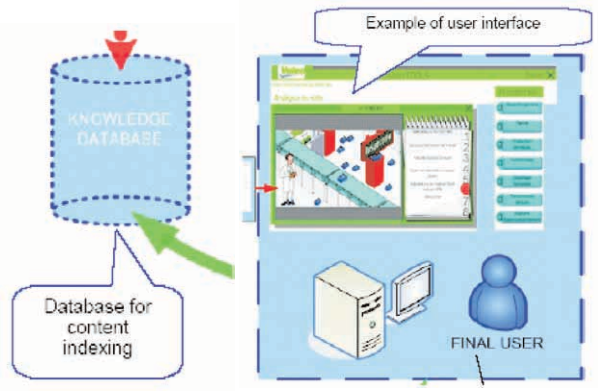

Fig. 8 The user's side of eMECHATRONICS with access to knowledge database, training tools, and decision-helping tools [18]

9. Analysis of digital documents

The first work in transformation of mechatronics to eContent will help to define precisely the amount, origin, format, type, language, quality and level of existing digital documents aimed to the use of the eContent strategy, which means documents in the field of mechanics (mathematics, physics), electronics and computer engineering which can be valorised and be used for training purpose. We will also refine our user comprehension by analysing their needs of information and training through case studies with students and employees on their workplace. Qualifying the available digital documents we have to:

- define the criteria of qualifying the available digital documents,
- put on a list of digital documents,
- analyse them by defining their origin (libraries, web, public databases), format (DOC, PDF, graphics, drawings, 3D models, videos, etc.), language, the level of difficulty or speciality, and usability (ready to use or need to be rewritten).

10. Description of the future work in eContent strategy

The investigation of transformation to the strategy eContent will cover the "in-faculty case study" starting from a "problem solving" methodology. Starting from the "mechatronics problems" encountered within the faculty, we have to proceed initially to a clear definition of the problems. This definition starts from a grid of collection, which specifies in particular the noted disfunction, the generated effects, the conditions of use, etc., and then applies a grid in several studies in real situation in the university and the companies. Once the problem identified, this stage of search for causes will be carried out in "expert system". The search for cause and the search for solution of a "mechatronic problem" (complex and relatively new) will constitute the guide for the consultation of databases. The case study will make it possible to check, in which proportion the technical documentary resources meet the mechatronics needs for the companies and will also make it possible to work to improve the access to these resources [18].

Conclusion

In response to the educational opportunities made available by dramatic technological innovation in the end of 1990s, the eContentplus 4-year programme (2005–2008), proposed by the European Commission in February 2004, will have a budget of _ 149 million to tackle the fragmentation of the European digital content market and improve the accessibility and usability of geographical information, cultural content and educational material. This article has presented far-reaching reason for an effective use of technology in mechatronics education to be better educated and better prepared for the role of eMECHATRONICS in the new Slovak knowledge-based economy. The principal stake of eMECHATRONICS with transformation of knowledge to eContent is to coordinate work and communication between individuals in the chain of value. Students and professionals to be taught eMECHATRONICS will develop multidisciplinary and management skills. Concerned with the aim of this article, we need to calculate with the fact that manufacturers are developing internal training cycles for mechatronics engineers. But at the standard level there is still a great disparity and overall lack of specific training in mechatronics. There are 6 – 7 universities in Slovakia proposing courses of mechatronics gathering nearly 400 students per annum (The University in Žilina has been teaching mechatronics since 1990). However, mechatronics educating supports do not exist as such in the form of courses, research, glossaries, and the few materials available are not accessible or adapted to such purpose. In order to face this complexity and versatility regarding mechatronics education contents for both initial and continuous training, there is a need to provide a knowledge base and enriched training contents, which will later help to solve manufacturing problems such as:

- design: appropriate solutions meeting customers' requirements,
- manufacturing: efficient and cost driven manufacturing process,
- interfaces design and development, tests, maintenance, between mechanical parts, electronic components and software,
- components manufacturing and maintenance processes and devices,
- implementation and test: know-how about implementing and testing more and more complex systems,
- operation: product performance, return of experience, reliability, safety issues,
- maintenance: safety, cost,
- breakdown: analyse of cause and prevent integration problems.

Concerning the number of eMECHATRONICS prospective professional end users, it can be evaluated in Europe to a potential of more than 1 million taking into account that only for the automotive industry, there is a potential of 20% of the 5 million employees in Europe.

Acknowledgement

This paper was created within support of the Grant Agency of the Ministry of Education of the Slovak Republic VEGA – Scientific Grant Agency of the Slovak Republic for project No. 1/3086/06 "Research of the New Methods of Modelling, Control and Simulation of Mechatronic Systems" and VEGA project No. 1/3123/06 "Research of Commutation Processes in the Power Transistor Structures and Optimisation of their Control at Soft-Switching Mode".

References

[1] PAVLÁSEK, P., PAVLÁSKOVÁ, V.: *Educational Technology (in Slovak)*, Textbook for Supplementary Pedagogical Education, EDIS - Editorial Centre of the University of Žilina, 2004, ISBN 80-8070-236-5, p. 83

[2] PAVLÁSEK, P., MEDVECKÝ, Š., CETL, M.: *Sophisticated Technologies - Tool for Success in Integrated Design,* Local Tradition – Global Future, Bratislava, 1997, pp. 55 – 56

[3] CETL, M., PAVLÁSEK, P., MEDVECKÝ, Š., HRČEKOVÁ, A.: *Modern Methods in the Product Design (in Slovak),* Strojárstvo 3/98, pp. 16 – 17

[4] PAVLÁSEK, P.: *Sofisticated Technologies in the Design of Products (in Slovak),* Strojárstvo 1/97, MEDIA/ST. pp. 24 – 25

[5] MEDVECKÝ, Š., HRČEKOVÁ, A., ŠTRBKA, P., PAVLÁSEK, P.: *Design of the Mechatronic Systems with Computer Aid,* Proc. of the Science Conference – Using of Unconventional Methods and Materials in Contruction, WPP, Poznaň, October 1996

[6] PAVLÁSEK, P., CETL, M.: *The Man and Mechatronics (in Slovak),* The Man in the Railway Transport, Proc. of the Seminar ŽELSEM '93, Loučeň, 1993, Part II, pp. 229 – 230

[7] PAVLÁSEK, P., CETL, M.: *Configuration of Integrated Mechatronic Systems (in Slovak),* Proc. of the International seminar: "Dynamic and solid analysis of the drive systems", Svratka, 1993, pp. 231 – 234
[8] KRÍŽIK, J.: *The Light and Shadow (in Slovak),* Imaginery in Autodesk 3DS MAX8. Inst. of Art and Science, University of Fine Arts, Bratislava, 2006
[9] PAVLÁSEK, P., KORENČIAK, D., PAVLÁSEK, M.: *Conceptual Design of Sophisticated On-board Measuring and Diagnostic System,* Proc. of the 5th Intern. Scientific Conf. ELEKTRO 2004, May 25-26, ISBN 80-8070-252-7, pp. 286 – 291
[10] *The Role of the Fine Art in Perspective of the Acivities of Mechatronics in Automobile Industry in Europe and in France),* Mechatronic Study of Renault PSA Cetim/Cabinet Décision – 7/2005
[11] JOCHEMS W., VAN MERRIËNBOER, J., KOPER, R.: *Integrated e-Learning: Implications for Pedagogy, Technology and Organization,* London, Routledge Falmer, 2004
[12] PAVLÁSEK, P.: *Mechatronical Aided Concept (MAC) in Intelligent Transport Vehicles Design. Advances in Electrical and Electronic Engineering,* 3-4/2003, ISSN 1336-1376, pp. 38 – 45
[13] PAVLÁSEK, P, GUTTEN, M., KORENČIAK, D.: *Measurements and Measuring Systems (in Slovak),* EDIS, Univ. of Žilina, 2005, ISBN 80-8070-286-1, pp. 33
[14] PAVLÁSEK, P.: *The Main signs of the Mechatronic Equipments (in Slovak),* Proc. of the Workshop „Mechatronics", Supplement of ŽELSEM _93, Loučeň, October 1993, pp. 7 – 12
[15] PAVLÁSEK, P., KORENČIAK, D., PAVLÁSEK, M. P.: *Virtual Instrumentation Based Development of Sophisticated Control System,* Proc. of the Inter. Conference Transcom 2005 - 6th European conference of youth research and science workers in transport and telecommunications, 27.-29. June 2005, Univ. of Žilina, ISBN 80-8070-417-1, pp. 117 – 124
[16] PAVLÁSEK, P., PAVLÁSEK, M. P.: *Sophisticated Biometrical System Development for Prompt Eefugee Personal Identification,* Proc. of the Intern. Conf. Trends in biomedical engineering, 7.-9. September 2005, Univ. of Žilina, ISBN 80-8070-443-0, pp. 143 – 148
[17] PAVLÁSEK, P., MEDVECKÝ, Š., MAČUŠ, P.*: Sophisticated Biomedical Systems: Product Technology, Design and Performance in Dental Medicine,* Proc. of the Intern. Conf. Trends in biomedical engineering, 7.-9. September 2005, Univ. of Žilina, ISBN 80-8070-443-0, pp. 149 – 154
[18] LAIRE, M., PAVLÁSEK, P., et al.: *eMechatronics. Online Web-based Training Solution Devoted to Transfer Emerging Mechatronic Scientific and Technological Knowledge Towards the Educational and Professional Communities,* Proposal No. 38217, eContentplus, FIEV, Souresnes, France, 2005.

P. Lehocký – R. Kohár – S. Hrček – J. Podhorský – B. Surmová – Š. Medvecký – A. Hrčeková *

AUTOMATIVE UNWINDING OF WASTE PAPER FROM REEL SPOOLS

Paper industry deals with procedures for conceptual and final design of a machine intended for unwinding paper that remains on reels during a certain phase of paper producing. Design procedure of the machine is a subject of this paper. The machine was designed as a mechatronic unit consisting of a mechanical part, an electric part and a pneumatic part. 3D CAD/CAM system Pro/ENGINEER was used for the design of the mechanical part. For the automation processes the PLC unit connected with the frequency changing unit and asynchronous drive were used as a central drive for the unwinding machine.

1. Introduction

In order to make production of paper faster, more effective and environmental friendlier, the paperwork in Ružomberok defined a task, the solution of which would approximate its production technology chain toward aforementioned goals. So far manually performed removal of wound-up rest of web paper that remains on a reel spool after a web unwinding – during a paper production - would be automated. The paper remains wound-up on a reel spool due to a used technology of production and due to production process tolerances. This unwound paper, the diameter of which varies, can not go for subsequent processing. Thus it is necessary to remove it from a reel and put it back to the production, recycle it. A former method of removing the paper from a reel was manual. With the use of knife, an operator had to cut the remaining paper off a reel and store the removed paper in a container from where it went for further processing. It is a time-consuming operation. Taking into consideration the weight and length of a reel, it is also physically hard.

The objective of the defined task was to minimise the manual operation of the removal of the rest of paper from a reel and speed up the process. The overall objective of the task was to design and to manufacture a fully automatic machine that would be able to unwind remained paper from a reel and would direct it for a recycling process. The emptying a reel must be done without damaging a reel itself. Furthermore, the machine must be able to place the removed paper on a conveyor that will transfer it for a recycling process and must be able to collect emptied reels at one particular place. As to a machine operator, the only activity he/she will perform will be loading rolls intended for unwinding and to unload empty reels.

The submitter of the task defined a set of initial parameters for the unwinding machine.

The parameters are:
- the width of a roll before unwinding: max. 400 mm
- the length of a reel: max. 2200 mm
- the diameter of a reel: 176 mm
- the unwinding speed: max. 150 m/min
- voltage: 3 x 400 V, 50 Hz
- compressed air pressure: max. 6 bar
- operating environment definition: standard, basic according the STN 33 0300 vol.3.1.1

The device can be divided into three basic parts:
- a mechanical part consisting of a machine frame, movable mechanisms, a machine covering,
- an electric part consisting of electric drive and power supply as a power part and a control part with PLC computer and sensors,
- a pneumatic part with pneumatic cylinders, valves and devices for compressed air parameters control.

2. Mechanical part of the machine

A procedure, in which the initial information is processed with respect to function requirements and in which also device parameters and working environment information are set up, is called a design process. The design process is divided into several steps. In the case of design of a machine intended for removing rest of paper off a reel spool, the steps were applied as well.

In the first phase, based on the submitter's specification of the task, general requirements for the machine capabilities and features were determined. Accordingly mechanical characteristics of the device were defined. The definition took into consideration the following attributes: the maximum weight and diameter of a roll to be unwound, need of using a fork lift for loading rolls, necessity of connection to the actual technical and technological

* P. Lehocký[1], R. Kohár[2], S. Hrček[2], J. Podhorský[2], B. Surmová[3], Š. Medvecký[2], A. Hrčeková[2]
[1] Faculty of Electronical Engineering, University of Žilina, e-mail: Pavel.Lehocky@fel.utc.sk
[2] Faculty of Mechanical Engineering, University of Žilina
[3] Rectors Office of the University of Žilina

infrastructure (electricity, compressed air). Also work safety conditions according STN must have been respected.

In the next step there were several solutions proposed to address the task of automatic removal of the rest of unwound paper. The solution had to consider changing length and diameter of a roll and to respect the requirements for unwinding speed and avoid damaging emptied reels.

Among proposed solutions, there was one in which the usual cutting procedure was considered. In order to remove the left paper from a reel by cutting it off, this solution, however, could not guarantee that during the cutting operation a reel would not be damaged. Prevention of damaging a reel is difficult due to a variable diameter of a reel that varies between 176 mm to 400 mm or even more. Such a solution requires the reel fixation and smooth regulation of depth of cut according to the actual diameter. The analysis and a feasibility study for this machine design showed that the expenditure for such a device would be excessive due to complicated loading and reel fixation mechanisms. The adjusting of the cut was problematic and the reliability of the cutting procedure was insufficient. Therefore this option of the task solution could not be applied.

Trying to find a reliable and effective solution for removing the rest of wound-up paper from a reel it was found out that the most effective way for emptying reels would be unwinding the left paper. Several options for unwinding were considered and analysed during the design process. In the end, using rotating cylinders or V-belts, as presented in Fig. 1, was considered the best and also the simplest solution.

Further analysis showed that rotating cylinders, used, for instance, for unwinding metal sheets, could not be accepted due to high speed required for paper unwinding. For high unwinding speed the additional device for a roll fixation is needed. Another additional device is necessary for releasing and transferring empty reels to storage. Assuming that the maximum weight of a roll before unwinding is 200 kg, and providing that an additional device for fixation and another one for after-unwinding manipulation would be needed, the mechanism (rotating cylinders and related devices) should be very robust. Therefore cost of material for such a device would negatively affect the final price of the device.

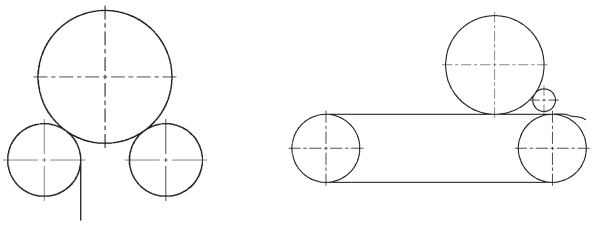

Fig. 1 Unwinding of the rest roll by rotational cylinders and V-belts principles

As the most appropriate solution, a V-belt solution was chosen as a principle for a machine design [2]. V-belt solution allows achieving speed required for unwinding and allows easy loading of rolls and unloading empty reels. A roll is placed in a system of V-belts. During loading it is important to place a roll on belts carefully in correct orientation. Owing to V-belts movement the roll is transferred to supporting cylinders, leans against them and the roll starts unwinding. The paper is directed under supporting cylinders and transported out of the unwinding space to a conveyor.

During the design process it is important to design particular parts and mechanisms of the machine. They are customised according the shape and dimension of the machine and they form groups. The proposed unwinder consists of two basic groups: a machine frame and an unwinding module. The machine frame consists of a loading plate for a roll, a device for loading a single roll to the unwinding module (a guide or a loader), a frame with supporting and guiding reels, covers, and storage for empty reel spools. Unwinding module consists of a frame of unwinding module and a movable V-belt part.

The design of the machine was done with CAD system Pro/ENGINEER Wildfire 2.0.

The system enables presenting the initial design of unwinding machine as a virtual 3D model. The initial 3D model of the machine is shown in Fig. 2.

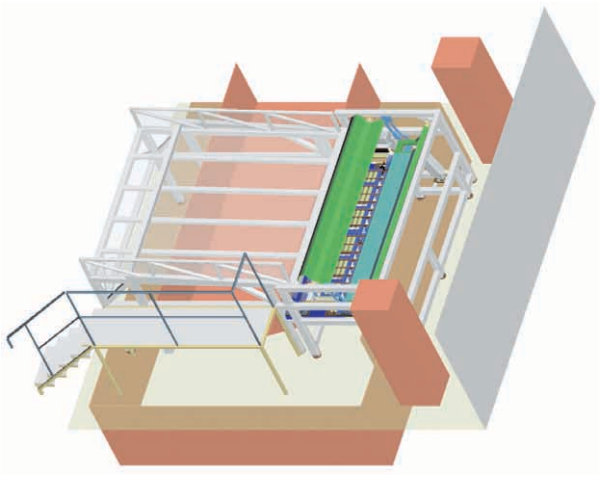

Fig. 2 Initial design of machine

Fig. 3 presents the final 3D model of the machine. In accordance with the demand of the customer, a storage box replaces a transportation box for empty reels with possibility of tying empty reels together. A frame of the machine is manufactured from welded steel profiles, which form a construction in which the particular mechanisms are installed. A loading ramp is used for loading rolls that are intended for unwinding. A guide – a device for loading one roll at a time on unwinding belts – prevents other rolls from being loaded if there is a roll already being unwound and at the same time it prevents the roll from dropping out of the

belts during the unwinding process. The function of the guide is to ensure that no other roll will interfere with a roll being just unwound. Supporting reels ensure rotation of a roll and consequent unwinding of the paper. Guiding reels ensure that the unwound paper will not wind back to the unwinding space. Supporting and guiding reels are placed in the same area. The unwinder has a safety cover, which guarantees that no foreign element or a person will get in the unwinding area. Thus injuries are prevented. The storage space under the loading plate is used for storing empty reels.

Fig. 3 Final from of frame

An unwinding device – Fig. 4 – consists of a frame assembled from aluminium profiles. Bearing boxes are placed here. A rotational part consists of two shafts, driving and driven, both equipped with a set of V-belt pulleys.

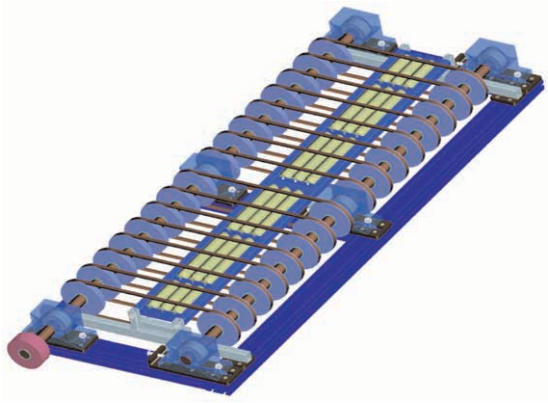

Fig. 4 Final form of unwinde

The final 3D model of the unwinding machine with the incorporated unwinding module is presented in Fig. 5.

CAD system Pro/ENGINEER allows not only creating 3D model of a designed device but is capable also of verifying functionality of the system by animation and simulation of the designed solution. This feature of the Pro/ENGINEER system was used for the design and verification of the functionality of the guide (loader) device, as well as the safety cover, as it is presented in Fig. 6.

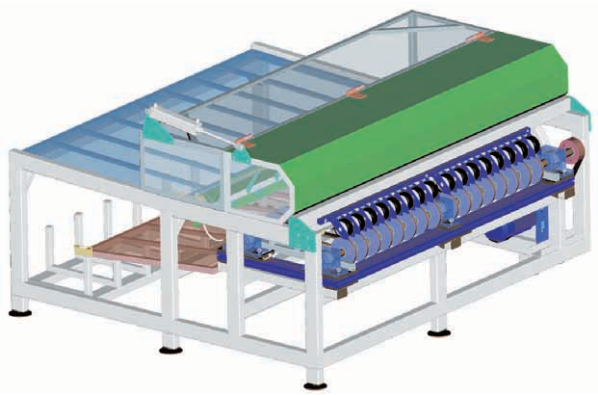

Fig. 5 Final 3D model of the machine

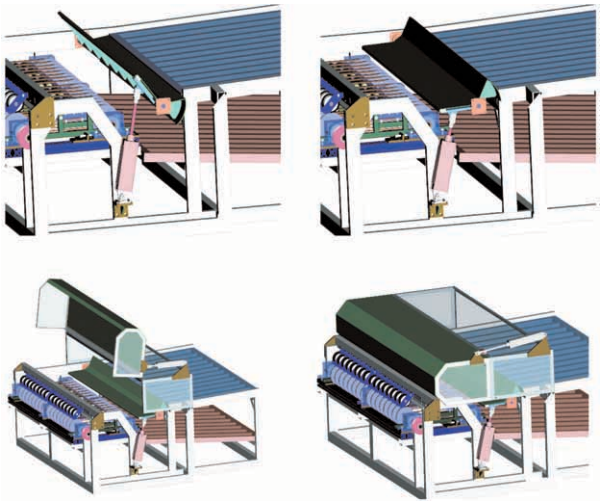

Fig. 6 The guide device simulation and the simulation sof the safety cover

During the process of a roll unwinding it is necessary to guarantee continuous rotation of the roll. The thickness of the unwinding paper changes during the unwinding process and so does the

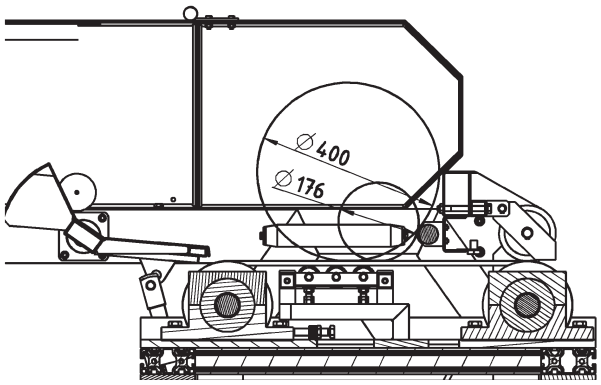

Fig. 7 Simulation of unwinding

points of contact between supporting reels and paper. Bearing in mind a changing diameter of a roll, in order to meet the condition of continuous rotation, the supporting reels must be placed in an appropriate way. Fig. 7 shows the simulation.

Reliable functioning of the machine is achieved through guaranteeing all pre-defined dimensions and tolerances during the machine manufacturing. Accuracy is important especially regarding to movable mechanisms and their placement. The guide device must be positioned aligned. As far as the unwinding unit, the position and proper alignment of shafts must be guaranteed as well. Each of the shafts lies in three bearing boxes. In case of inaccurate position of either of the shafts some bearing can be damaged due to inappropriate alignment. Alignment of the shafts must be measured carefully before putting the device into operation.

The measurement was done by 3D measuring device FARO Laser Scan Arm. The device is presented in Fig. 8. The FARO Laser Scan Arm is a device with no need for special laboratory conditions.

The measurement of an existing device or a product carried out by FARO Laser Scan Arm is called 3D scanning. This method of collecting data is called Reverse Engineering. Reverse Engineering enables transformation of a real existing object into a virtual object. The result of the 3D scanning procedure is usually a data cloud, which is transformed to the regular surfaces and volumes by means of specialised software.

Fig. 8 Measuring of the object with FARO

In the process of the machine design, Reverse Engineering [3] was used for control of the shaft alignment. The scanned data were processed in PolyWorks software. PolyWorks enables to compare measured parameters of a real object with the virtual 3D model. Fig. 9 shows the example of the output of the PolyWorks software. Grey colour represents 3D virtual model of a shaft lying on bearing boxes. The colourful object projected in a spectrum of colours represents a real scanned shaft. Each particular colour of the spectrum gives information about how much the real object differs from the virtual one. Such procedure allows adjusting the shafts into desired position.

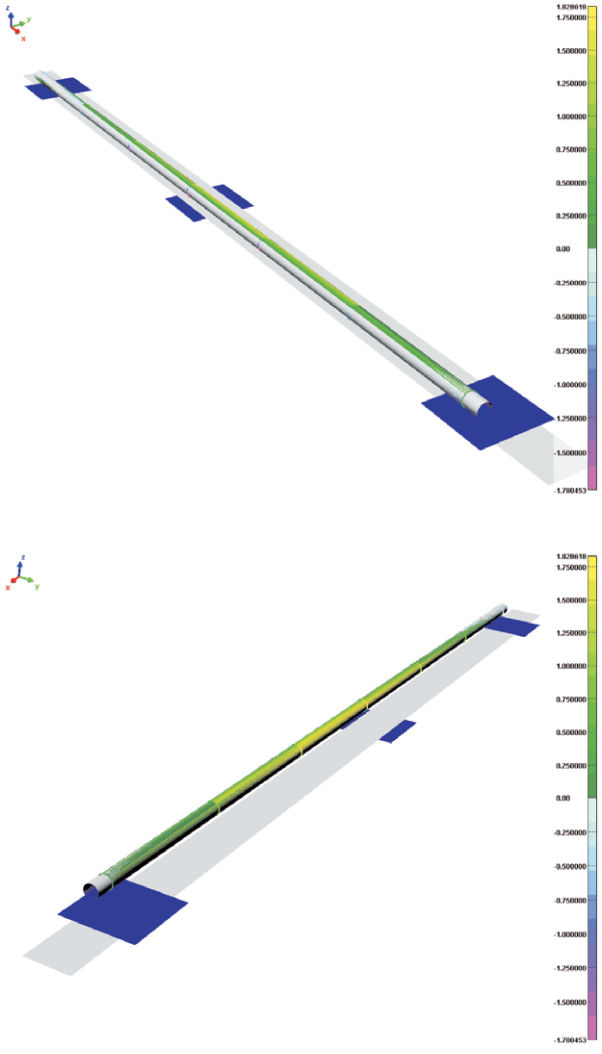

Fig. 9 Graphic outputs from PolyWorks software

3. Electric part of the machine

In order to fully meet the customer's requirements, attention is given to all parts of the machine. An electric part of the machine is tailored accordingly and connected to the mechanical part. It is

composed of driving units and control parts. The function of the driving part is to put the mechanisms of unwinding unit into movement. The control part controls the mechanisms in accordance with the technological demands. The integrated parts of the electrical part are sensors, switches, circuit breakers and electro installation. Electric part of designed machine is divided into two parts:

- a power unit consisting of electric drive, a frequency changer, control elements (switches, fuses, main switch, emergency switch, ...),
- a control part consisting of a PLC computer unit, control elements (switches), sensors, output action elements (electromagnetic valves, signalization,...).

The design of the electric part of the unwinding machine must correspond to the basic data requested by the customer:

- supply voltage - 3PEN ~ 50Hz 400V / TN-S ,
- operating environment – standard, basic according STN 33 0300.

The design of the electric part of the unwinder consist of a design of a switchboard with all its parts optimally arranged and connected and a design of electric circuits and connections of all instruments and electric devices located in the machine.

According to the task definition, the required unwinding speed of the machine is 150 m/min. The speed and a total moment of inertia of the system calculated from rotation of electro drive shaft determine parameters of the electro drive, such as power output, turns per minute, torque moment. It is necessary to ensure that the electro drive will reach the requested turns per minute under load in such time period that overheating of the electric drive will not occur. For asynchronous drives with intermediate power range such effect can occur when the moment of inertia is 20 – 30 times higher than moment of inertia of an armature. For a two-pole asynchronous electric drive the critical value occurs when moment of inertia is 8 – 12 times higher than moment of inertia of an armature [1]. The effect of overheating of the asynchronous drive is caused by the fact, that during acceleration of the drive at high load the power losses are 25 – 35 times higher than losses of a drive running at normal load. The high losses cause that the drive winding reaches the highest allowed temperature within 10 – 15 seconds. In case of large moment of inertia of the system the drive acceleration time exceeds 10 – 15 seconds, which leads to immediate damage of the drive isolation. With respect to the above mentioned facts and taking into consideration the input parameters and safety limit of 1,3, a drive with economic asynchronous motor with integrated front gearbox is considered as the best option, as shown in Fig. 10. This type of asynchronous motor differs from others by a cage of a rotor. In the case of the economic asynchronous motor the cage is manufactured from copper. The use of copper reduces the losses in the motor, increases the efficiency of the motor and decreases the power consumption with respect to the requested output

Following are the parameters of the asynchronous motor: power is 4 kW, nominal current at 400V is 8,1 A, nominal turns per minute is 1460 rpm, nominal torque moment is 26,9 Nm. As to the gearbox, its input parameter is gear ratio of 5, 64.

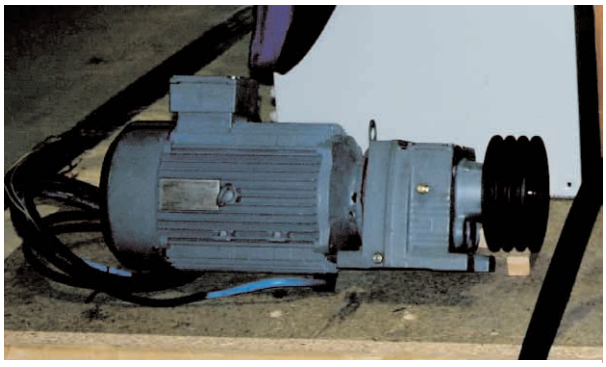

Fig. 10 Asynchronous motor with gearbox

The asynchronous motor and the gearbox is a driving unit of the unwinding mechanism. The transfer of power is done by V-belt gear. The motor is supplied by frequency changing unit with vector control. The need of the frequency-changing unit is due to the fact that the machine works in several modes in which different turns per minutes are requested. Also with respect to need of a run-up and a run-down ramp for loading rolls and unloading empty reels and due to securing fluent start of paper unwinding it is necessary to use the frequency-changing unit. According to the customer's request, the ABB frequency changing unit, ACS 350-03E-08A8-4, is opted for. Following are the parameters of the unit: power of 4 kW, nominal current of 8,8 A, voltage Un=400V, 50Hz. The frequency-changing unit is placed in a separate distribution panel R2, Fig. 11.

Fig. 11 Instrument panel R2

A switchboard R1 shown in the Fig. 12 contains electrical devices, such as terminals, circuit breakers, switches, fuses, voltage transformer and supply 24V DC, PLC automat, technological socket 230V for connecting of computer for PLC programming. The upper side of the switchboard is used for control elements.

To ensure the automatic operation of the machine without the need of manual control it is necessary to equip the machine with

Fig. 12 Switchboard R1

a control unit. The control unit is PLC automat SIEMENS S7-222 with extension module for digital inputs and outputs EM 223. Signals coming from sensors and control elements go to PLC input. PLC automat then controls automat outputs connected to active elements or signalization. The outputs are switched on according to the pre-programmed sequences requested by technology. The PLC automat SIEMENS S7-2xx is programmed in the Step7 – MicroWin environment. MicroWin allows to create virtual logical circuit (to program the PLC automat) and then to control the machine. The feature of the PLC automat to create virtual logical circuits enables debugging, testing or changing solution operatively with no need of mechanical changes in the system.

The machine was equipped with the following optical sensors according to the function requirements:

- optical sensor (transmitter – receiver) for detection of presence of a roll at a loading ramp,
- optical sensor (diffuse sensor with reflector) for detection of a roll by a device for loading a single roll to an unwinding unit,
- optical sensor (transmitter – receiver) for a roll detection at an unwinding V-belts unit,
- optical sensor (diffuse sensor) for detection of paper inserted under presser rollers,
- optical sensor (diffuse sensor with reflector) for detection of status of fullness of the box that stores empty reels.

There are also induction sensors in the machine, the function of which is to monitor position of pneumatic cylinders. One of the induction sensors has a safety function on the movable cover of the machine.

The machine can operate either in an automatic or a manual mode. If the machine operates in the automatic mode, a green signalization light starts flashing. When malfunction of the system occurs, the movable safety cover opens. The fact that a roll remains on the unwinding belts whilst the cover is open, is not in line with the normal operational regime of the machine. Therefore the machine automatically stops and a red light starts lighting. Under the seamless automatic mode the machine performs a set of operations automatically according the actual need. At the beginning the machine waits until a roll is loaded at a loading station. As soon as a roll is loaded and an optical sensor detects it, a command is triggered towards the belts to start moving. The roll is then transferred to a guide unit – a loader, the function of which is to guide and load a simple roll at the time onto the unwind belts. At this stage the belts move at reduced speed that is required for guiding the end of paper under the pressure reels. If within a certain interval the paper is not detected and the paper is not inserted properly the machine stops and the red light starts flashing. The paper insertion is monitored by the optical sensors connected to the pressure reels. There are eight sensors to detect rolls of varied diameters. Immediately after the paper is led under the pressure reels, the machine increases the unwinding speed to maximum. The unwinding process is also dependent on the technology of further processing of unwound paper. It is important not to overload the machine for further processing. The unwinding speed is reduced again as soon as the optical sensors register no paper under the pressure reels when the reel is successfully emptied. The loader is positioned back to the load position. The induction sensors connected to the pneumatic cylinder send information to the PLC unit. The unit then reverses the movement of the belts and the empty reel is launched to the storage space where emptied reels are stored. The capacity of the storage space is controlled by an optical sensor and the fullness of it is signalized by orange light. When the unwinding unit is empty the process starts from the very beginning by loading a new roll. If a roll is at the loading plate but it is not transferred to the loader the orange light flashes.

In a manual mode the operator can control each operation individually.

4. Pneumatic part of machine

Pneumatic part is composed of two pneumatic cylinders. One cylinder controls the loader, the function of which is to assure loading one simple roll at a time to the unwinding unit. The second one controls the cover of the machine. Fig. 13 illustrates the pneumatic cylinders. A component part of the pneumatic cylinders are electro pneumatic double action valves. They open and close in accordance with signals transmitted from PLC unit and thus they control the pneumatic cylinders.

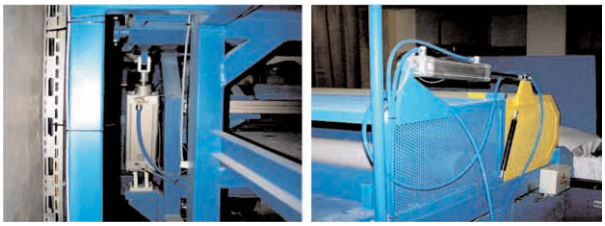

a) *b)*

Fig. 13 a) pneumatic cylinder – loader
b) pneumatic cylinder – cover

In order to assure proper function of the pneumatic unit it must also contain:

Fig. 14 Valve terminal

- a closing valve, which traps the compressed air in the pneumatic cylinders and releases pressure in the cylinders,
- a regulation valve, by regulation of which the pneumatic cylinders operate at constant pressure
- a lubrication set, that is needed for lubrication of the pneumatic cylinders which increases their durability.

Fig. 14 illustrates a valve terminal and a device for compressed air preparation.

Conclusion

Fig. 15 presents the final version of the unwinding machine after its installation in the Mondi BP paperwork. The operation-testing period was already done and the machine is prepared for full operation as soon as it receives a certification protocol from the Technical Inspection.

Fig. 15 Unwinding machine installed at the paperwork

References:

[1] BEDNÁRIK, B. et al.: *Electroenergetics in Transport (in Slovak)*, ALFA Bratislava, 1983
[2] MÁLIK, L. et al.: *Machine Elements and Mechanisms (in Slovak)*, EDIS Žilina, 2003, ISBN 80-8070-043-5,
[3] KUČERA, Ľ., MAČUŠ, P.: *The possibilities of 3D scaning for measurement of deformation of steel frames.* XLV konferencia katedier častí strojov, Blansko, 2004, ISBN 80-214-2702-7.

Adam Balawejder – Mieczyslaw Chalfen – Tadeusz Molski – Andrzej Surowiecki *

THE STABILITY OF HYDRO TECHNICAL EMBANKMENTS UNDER VARIOUS SEEPAGE CONDITIONS

The flood control devices in Bytom Odrzanski protect the city against the Odra water flooding with a probability p = 10 ÷ 20 %. The flood protection devices (class validity II) of hydro-technical structures are designed and realized for protection improvement and designed on the flow in the Odra river with a probability p = 1 % . The earth embankment (2044 total in length) will be built with local non-cohesive grounds. On the 900 m length, the base of the embankment presents no cohesive grounds. It causes conditions for free filtration through the base and body of the embankment. The computer calculations of filtration showed high (locally) hydraulic heads (I_{max} = 0,984) that cause the need for ground protection against flux and erosion by using filtration geotextile. The smallest value of the stability coefficient obtained using the 'Fellenius' method was F_s = 1.439 > 1.2 . The exact analysis of filtration conditions and stability allowed for the undertaking of solutions ensuring the safety for the structure.

1. Introduction

The safety of hydro technical buildings such as soil banks, flood embankments and earth dams is a very important and essential issue because of two aspects: The safety of the constructions themselves and the prevention of water-logging adjacent areas in cases of high river levels. One of more important elements affecting safety (stability of the earth dam) is filtration of water through permeable grounds used for building the dam. Water percolated in the conditions of the high flow gradient could cause occurrence of such phenomena as suffosion, washing out and/or hydraulic uplift which negatively influences the stability of the construction. It is very important that the filtration analysis is not limited to only determining the hydroisohypses course. It should also include a calculation of the length and direction of the velocity water flow vectors. It will allow the determination of regions where the hydraulic head could exceed admissible and critical values.

The results of water flow to flood embankment protection with negative effects of filtration are presented in this paper using the example of the left-bank of the Odra valley in the Bytom Odrzański region. The flood protection program for this locality predicts a two stage investment task [5, 6]. Stage I presents the improvement of protection of the most at risk of flooding, north – west part of the city. Stage II includes further building-up the left-hand flood embankment of the Odra river: km 416.95 + 419.20. With reference to embankment distance, it is a section of 2+044 km in length from km 0+550 to km 2+594, thus from a newly built surrounding embankment in stage I to the urban sewage treatment plant (Fig. 1). Whilst preparing the engineering project (flood protection of the Bytom Odrzański region) – stage II, there was a need to carry out the investigation of free seepage and stability of the embankment, which is the object of this work.

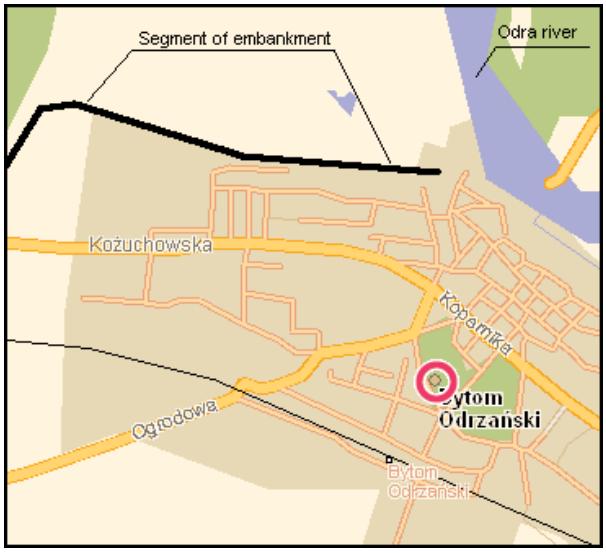

Fig. 1 Situation map

2. Geology and hydrogeology

In the foundation of the projected embankment (section km 1+700 ÷ 2+594) mineral bearing soils were discovered representing Holocene and Pleistocene formations of the river lagoon, glacier and river origin (Fig. 2). Also were discovered sands, medium sands and sandy gravels but seldom dust sands or coarse sands with gravel. These are permeable and very permeable grounds with filtration coefficient from 0.5 m/d in the case of fine sands and silty sands to 55 m/d in the case of sandy gravels. Sporadically among

* Adam Balawejder[1], Mieczyslaw Chalfen[2], Tadeusz Molski[1], Andrzej Surowiecki[3]
[1] Institute of Environmental Engineering, Wroclaw University of Environmental and Live Sciences, Poland, E-mail: mch@ozi.ar.wroc.pl
[2] Department of Mathematics, Wroclaw University of Environmental and Live Sciences, Poland
[3] Institute of Building Engineering and Landscape Architecture, Wroclaw University of Environmental and Live Sciences, Poland

the sands there are also the river lagoon's inclusion of cohesive grounds, therefore, clays and silty clays [3].

The groundwater depths are shallow and very shallow. The free groundwater table is at a levels of about 0.5 ÷ 2.0 m below the surface of the terrain (in the period of the mean levels) depending on the region and distance from the Odra bed.

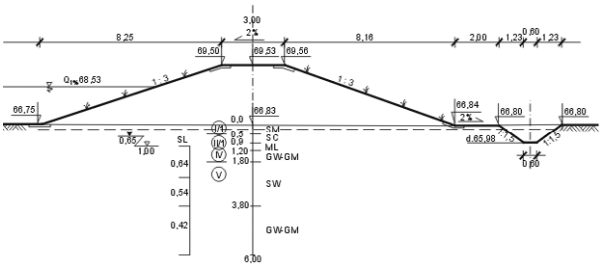

Fig. 2 Vertical cross-section of embankment

3. Characterization of the researched object

The left bank embankment of the Odra river protecting built-up areas of Bytom Odrzański was qualified to a class II validity of structure. The embankment location corresponds to "A general strategy against flood protection in the upper and middle Odra basin". The relative safe height of the dam crest below the reliable water level was taken 1.0 m [6, 7], which met technical standards for water management objectives – class II validity structure. The investigations of the filtration and stability conditions for the section of embankment from stage II of the investment were done on the stage of studying project [1,2]. The following embankment parameters were assumed:

- width of the dam crest 3.0 m
- slope 1:3
- total length 2 044 m
- height 1.8 ÷ 3.8.

The slope and crest of the dam are stabilized by grassing on the humus.

There is a local alluvial soil layer in the foundation of the embankment which causes conditions for the seepage under pressure. However, on the embankment section (length 894 m, in km 1+700 ÷ 2+594) where alluvial soil does not occur, seepage through the dam and subsoil foundation will not appear. [1].

4. Computation for free filtration in typical vertical cross-section of embankment

The vertical flat flow occurs in the case of liquid filtration through the objects where the flow in a perpendicular direction to the cross section could be recognized as inessential (dams, embankments and others barriers from porous materials). The equation which describes the potential of the liquid flow area [4, 8, 10] is presented:

$$\frac{\partial}{\partial x}\left(k_s \frac{\partial h}{\partial x}\right) + \frac{\partial}{\partial z}\left(k_s \frac{\partial h}{\partial z}\right) = 0 \qquad (1)$$

And in the case of homogenous and isotropic medium, where the conductivity is $k_x = k_z$, the Laplace's equation is given:

$$\frac{\partial^2 h}{\partial x^2} + \frac{\partial^2 h}{\partial z^2} = 0 \qquad (2)$$

Solving the issue of stationary flow with a free surface there remains the problem of determining the depression curve location where kinematics boundary conditions must be implemented ($p = 0 \rightarrow h = z$ – potential is equal to the position head) and $q_n = 0$ – showing a shortage of flow in the normal direction to the depression curve. It demands starting the iterative process where the differences of depression curve location in two following iteration are taken as a criterion of the accurate assessment of the solution.

The computer program FILTR based on the finite elements method was used for solving the problem. The program generates the net of trianglular elements for which the function approximating the potential in the element is the linear function of two variables. The consequence of this fact is the constant value of the filtration velocity in the element. The results of the computations are presented as the velocity field in the filtration area and hydrodynamic network. The total discharge of flow is also given.

Assumptions and results of computations

The computation scheme presented in Fig. 3 was taken into the research. The computer calculations of filtration were done with the following alternative assumptions:

Variant B_1:

- $H = 2.5$ m,
- thickness of the permeable ground $M = 10$ and filtration coefficient $k = 18$m/d,
- permeable embankment body ($k = 18$m/d) with tight screen on the water side slope,
- surrounding collector trench with groundwater depth at 0.5 m below the surface of the terrain.

The filtration process takes place in the free filtering conditions through the basement soil and embankment.

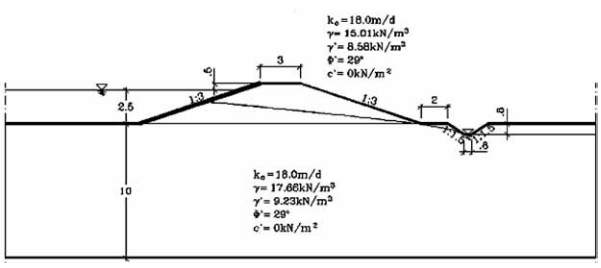

Fig. 3 Computation scheme for vertical cross-section of embankment (variant B_1 and B_2)

Variant B_2:

The assumptions are similar to the variant B1, only the depth of water level in the trench is 0.8 m below the surface of the terrain.

It was stated, basing on the computer calculations of filtration, that:

For the variant B_1:
- value of the inflow rate on the linear metre of trench amounts to $q_r = 1.017*k_o = 1.017*18.0 = 18.31$ m^3/d,
- maximum velocity of inflow to the surrounding collector trench $V_{max} = 0.581*k_o = 0.581*18.0 = 10.46$ m/d,
- maximum value of the hydraulic head in the zone of the inflow to the trench $I_{max} = 0.581$.

For the variant B_2:
- value of the inflow rate on the linear metre of trench amounts to $q_r = 1.088*k_o = 1.088*18.0 = 19.58$ m^3/d,
- maximum velocity of inflow to the surrounding collector trench $V_{max} = 0.942*k_o = 0.942*18.0 = 17.71$ m/d,
- maximum value of the hydraulic head in the zone of the inflow to the trench $I_{max} = 0.984$.

The example of computation results are showen on Figs. 4 and 5.

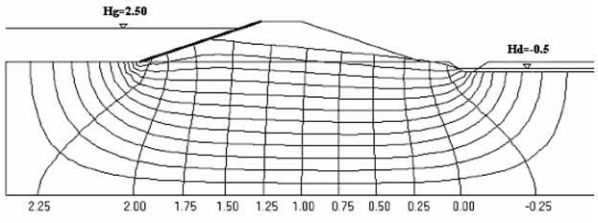

Fig. 4 Result of computations - hydrodynamic network and velocity field (variant B1)

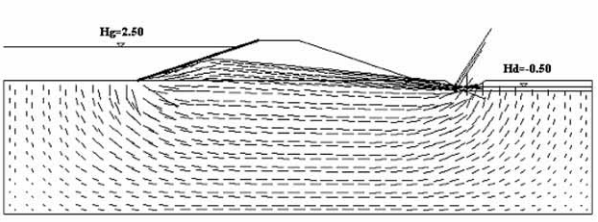

Fig. 5 Result of computations - hydrodynamic network and velocity field (variant B2)

5. Calculations of embankment stability

The stability calculations of the downstream slope of embankment were done for the representative cross-section shown on the scheme (Fig. 3). The scheme contains the assumed dimensions and geotechnical parameters of the basement soil and body of embankment. The computations were done using the 'Fellenius' method using our own computer program SZMF. The lowest value of stability coefficient was $F_s = 1.439$.

6. Result of computations for seepage (variant B1 and B2)

The result of computations are given in 4 parts of this paper. The hydrodynamic network and velocity fields are presented in Figs. 4 and 5. There was a seepage on the toe of the upstream slope of the embankment in the variant B1 (fig. 4). However in the variant 62 there was not direct seepage but the depression curve was almost on the surface of the terrain on the toe of embankment. The values of the inflow rate on 1 linear meter of the trench in variants B_1 and B_2 amount accordingly to $q_r = 18.31$ m^3/d and 19.58 m^3/d .

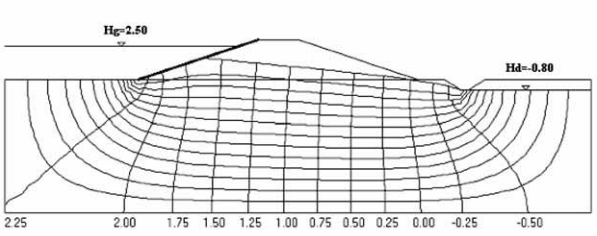

Fig. 6 Results of embankment stability computations

The maximal values of the hydraulic head in the inflow zone to the surrounding collector trench amount to: for variant B_1 - $I_{max} = 0.581$ and for variant B_2 - $I_{max} = 0.984$.

The critical slope of base of embankment amount to $I_{crit} = 0.99$ and the porosity $n = 0.40$ so the constant coefficient of destruction of the hydro technical structure is:

For variant B_1

$$\gamma_n = \frac{I_{crit}}{I_{max}} = \frac{0.99}{0.581} = 1.70 > 1.2 \qquad (3)$$

For variant B_2

$$\gamma_n = \frac{I_{crit}}{I_{max}} = \frac{0.99}{0.984} = 1.70 > 1.2 \qquad (4)$$

The computer calculations of filtration were done for the afore-mentioned schemes assuming that the filtration coefficients were given on the background of the geotechnical research referring to the object [3]. The permeable basement of the embankment with a growing depth characterizes the increase of water permeability. The value $k = 18.0$ m/d was assumed by computations. The filtration process through the base of the embankment's upper section with a smaller filtration coefficient, had an essential influence on the value of flow. The calculated values of the velocities and rate of inflows to the drainage devices could be overestimated proportionally to assumed the value of the filtration coefficient.

The shape and location of the depression curve confirms the appropriateness of using the tight screen on the upstream slope and also suggests the need for drainage (breakstone) in the lower section of the downstream slope. The high (locally) hydraulic heads ($I_{max} = 0.984$) on the inflow to the trench induce the need for ground protection against flux and erosion by using filtration geotextile. The assumed scheme for calculations (Fig. 3) takes into consideration the unfavorable conditions of stability, meaning a basement and body of embankment are water permeable. The obtained value of the smallest stability coefficient $F_s = 1.439$ (Fig. 6) meets the stability condition because $F_s = 1.439 > 1.2$.

7. Conclusions

1. For ensuring the safe conditions of filtration it is necessary to expect a tight screen on the water side slope on all the length of the designed embankment on firm grounds.
2. There is a need for ground protection against flux and erosion by using the filtration geotextile because of the high (locally) hydraulic heads ($I_{max} = 0.984$) on the inflow to the trench in free water table conditions.
3. To ensure the stability it is necessary to expect drainage (breakstone) on all the lengths of embankment in the lower section of the downstream slope protecting it against the water outflow on the slope.
4. The obtained calculated value of the smallest stability coefficient using the 'Fellenius' method meets the stability condition of the downstream slope of embankment.
5. Computer analysis of conditions of free filtration and stability of the embankment allowed, at the stage of working out of engineering design, the undertaking of solutions ensuring the safety for the structure.

References

[1] BALAWEJDER, A., CHALFEN, M., MOLSKI, T.: *Investigation of filtration conditions of the dam and stability constituting the protection of Bytom Odrzanski against flooding - stage II,* Wroclaw 2003.

[2] BALAWEJDER, A., CHALFEN, M., MOLSKI, T.: *Pressure filtration conditions effecting the substructure of the dam constituting the protection of Bytom Odrzanski against flooding,* IV. Technical scientific conference on the subject: Military engineering – teamwork response to non-military crisis situations, Wroclaw 2003.

[3] *Geological engineering documentation - Environment and land improvement design office "Ekoprojekt" Sp. z o. o. (Ltd company),* Zielona Gora 2002.

[4] KOWALSKI, J.: *Hydrogeology with the foundations of geology,* Agricultural University Press, Wroclaw, 1998.

[5] *Building design, protection of Bytom Odrzanski against flooding - stage I, Environment and land improvement design office "Ekoprojekt" Sp. z o. o. (Ltd company)*, Zielona Góra 2001.

[6] *Building design, protection of Bytom Odrzanski against flooding - stage II, Environment and land improvement design office "Ekoprojekt" Sp. z o. o. (Ltd company)*, Zielona Góra 2002.

[7] *Ordinance of the minister for the protection of the environment, natural resources and forestry* (20. 12. 1996) on the technical conditions necessary for the water management facility to satisfy, and its position.

[8] WIECZYSTY A.: *Engineering hydrogeology*, State Science Press (Panstwowe Wydawnictwo Naukowe), Warszawa 1982.

[9] WILUN, Z.: *A geotechnical outline,* WKiL, Warszawa 1987.

[10] ZIENKIEWICZ, O.C.: *Finite elements method,* Arkady Warszawa 1972.

Tatiana Olejníková *

THE LINEAR ELLIPTIC – SURFACES OF REVOLUTION

The paper presents a category of revolution surfaces which may be generated by the metrical Euclidean transformation compounded by revolutions and displacements. These surfaces are created by a straight line revolution around a revolution axis moving on an ellipse. This surface group is classified according to the relative positions of a revolution axis moving in contact with an ellipse, and according to the relative positions of a straight line and a revolution axis . The straight line revolution and axis motion can be for equal or different orientation and both can have equal or different radian frequencies. The transformation matrices for the vector equations of the surface and also some properties of these surfaces are presented in this paper.

1 Introduction

The linear elliptic-surface of revolution is generated by a straight line revolution around the revolution axis o moving on the ellipse k and it has the specified direction with respect to the ellipse and one point $R = a \cap k$ lies on the ellipse k. We can create the corresponding metrical transformation for this revolution by the composition of three-dimensional transformations, a revolution and displacement. We can represent this transformation by a regular square matrix of 4^{th} dimension whose elements are the real functions of one variable

$$T(\epsilon) = \begin{pmatrix} a_{11}(\epsilon) & a_{12}(\epsilon) & a_{13}(\epsilon) & 0 \\ a_{21}(\epsilon) & a_{22}(\epsilon) & a_{23}(\epsilon) & 0 \\ a_{31}(\epsilon) & a_{32}(\epsilon) & a_{33}(\epsilon) & 0 \\ a_{41}(\epsilon) & a_{42}(\epsilon) & a_{43}(\epsilon) & 1 \end{pmatrix}.$$

We may express the vector equation of this revolution surface as a product of the vector function of the straight line p $r(t) = (x(t)\ y(t)\ z(t)\ 1)$, $t \in \langle -\infty, +\infty \rangle$ and the corresponding transformation matrix $T(\epsilon) : p(\epsilon, t) = r(t)\ .\ T(\epsilon)$.

2 Classification of surfaces

The above described linear revolution surfaces may be classified according to the relative positions of the revolution axis o and the ellipse $k = (0, a, b) \subset xz$ with parametric equations

$$\begin{aligned} x &= a \cos \epsilon \\ y &= 0 \qquad , \epsilon \in \langle 0, 2\pi \rangle \\ z &= b \sin \epsilon \end{aligned}$$

to the five subgroups:

I. $o \parallel z$ (z – minor axis of ellipse k),
II. $o \parallel x$ (x – major axis of ellipse k),
III. $o = n$ (n – a normal to the ellipse k),
IV. $o = t$ (t – tangent to the ellipse k),
V. o $\parallel$ y (y – perpendicular to the plane xz).

In case of I – IV subgroups, the revolution axis o lies in the plane of ellipse $k \subset xz \perp y$ and these surfaces are of the *spherical* (when $o \times y$) or *Euler* type (when $0 \not\parallel y$), in case of V subgroup the axis of revolution o is perpendicular to the plane of the ellipse $o \perp xz$ and these surfaces are of the *cycloidal* type.

Next, these surfaces may be classified according to the relative position of the straight line p and the revolution axis o:

a) cylindrical $p \parallel o$ (parallel),
b) conical $p \times o$ (concurrent),
c) hyperbolical $p \not\parallel o$ (skew).

2.1 Surfaces of the subgroup I (o is parallel to the minor axis of the ellipse k)

We will formulate the transformation matrix of the revolution surface, which is created by a revolution around the axis $o \parallel z$ as a product of matrices, which represents the displacement parallel to the vector $(-a, 0, 0)$, the revolution through the angle $\epsilon' = \pm m\epsilon$, $\epsilon \in \langle 0, 2\pi \rangle$ about the coordinate axis z and displacement parallel to the vector $(a \cos \epsilon, 0, b \sin \epsilon)$, where the addition sign $(+)$ is in the case of equal orientation, the minus sign $(-)$ is in the case of different orientations of the line p revolution and the axis o motion, the coefficient m is a multiple of the radian frequency of the axis o motion of

$$T(\epsilon) = \begin{pmatrix} \cos \epsilon' & \sin \epsilon' & 0 & 0 \\ -\sin \epsilon' & \cos \epsilon' & 0 & 0 \\ 0 & 0 & 1 & 0 \\ a(\cos \epsilon - \cos \epsilon') & -a \sin \epsilon' & b \sin \epsilon & 1 \end{pmatrix}.$$

If the straight line p parallel to the axis o (Fig. 1) is determined by the point $A(x_A, 0, 0)$, where $x_A \neq a$, then its vector equation is $r(t) = (x_A, 0, t, 1)$. In Fig. 2 the surface of the cylindrical type for a sign $(-)$ of orientation of motions and for $m = 6$ is shown.

* **Tatiana Olejníková**
Department of Mathematics and Descriptive Geometry, Faculty of Civil Engineering, Technical University, Vysokoškolská 4, 040 01 Košice,
E-mail: tatiana.olejnikova@tuke.sk

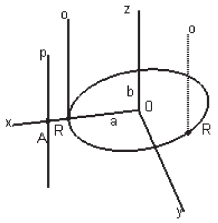

Fig. 1

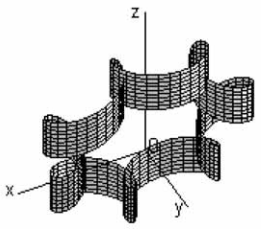

Fig. 2

If the straight line p concurrent to the axis o is determined by the point $A(a, y_4, z_A)$, and the distance v of the point $C = p \cap xz$ from the axis x, $v = |C_x|$, we will express it by the vector equation $r(t) = (a, y_A(1 - t), tv, 1)$ (Fig. 3).

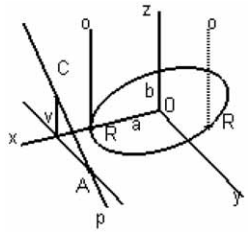

Fig. 3

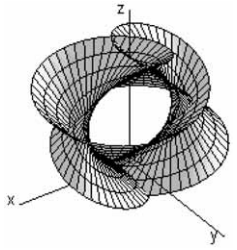

Fig. 4

If $p \perp o$, $p \perp x$, then the surface includes an ellipse k and two congruent ellipses located in mutually perpendicular planes (Fig. 5). For $p \perp o$, $p = x$, the surface is elliptic conoid of 4^{th} degree, where the generating line is perpendicular to the plane of the generating ellipse (Fig. 6).

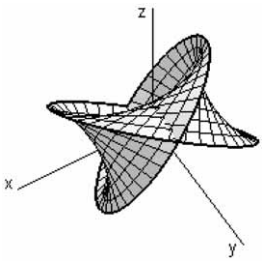

Fig. 5

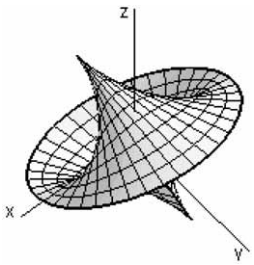

Fig. 6

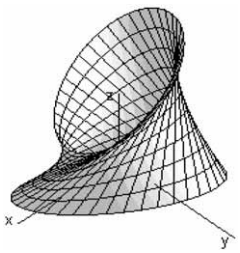

Fig. 7

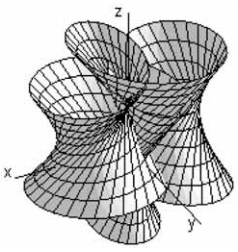

Fig. 8

The straight line p skew to the axis o (Fig. 3) is given by the point $A(x_A, y_A, z_A)$, $x_A \neq a$ and by distance of the point $C = p \cap xz$ from the axis x, $v = |Cx| \neq 0$. We can express the straight line p by the vector equation $r(t) = (x_A, y_A(1 - t), z_A + t(v - z_A), 1)$. Surfaces of the hyperbolic type for $m = 1$ and $m = 3$ are shown in Figs. 7, 8.

2.2 Surfaces of the subgroup II (o is parallel to the major axis of the ellipse k)

We will formulate the transformation matrix of the revolution surface where $o \parallel x$ as a product of matrices, which represent the displacement parallel to the vector $(-a, 0, 0)$, the revolution through the angle $\epsilon' = \pm m\epsilon$, $\epsilon \in \langle 0, 2\pi \rangle$ about the coordinate axis x and displacement parallel to the vector $(a \cos \epsilon, 0, b \sin\epsilon)$

$$T(\epsilon) = \begin{pmatrix} 1 & 0 & 0 & 0 \\ 0 & \cos\epsilon' & -\sin\epsilon' & 0 \\ 0 & \sin\epsilon' & \cos\epsilon' & 0 \\ a(\cos\epsilon - 1) & 0 & b\sin\epsilon & 1 \end{pmatrix}.$$

If the straight line p is parallel to the axis o (Fig. 9) and given by the point $A(x_A, y_A, zA)$, $y_A \neq 0$, its vector equation is $r(t) = (x_A(1 - t), y_A, z_A, 1)$. In Fig. 10 the surface of the cylindrical type for a sign $(-)$ of orientation of motions and is shown.

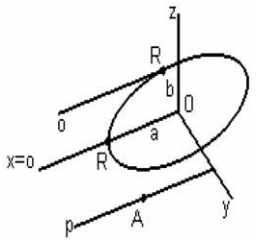

Fig. 9

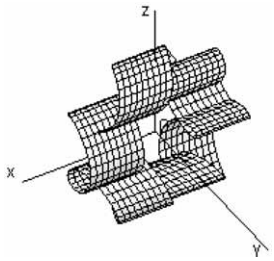

Fig. 10

If the straight line p is concurrent to the axis o (Fig. 11), given by the points $A(x_A, 0, z_A)$ and $C(a, 0, 0)$, then it creates the surface of the conical type, which is in Fig. 12 for $m = 5$ and for sign $(-)$ for the orientation of movements. Because the point $C = a \cap k$, then the surface contains the ellipse k.

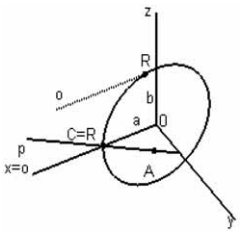

Fig. 11

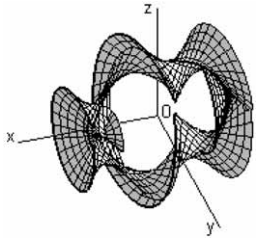

Fig. 12

If the straight line p is skew to the axis o (Fig. 13), given by the points $A(x_A, y_A, z_A)$ and $C(a, y_A, 0)$, then it creates the surface

of the hyperbolical type, which in Fig. 14 for $m = 3$ and for a sign $(-)$ for the orientation of movements is shown.

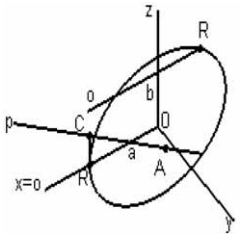

Fig. 13

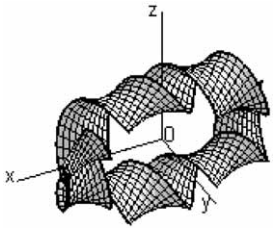

Fig. 14

2.3 Surfaces of the subgroup III (*o* is a normal to the ellipse *k*)

We will formulate the transformation matrix of the revolution surface with the axis $o = n$ as a product of matrices which represents the displacement parallel to the vector $(-a, 0, 0)$, the revolution through the angle $\epsilon' = \pm\, m\epsilon$, $\epsilon \in \langle 0,\ 2\pi \rangle$ about the co-ordinate axis x, the displacement parallel to the vector $(d, 0, 0)$, where $d = |O'\,R|$, $O' = n \cap x$, the revolution through the angle ϵ'' about the coordinate axis y and displacement parallel to the vector $(d', 0, 0)$, $d' = |O\,O'|$ (Fig. 15)

$$T(\epsilon) = \begin{pmatrix} \cos\epsilon'' & 0 & \sin\epsilon'' & 0 \\ \sin\epsilon'\sin\epsilon'' & \cos\epsilon' & -\sin\epsilon'\cos\epsilon'' & 0 \\ -\cos\epsilon'\sin\epsilon'' & \sin\epsilon' & \cos\epsilon'\cos\epsilon'' & 0 \\ (d-a)\cos\epsilon'' + d' & 0 & (d-a)\sin\epsilon'' & 1 \end{pmatrix}$$

where $\epsilon'' = \pm arcos \dfrac{b\cos\epsilon}{\sqrt{a^2\sin^2\epsilon + b^2\cos^2\epsilon}}$, + for $\epsilon \in \langle 0,\ \pi \rangle$,

− for $\epsilon \in \langle \pi,\ 2\pi \rangle$, $d = \dfrac{b}{a}\sqrt{a^2\sin^2\epsilon + b^2\cos^2\epsilon}$,

$d' = \dfrac{a^2 - b^2}{a}\cos\epsilon$.

The direction vector of the tangent is $t(-a\,sin\epsilon,\ 0,\ b\cos\epsilon)$, the direction vector of the normal is $n(-b\cos\epsilon,\ 0,\ -\,a\,sin\epsilon)$.

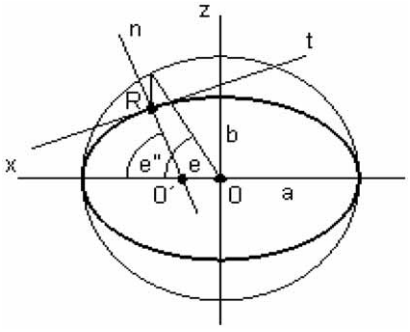

Fig. 15

The straight line p parallel to the axis o (Fig. 16) and given by the point $A(a, y_A, 0)$ creates the surface of the cylindrical type for the sign $(+)$ for orientation of motions and for $m = 5$ which is shown in Fig. 17.

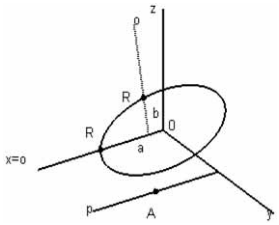

Fig. 16

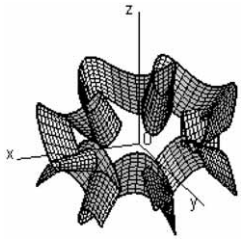

Fig. 17

The straight line p concurrent to the axis o creates the surface of the conical type (Fig. 18). If $p \perp o$ $p \subset xz$ and $x_A = a$, the straight line p is a tangent to the ellipse k and it creates the surface of the conical type (Fig. 19).

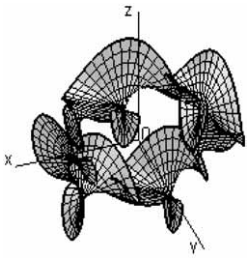

Fig. 18

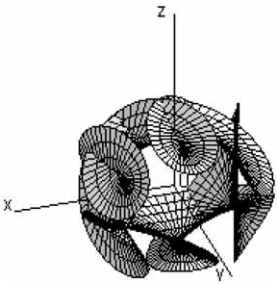

Fig. 19

The surface of the hyperbolical type created by p/o for $m = 4$ and equal orientation of the movements is shown in Fig. 21.

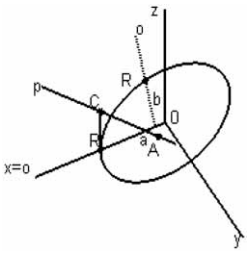

Fig. 20

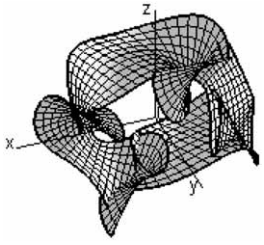

Fig. 21

2.4 Surfaces of the subgroup IV (*o* is a tangent to the ellipse *k*)

We will formulate the transformation matrix of the surface created by a revolution for $o = t$ as a product of matrices, which

represents displacement parallel to the vector $(-a, 0, 0)$, the revolution through the angle $\epsilon' = \pm m\epsilon$, $\epsilon \in \langle 0, 2\pi \rangle$ about the coordinate axis z, displacement parallel to the vector $(d, 0, 0)$, where $d = |O'\ R|$, $O' = n \cap x$ the revolution through the angle ϵ'' about the co-ordinate axis y and displacement parallel to the vector $(d', 0, 0)$, $d' = |O\ O'|$ (Fig. 15)

$$T(\epsilon) = \begin{pmatrix} \cos\epsilon' \cos\epsilon'' & \sin\epsilon' & \cos\epsilon' \sin\epsilon'' & 0 \\ -\sin\epsilon' \cos\epsilon'' & \cos\epsilon' & -\sin\epsilon' \sin\epsilon'' & 0 \\ -\sin\epsilon'' & 0 & \cos\epsilon'' & 0 \\ u_1 & -a\sin\epsilon' & u_2 & 1 \end{pmatrix}$$

where $u_1 = (-a\cos\epsilon' + d)\cos\epsilon'' + d'$, $u_2 = (-a\cos\epsilon' + d)\sin\epsilon''$,

$\epsilon'' = \pm arcos \dfrac{b\cos\epsilon}{\sqrt{a^2\sin^2\epsilon + b^2\cos^2\epsilon}}$, + for $\epsilon \in \langle 0, \pi \rangle$,

− for $\epsilon \in \langle \pi, 2\pi \rangle$, $d = \dfrac{b}{a}\sqrt{a^2\sin^2\epsilon + b^2\cos^2\epsilon}$,

$d' = \dfrac{a^2 - b^2}{a}\cos\epsilon$.

The straight line $p \parallel o$ (Fig. 22) creates the surface of the cylindrical type (Fig. 23). The straight line $p \times o$ creates the surface of the conical type (Fig. 24) and the straight line $p\ /\ o$ creates the surface of the hyperbolical type (Fig. 25).

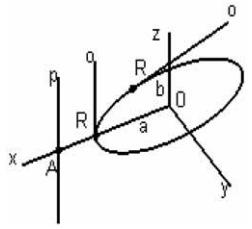

Fig. 22

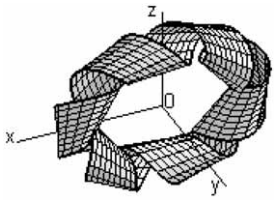

Fig. 23

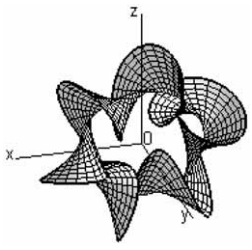

Fig. 24

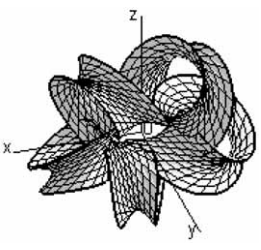

Fig. 25

2.5 Surfaces of the subgroup V (*o* is perpendicular to the plane of ellipse *xz*)

We will formulate the transformation matrix of the surface created by a revolution of straightline p around axis $o \perp xz$ as a product of matrices, which represents the displacement parallel to the vector $(-a, 0, 0)$, a revolution through the angle $\epsilon' = \pm m\epsilon$, $\epsilon \in \langle 0, 2\pi \rangle$, about the coordinate axis y, displacement parallel to the vector

$$T(\epsilon) = \begin{pmatrix} \cos\epsilon' & 0 & \sin\epsilon' & 0 \\ 0 & 1 & 0 & 0 \\ -\sin\epsilon' & 0 & \cos\epsilon & 0 \\ a(\cos\epsilon - \cos\epsilon') & 0 & b\sin\epsilon - a\sin\epsilon' & 1 \end{pmatrix}.$$

The straight line p parallel to the axis o creates the surface of the cycloidal type and ϵ-curves of this surface are similar to epicycloids or hypocycloids, i.e. the curves which are created by roll a circle along ellipse. The surface in Fig. 26 is of the epicycloidal type, where orientation of the motions is equal and surface in Fig. 27 is of the hypocycloidal type, where orientation of the motions is different.

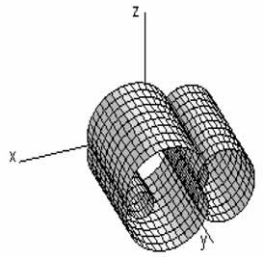

Fig. 26

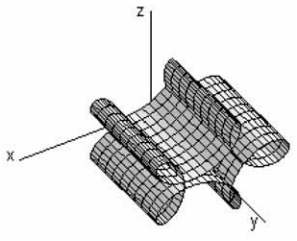

Fig. 27

The surface of the conical type, which is created by the straight line p concurent to the axis o and has the sign (+) for orientation of motions, is the surface of the epicycloidal type (Fig. 28). The surface for the sign (−) is the surface of the hypocycloidal type (Fig. 29).

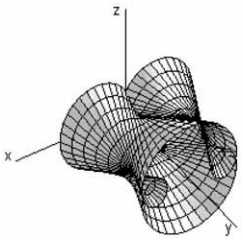

Fig. 28

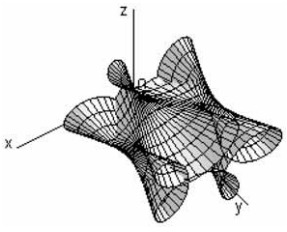

Fig. 29

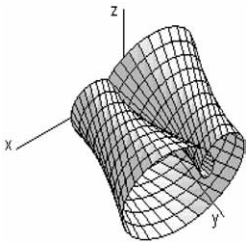

Fig. 30

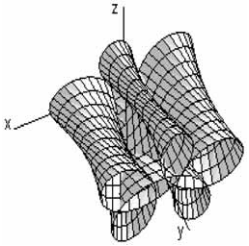

Fig. 31

The surface of the hyperbolical type, which is created by the straight line p skew to the axis o and has the sign $(+)$ for orientation of motions is the surface of the epicycloidal type (Fig. 30), the surface for the sign $(-)$ is the surface of the hypocycloidal type (Fig. 31).

3. Conclusion

We searched the group of linear revolution surfaces which were generated by a straight line revolution with a revolution axis of moving in contact with a curve. We specified the ellipse as a generating curve, which lies in the plane xz, its center is congruent to the origin O of coordinate system and its major axis is congruent to the axis x, the minor axis is congruent to z.

The coordinate axis y is perpendicular to the ellipse plane xz. If we search relative positions of the axis o and coordinate axis y, we can classify these surfaces by three subgroups. The first subgroup contains surfaces of the *spherical type* with above mentioned concurrent lines, the second subgroup contains surfaces of the *Euler type* with above mentioned skew lines and the third subgroup contains surfaces of the *cycloidal type* with above mentioned parallel lines. The surface-type also changes depending upon relative positions of the straight line p and the axis o. For better visualization, only particular segments of each surface displayed.

This work was solve by the Grant VEGA 1/4002/07.

References

[1] GRANÁT, L., SECHOVSKÝ, H.: *Computer graphic (in Czech)*, SNTL Nakladatelství technické literatury, Praha, 1980
[2] DRS, L.: *Surface in computer graphic (in Czech)*, SNTL Nakladatelství technické literatury, Praha, 1984
[3] VELICHOVÁ, D.: *Biaxial rotary surfaces (in Slovak),* Sborník příspěvku, 24. roč. mezinárodní konference Geometrie a počítačová grafika, Jeseníky, 2004, ISBN 80-248-0581-2
[4] VELICHOVÁ, D.: *Biaxial rotary surfaces II (in Slovak)*, Sborník 25. konference o geometrii a počítačové grafice, ČR, 2005, ISBN 80-7015-013-0
[5] BUDINSKÝ, B., KEPR, B.: *Basis of differential geometry with technical applications (in Czech)*, SNTL Nakladatelství technické literatury, Praha, 1970.

COMMUNICATIONS – Scientific Letters of the University of Žilina
Writer's Guidelines

1. Submissions for publication must be unpublished and not be a multiple submission.
2. Manuscripts written **in English language** must include abstract also written in English. The submission should not exceed 7 pages (format A4, Times Roman size 12). The **abstract** should not exceed 10 lines.
3. Submissions should be sent: **by e-mail** (as attachment in system Microsoft WORD) to one of the following addresses: *holesa@nic.utc.sk* or *vrablova@nic.utc.sk* or *polednak@fsi.utc.sk* **with a hard copy** (to be assessed by the editorial board) **or on a 3.5″ diskette** with a hard copy to the following address: Zilinska univerzita, OVaV, Univerzitná 1, SK-10 26 Zilina, Slovakia.
4. Abbreviations, which are not common, must be used in full when mentioned for the first time.
5. Figures, graphs and diagrams, if not processed by Microsoft WORD, must be sent in electronic form (as GIF, JPG, TIFF, BMP files) or drawn in contrast on white paper, one copy enclosed. Photographs for publication must be either contrastive or on a slide.
6. References are to be marked either in the text or as footnotes numbered respectively. Numbers must be in square brackets. The list of references should follow the paper (according to **ISO 690**).
7. The author's exact **mailing address of the organisation where the author works, full names, e-mail address or fax or telephone number,** must be enclosed.
8. The editorial board will assess the submission in its following session. In the case that the article is accepted for future volumes, the board submits the manuscript to the editors for review and language correction. After reviewing and incorporating the editor's remarks, the final draft (before printing) will be sent to authors for final review and adjustment.
9. The deadlines for submissions are as follows: September 30, December 31, March 31 and June 30.
10. Topics for the next issues: 2/2007 – Educational Sciences in Dimenzions of the Informations Society, 3/2007 – Construction of Transport Buildings.

POKYNY PRE AUTOROV PRÍSPEVKOV DO ČASOPISU KOMUNIKÁCIE – vedecké listy Žilinskej univerzity

1. Redakcia prijíma iba príspevky doteraz nepublikované alebo inde nezaslané na uverejnenie.
2. Rukopis musí byť **v jazyku anglickom**. Príspevok by nemal prekročiť 7 strán (formát A4, písmo Times Roman 12 bodové). K článku dodá autor **resumé** v rozsahu maximálne 10 riadkov (v anglickom jazyku).
3. Príspevok prosíme poslať: **e-mailom**, ako prílohu spracovanú v aplikácii Microsoft WORD, na adresu: *holesa@nic.utc.sk* alebo *polednak@fsi.utc.sk* príp. *vrablova@nic.utc.sk* (alebo doručiť na diskete 3,5″) **a jeden výtlačok** článku na adresu Žilinská univerzita, OVaV, Univerzitná1, 010 26 Žilina.
4. Skratky, ktoré nie sú bežné, je nutné pri ich prvom použití rozpísať v plnom znení.
5. Obrázky, grafy a schémy, pokiaľ nie sú spracované v Microsoft WORD, je potrebné doručiť buď v digitálnej forme (ako GIF, JPG, TIFF, BMP súbory), prípadne nakresliť kontrastne na bielom papieri a predložiť v jednom exemplári. Pri požiadavke na uverejnenie fotografie priložiť ako podklad kontrastnú fotografiu alebo diapozitív.
6. Odvolania na literatúru sa označujú v texte alebo v poznámkach pod čiarou príslušným poradovým číslom v hranatej zátvorke. **Zoznam použitej literatúry** je uvedený za príspevkom. Citovanie literatúry musí byť **podľa STN 01 0197 (ISO 690)** „Bibliografické odkazy".
7. K rukopisu treba pripojiť **plné meno a priezvisko autora a adresu inštitúcie v ktorej pracuje, e-mail adresu** alebo číslo telefónu event. faxu.
8. Príspevok posúdi redakčná rada na svojom najbližšom zasadnutí a v prípade jeho zaradenia do niektorého z budúcich čísiel podrobí rukopis recenziám a jazykovej korektúre. Pred tlačou bude poslaný autorovi na definitívnu kontrolu.
9. Termíny na dodanie príspevkov do čísiel v roku sú: 30. september, 31. december, 31. marec a 30. jún.
10. Nosné témy ďalších čísiel: 2/2007 – Edukačné vedy v dimenziách informačnej spoločnosti, 3/2007 – Konštrukcia dopravných stavieb.

COMMUNICATIONS

SCIENTIFIC LETTERS OF THE UNIVERSITY OF ŽILINA
VOLUME 9

Address of the editorial office:
Žilinská univerzita
Office for Science and Research
Univerzitná 1, Slovakia
SK 010 26 Žilina
E-mail: komunikacie@nic.utc.sk, polednak@fsi.utc.sk,

Each paper was reviewed by two reviewers.

Journal is excerpted in Compendex

It is published by the University of Žilina in
EDIS - Publishing Institution of Žilina University
Registered No: 1989/98
ISSN 1335-4205

Published quarterly

Single issues of the journal can be found on:
http://www.utc.sk/komunikacie